GEORGIA INSTITUTE OF TECHNOLOGY — OFFICE OF CONTRACT ADMINISTRATION

PROJECT ADMINISTRATION DATA SHEET

[x] ORIGINAL [ ] REVISION NO. _____

Project No. A-3520 GTRI/~~GIT~~ DATE 5/3/83

Project Director: E. O. Rausch ~~School~~/Lab RAIL-AD

Sponsor: Lockheed-Georgia Company

Type Agreement: Purchase Order No. CA20741 & Agmt. dated 3/14/83.

Award Period: From 4/13/83 To ~~8/13/83~~ 12-31-83 4-30-84 (Performance) _____ (Reports)

Sponsor Amount: Total Estimated: $ 29,444 Funded: $ 29,444 (Phase I)

Cost Sharing Amount: $ None Cost Sharing No: N/A

Title: Fiber Optic RF Strain Sensor

ADMINISTRATIVE DATA

OCA Contact William F. Brown Ext. 4820

1) Sponsor Technical Contact:

Dr. M. C. Whiffen, D/72-11, Z403
Lockheed-Georgia Co.
Marietta, GA 30063

2) Sponsor Admin/Contractual Matters:

Mr. Bill Britton, D/52-25, Z630
Lockheed-Georgia Co.
Marietta, GA 30063

(404) 425-4596

Defense Priority Rating: None

Military Security Classification: None

(or) Company/Industrial Proprietary: See Comments below

RESTRICTIONS

See Attached _____ Supplemental Information Sheet for Additional Requirements.

Travel: Foreign travel must have prior approval – Contact OCA in each case. Domestic travel requires sponsor approval where total will exceed greater of $500 or 125% of approved proposal budget category.

Equipment: Title vests with None proposed

COMMENTS:

The total P.O. amount of $29,444 includes $500 to be added by forthcoming P.O. revision per 4/25/83 telecon between L. Bowman of OCA and B. Britton of Lockheed. The $500 is consideration for restriction of publications from the research for a period of 2 years after project completion.

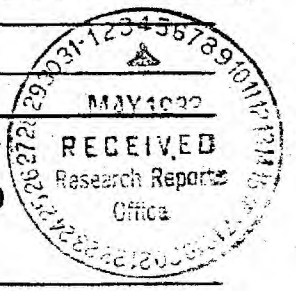

COPIES TO:

Research Administrative Network
Research Property Management
Accounting
Procurement/EES Supply Services
Research Security Services
Reports Coordinator (OCA)
GTRI
Library
Research Communications (2)
Project File
Other Rausch
Other I. Newton

FORM OCA 4-79I (Rev 982)

EORGIA INSTITUTE OF TECHNOLOGY OFFICE OF CONTRACT ADMINISTRATION

SPONSORED PROJECT TERMINATION/CLOSEOUT SHEET

Date 6/14/84

oject No. A-3520 School/Lab RAIL-AD

cludes Subproject No.(s)

oject Director(s) E. O. Rausch GTRI XX6XX

onsor Lockheed-Georgia Company, Marietta, GA

tle Fiber Optic RF Strain Sensor

fective Completion Date: 4/30/84 (Performance) 4/30/84 (Reports)

rant/Contract Closeout Actions Remaining:

- [ ] None
- [X] Final Invoice or Final Fiscal Report
- [ ] Closing Documents
- [ ] Final Report of Inventions
- [ ] Govt. Property Inventory & Related Certificate
- [ ] Classified Material Certificate
- [ ] Other

ontinues Project No. Continued by Project No.

OPIES TO:

oject Director
esearch Administrative Network
esearch Property Management
ccounting
ocurement/EES Supply Services
esearch Security Services
eports Coordinator (OCA)
egal Services

Library
GTRI
Research Communications (2)
Project File
Other

orm OCA 60:1028

ENGINEERING EXPERIMENT STATION
Georgia Institute of Technology
A Unit of the University System of Georgia
Atlanta, Georgia 30332

May 27, 1983

Dr. M. C. Whiffen
D/72-11,7403
Lockheed-Georgia Company
Marietta, Georgia 30063

Subject: Monthly Technical Status Report No. 1, "Fiber Optic RF Strain Sensor," Purchase Order No. CA20741, Georgia Tech Project A-3520

Dear Dr. Whiffen:

This report summarizes project activities performed under the subject contract for the period April 13, 1983 through May 13, 1983.

TECHNICAL ACTIVITIES

In order to satisfy Task 1 of Phase I of the Fiber Optic RF Strain Sensor Program Georgia Tech initiated a literature search concerning noise in fiber optic transmission systems utilizing solid state diode lasers and light emitting diodes. Information extracted from this body of literature was incorporated into an equation that specifies the signal-to-noise ratio (S/N) as a function of various parameters. A number of computer programs were generated to calculate and produce the data outlined in a memorandum to Lockheed-Georgia dated May 9, 1983.

FUTURE ACTIVITIES

During the period May 14, 1983 through June 13, 1983 the relationships between the S/N ratio at the input and output of the RF mixer will be determined. Production of the required S/N ratio plots will then be initiated.

Respectfully submitted,

Ekkehart O. Rausch, Ph.D.
Senior Research Scientist

APPROVED:

Robert N. Trebits, Ph.D.
Chief, Analysis Division

ENGINEERING EXPERIMENT STATION
Georgia Institute of Technology
A Unit of the University System of Georgia
Atlanta, Georgia 30332

June 29, 1983

Dr. M. C. Whiffen
D/72-11,7403
Lockheed-Georgia Company
Marietta, Georgia 30063

Subject: Monthly Technical Status Report No. 2, "Fiber Optic RF Strain Sensor," Purchase Order No. CA20741, Georgia Tech Project A-3520

Dear Dr. Whiffen:

This report summarizes project activities performed under the subject contract for the period May 14, 1983 through June 13, 1983.

TECHNICAL ACTIVITIES

Signal-to-noise ratios (S/N) as a function of fiber length for various bandwidth and frequencies were computed and plotted. These ratios were converted to a minimum observable phase shift, $\Delta\phi$, and a minimum observable strain, $\Delta\varepsilon$, (i.e. strain sensitivity). Computed values are in good agreement with experimental data. To date, only sensor systems utilizing a laser diode have been computer modelled. LED sensor systems will be addressed during the next reporting period.

Phase changes due to $1^{o}C$ temperature variations have been calculated and compared with minimum observable phase changes. These results show the RF strain sensor to be temperature sensitive at a frequency of 1 GHz for bandwidths less than 1 MHz and fiber lengths greater than 1 m. In general, increased strain sensitivity can be obtained by increasing RF frequency, decreasing bandwidth, increasing fiber length, or a combination thereof. Economic considerations favor an LED system with variable bandwidth to obtain the required strain sensitivity.

FUTURE ACTIVITIES

During the next reporting period S/N, $\Delta\phi$, and $\Delta\epsilon$ will be derived for an LED sensor system and $\Delta\phi$ as a function of pressure changes will be computed.

Respectfully submitted,

Ekkehart O. Rausch, Ph.D.
Senior Research Scientist

APPROVED:

Robert N. Trebit, Ph.D.
Chief, Analysis Division

ENGINEERING EXPERIMENT STATION
Georgia Institute of Technology
A Unit of the University System of Georgia
Atlanta, Georgia 30332

July 29, 1983

Dr. M. C. Whiffen
D/72-11,7403
Lockheed-Georgia Company
Marietta, Georgia 30063

Subject: Monthly Technical Status report No. 3 "Fiber Optic RF Strain Sensor," Purchase Order No. CA20741, Georgia Tech Project A-3520.

Dear Dr. Whiffen:

This report summarizes project activities performed under the subject contract for the period June 14, 1983 through July 13, 1983.

TECHNICAL ACTIVITIES

Signal-to-noise ratios as a function of fiber length, RF frequency and pulse width were computed utilizing an LED. These ratios were converted to a minimum observable phase shift, a minimum observable strain, and an expected dynamic range.

Phase changes due to atmospheric pressure differentials between sea level and 33000 ft. were also calculated. These phase values were superimposed on the minimum observable phase shifts to compare the magnitudes of these parameters. Task I of Phase I is now complete.

FUTURE ACTIVITIES

During the next reporting period a block diagram, a parts list and an electrical schematic of the system will be generated.

Respectfully submitted,

Ekkehart O. Rausch, Ph.D.
Senior Research Scientist

APPROVED:

Robert N. Trebit, Ph.D.
Chief, Analysis Division

EOR/ss

Georgia Institute of Technology
ENGINEERING EXPERIMENT STATION
Atlanta, Georgia 30332

January 9, 1984

Dr. M. C. Whiffen
D/72-11,7403
Lockheed-Georgia Company
Marietta, Georgia 30063

Subject: Monthly Technical Status Report No. 4 "Fiber Optic RF Strain Sensor," Purchase Order No. CA20741, Georgia Tech Project A 3520.

Dear Dr. Whiffen:

This report summarizes project activities performed under the subject contract for the period July 14, 1983 through December 31, 1983.

TECHNICAL ACTIVITIES

A block diagram, a parts list and an electrical schematic of the proposed sensor system was generated and delivered to Lockheed. Parts for the system were purchased. All parts were delivered to Georgia Tech (via Lockheed) with the exception of the LED transmitters and photodiode receivers. A layout of the system was completed and assembly of the RF fiber optic sensor is currently in progress. Completion of the unit is scheduled for mid-February.

FUTURE ACTIVITIES

The next reporting period will cover progress in system assembly and, possibly, testing.

Respectfully submitted,

Ekkehart O. Rausch, Ph.D.
Senior Research Scientist

APPROVED:

Robert N. Trebits, Ph.D.
Chief, Analysis Division

EOR/mhl

Georgia Institute of Technology
ENGINEERING EXPERIMENT STATION
Atlanta, Georgia 30332

January 17, 1984

Dr. M. C. Whiffen
D/72-11,7403
Lockheed-Georgia Company
Marietta, Georgia 30063

Subject: Monthly Technical Status Report No. 6 "Fiber Optic RF Strain Sensor," Purchase Order No. CA20741, Georgia Tech Project A-3520.

Dear Dr. Whiffen:

This report summarizes project activities performed under the subject contract for the period January 1, 1984 through January 31, 1984.

TECHNICAL ACTIVITIES

A wirewrapped prototype of the control logic circuit board was built and tested. Final versions of the control logic and amplifier boards have been completed and tested. The rear panel of the unit has been finished. Power supplies and power wiring have been installed. Fabrication of mountings for the coaxial components is in progress.

Delivery of the fiber optic transceiver will be postponed by LeCroy Corporation for another two weeks.

FUTURE ACTIVITIES

Assembly of the main unit will continue into the next reporting period and preliminary testing will begin.

Respectfully submitted,

Ekkehart O. Rausch, Ph.D.
Senior Research Scientist

Approved:

Robert N. Trebits, Ph.D.
Chief, Analysis Division

EOR/dmp

Georgia Institute of Technology
ENGINEERING EXPERIMENT STATION
Atlanta, Georgia 30332

March 15, 1984

Dr. M. C. Whiffen
D/72-11,7403
Lockheed-Georgia Company
Marietta, Georgia 30063

Subject: Monthly Technical Status Report No. 7 "Fiber Optic RF Strain Sensor," Purchase Order No. CA20741, Georgia Tech Project A-3520.

Dear Dr. Whiffen:

This report summarizes project activities performed under the subject contract for the period February 1, 1984 through February 29, 1984.

TECHNICAL ACTIVITIES

Assembly of the coaxial components was completed and system testing was begun. Signal levels were verified and attenuator values were optimized. The unit was also connected to the Apple computer to verify software control of system operating modes, calibration and data logging. Program debugging and optimization are well underway. Engraving of the front panel has begun.

Delivery of the fiber optic tranceiver pairs has been postponed by LeCroy Corporation until end of March.

FUTURE ACTIVITIES

The front panel and tranceiver pairs will be installed, completing assembly of the unit. Operation of the strain sensor will be initiated.

Respectfully submitted,

Ekkehart O. Rausch, Ph.D.
Senior Research Scientist

APPROVED:

Robert N. Trebits, Ph.D.
Chief, Analysis Division

EOR/mhl

Georgia Institute of Technology
ENGINEERING EXPERIMENT STATION
Atlanta, Georgia 30332

May 14, 1984

Dr. M. C. Whiffen
D/72-11, 7403
Lockheed-Georgia Company
Marietta, Georgia 30063

Subject: (Final) Technical Status Report No. 8 "Fiber Optic RF Strain Sensor," Purchase Order No. CA20741, Georgia Tech Project A-3520.

Dear Dr. Whiffen:

This report summarizes project activities performed under the subject contract for the period April 13, 1984 through April 30, 1984.

TECHNICAL ACTIVITIES

All required components were delivered and incorporated into the strain sensor. The system is complete. Final test procedures have indicated a phase sensitivity of 0.018° and a strain sensitivity of 10^{-4}. The modulation frequency was 100 MHz and the low pass filter width was 1 KHz. Integration, i.e., averaging of multiple samples, can provide better sensitivity. The strain sensor unit will be delivered within two weeks following some minor cosmetic changes.

Respectfully submitted,

Ekkehart O. Rausch, Ph.D.
Senior Research Scientist

APPROVED:

Robert N. Trebits, Ph.D.
Chief, Analysis Division

/mhl

INTERIM TECHNICAL REPORT
GIT/EES PROJECT A-3520

RF FIBER OPTIC SENSOR

By

E. O. Rausch, B. E. Huitt, and B. S. Bostatter

Prepared for

LOCKHEED-GEORGIA COMPANY
A Division of Lockheed Corporation
Marietta, Georgia 30332

Under

Purchase Order No. CA20741

January 1984

GEORGIA INSTITUTE OF TECHNOLOGY
A Unit of the University System of Georgia
Engineering Experiment Station
Atlanta, Georgia 30332

INTERIM TECHNICAL REPORT
GIT/EES PROJECT A-3520

RF FIBER OPTIC SENSOR

By:

E. O. Rausch, B. E. Huitt, and B. S. Bostatter

Prepared for:

Lockheed-Georgia Company
A Division of Lockheed Corporation
Marietta, Georgia 30332

Under

Purchase Order No. CA20741

January 1984

GEORGIA INSTITUTE OF TECHNOLOGY
A Unit of the University System of Georgia
Engineering Experiment Station
Atlanta, Georgia 30332

TABLE OF CONTENTS

SECTION	TITLE	PAGE
1	INTRODUCTION	1
1.1	Objectives	1
1.2	Background	1
2	SIGNAL-TO-NOISE RATIO ANALYSIS	9
2.1	Introduction	9
2.2	Derivation of SNR for a System with Monomode Fiber-CW Signal - ILD	9
2.2.1	Derivation of Signal Power	9
2.2.2	Derivation of Noise Power	13
2.2.3	Numerical Estimations	15
2.3	Derivation of SNR for a System with Multimode Fiber-CW Signal-ILD	19
2.4	SNR Calculations of a System with Multimode Fiber - Pulsed Signal - ILD	23
2.5	Maximum Measured SNR in a Multimode System with CW Signal and ILD	25
2.6	Derivation of SNR for a System with an LED Source	25
3	SENSITIVITY ANALYSIS	29
3.1	Mixer Transfer Functions	29
3.2	Minimum Observable Phase Shift	32
3.3	Minimum Observable Strain Sensitivity	41
3.4	Estimated Dynamic Range	42
3.5	Temperature Sensitivity	43
3.6	Pressure Sensitivity	45
3.7	Comparisons Between Predicted and Measured Phase Shifts	45
3.8	Analytical Results	48
APPENDIX A	The Sum of Two Sinusoids	84
APPENDIX B	Derivation of the Output Power of a CW Signal Propagating Through a Multimode Fiber	86
APPENDIX C	The Convolution of a Gaussian Pulse with a Gaussian Response Function	90
APPENDIX D	Gaussian Statistics	96

THIS PAGE IS LEFT INTENTIONALLY BLANK

LIST OF FIGURES

FIGURE	TITLE	PAGE
1	Simplified block diagram of an optical interferometer using fiber optics	3
2	Simplified block diagram of a fiber optic RF interferometer	5
3	Block diagram of a practical RF fiber optic interferometer	7
4	Relative photon noise spectrum	11
5	Low frequency relative photon noise per 1 Hz bandwidth as a function of laser output power	11
6	Noise power as a function of total attenuation in fiber	18
7	Signal-to-noise ratio as a function of total attenuation in a monomode fiber optic link for various system bandwidths	20
8	Signal-to-noise ratio versus total attenuation in a multimode fiber optic link	22
9	Peak to peak Output voltage of multimode fiber optic transmission link versus peak to peak input voltage	26
10	Signal-to-noise ratio as a function of total attenuation in a multimode fiber link for various system bandwidths	28
11	Block diagram of a practical fiber optic RF sensor	30
12	Relationship between I and Q components	33
13	Transfer function of the Q mixer	33
14	Relationship between observable phase shift due to noise, and phase noise vector	35
15	Relationship between minimum observable phase shift and phase shift due to noise	37
16	Definition of probability of detecting a false phase shift or false alarm (PFA) and probability of detecting a true phase shift (PD)	39
17	Mixer output as a function of fiber displacement	50
1-1-1	Signal-to-noise ratio as a function of fiber length for various bandwidths. RF frequency was set to 1 GHz. The optical source is a laser diode	51
1-1-2	Minimum observable phase shift, as a function of fiber length for various bandwidths. RF frequency was set to 1 GHz. The optical source is a laser diode. At 1 GHz the temperature sensitivity is 2.1096×10^{-4} rad/^{o}C-m and the pressure sensitivity is 7.638×10^{-5} rad/atm-m	52

LIST OF FIGURES (Cont.)

FIGURE	TITLE	PAGE
1-1-3	Minimum observable strain (strain sensitivity) as a function of fiber length for various bandwidths. RF frequency was set to 1 GHz. The optical source is a laser	53
1-1-4	Expected dynamic range as a function of fiber length for various bandwidths. RF frequency was set to 1 GHz. The optical source is a laser. Maximum strain value is 1.23×10^{-2}. Minimum strain value is strain sensitivity	54
1-2-1	Signal-to-noise ratio as a function of fiber length for various RF frequencies. Bandwidth was set to 1 kHz. The optical source is a laser diode	55
1-2-2	Minimum observable phase shift, as a function of fiber length for various RF frequencies. Bandwidth was set to 1 kHz. The optical source is a laser diode	56
1-2-3	Minimum observable strain (strain sensitivity) as a function of fiber length for various RF frequencies. The bandwidth was set to 1 kHz. The optical source is a laser	57
1-2-4	Expected dynamic range as a function of fiber length for various RF frequencies. Bandwidth was set to 1 kHz. The optical source is a laser. Maximum strain value is 1.23×10^{-2}. Minimum strain value is strain sensitivity	58
1-3-1	Signal-to-noise ratio as a function of RF frequency for various fiber lengths. Bandwidth was set to 1 kHz. The optical source is a laser	59
1-3-2	Minimum observable phase shift, as a function of RF frequency for various fiber lengths. Bandwidth was set to 1 kHz. The optical source is a laser	60
1-3-3	Minimum observable strain (strain sensitivity) as a function of RF frequency for various fiber lengths. Bandwidth was set to 1 kHz. The optical source is a laser	61
1-3-4	Expected dynamic range as a function of RF frequency for various fiber lenghts. Bandwidth was set to 1 kHz. The optical source is a laser. Maximum strain value is 1.23×10^{-2}. Minimum strain value is strain sensitivity	62
1-4-1	Signal-to-noise ratio as a function of pulse width for various fiber lengths. RF frequency was set to 100 MHz. The optical source is a laser	63

LIST OF FIGURES (Cont.)

FIGURE	TITLE	PAGE
1-4-2	Minimum observable phase shift, as a function of pulse width for various fiber lengths. RF frequency was set to 100 MHz. The optical source is a laser	64
1-4-3	Minimum observable strain (strain sensitivity) as a function of pulse width for various fiber lengths. RF frequency was set to 100 MHz. The optical source is a laser	65
1-4-4	Expected dynamic range as a function of pulse width for various fiber lengths. RF frequency was set to 100 MHz. The optical source is a laser. Maximum strain value is 1.23 x $^{-2}$. Minimum strain value is strain sensitivity	66
2-1-1	Signal-to-noise ratio as a function of fiber length for various bandwidths. RF frequency was set at 100 MHz. The optical source is an LED	67
2-1-2	Minimum observable phase shift, as a function of fiber length for various bandwidths. RF frequency was set to 100 MHz. The optical source is an LED. At 100 MHz the temperature sensivitity is 2.1096 x 10^{-5} rad/^{o}C-m and the pressure sensitivity is 7.638 x 10^{-6} rad/atm-m	68
2-1-3	Minimum observable strain (strain sensitivity) as a function of fiber length for various bandwidths. RF frequency was set to 100 MHz. The optical source is an LED	69
2-1-4	Expected dynamic range as a function of fiber length for various bandwidths. RF frequency was set to 100 MHz. The optical source is an LED. Maximum strain value is 1.23 x 10^{-2}. Minimum strain value is strain sensivitity	70
2-2-1	Signal-to-noise ratio as a function of fiber length for various RF frequencies. Bandwidth was set to 1 kHz. The optical source is an LED	71
2-2-2	Minimum observable phase shift, as a function of fiber length for various RF frequencies. Bandwidth was set to 1 kHz. The optical source is an LED	72
2-2-3	Minimum observable strain (strain sensitivity) as a function of fiber length for various RF frequencies. Bandwidth was set to 1 kHz. The optical source is an LED	73
2-2-4	Expected dynamic range as a function of fiber length for various RF frequencies. Bandwidth was set to 1 kHz. The optical source is an LED. Maximum strain value is 1.23 x 10^{-2}. Minimum strain value is strain sensitivity	74

LIST OF FIGURES (Cont.)

FIGURE	TITLE	PAGE
2-3-1	Signal-to-noise ratio as a function of RF frequency for various fiber lengths. Bandwidth was set to 1 kHz. The optical source is an LED	75
2-3-2	Minimum observable phase shift, as a function of RF frequency for various fiber lengths. Bandwidth was set to 1 kHz. The optical source is an LED	76
2-3-3	Minimum observable strain (strain sensitivity) as a function of RF frequency for various fiber lengths. Bandwidth was set to 1 kHz. The optical source is and LED	77
2-3-4	Expected dynamic range as a function of RF frequency for various fiber lenghts. Bandwidth was set to 1 kHz. The optical source is an LED. Maximum strain value is 1.23×10^{-2}. Minimum strain value is strain sensitivity	78
2-4-1	Signal-to-noise ratio as a function of pulse width for various fiber lengths. RF frequency was set to 100 MHz. The optical source is an LED	79
2-4-2	Minimum observable phase shift, as a function of pulse width for various fiber lengths. RF frequency was set to 100 Mhz. The optical source is an LED	80
2-4-3	Minimum observable strain (strain sensitivity) as a function of pulse width for various fiber lengths. RF frequency was set to 100 MHz. The optical source is an LED	81
2-4-4	Expected dynamic range as a function of pulse width for various fiber lengths. RF frequency was set to 100 MHz. The optical source is an LED. Maximum strain value is 1.23×10^{-2}. Minimum strain value is strain sensitivity	82

SECTION 1
INTRODUCTION

1.1 OBJECTIVES

From April to September 1982, the Radar and Instrumentation Laboratory of the Georgia Institute of Technology Engineering Experiment Station, working under a Lockheed-Georgia Company Contract (Purchase Order No. CA20741), conducted the first phase of a two-phase research program to analyze, construct, and test an RF fiber optic strain sensor. The goals of Phase 1 were to:

1. Conduct an analysis of the sensor that specifies the minimum observable change in phase shift as a function of system bandwidth, fiber length, and modulation frequency. Included in this analysis were the sensor's sensitivity to temperature and pressure changes, the impact of vibrations on sensor operation, and changes in the sensor's phase resolution for pulsed versus CW operating modes.
2. Review the analysis and formulate design specifications that will serve as a guide in the construction of the sensing device, translate these parameters into a specific system design, and produce an electrical schematic diagram and an associated parts list.

The objectives of Phase 2 are to: (1) construct the sensor and (2) quantify experimentally the sensor's performance. In this report, only the results of the analysis completed in Phase 1 and the associated mathematical apparatus are presented.

1.2 BACKGROUND

In recent years, glass fibers for use as a transmission medium of broadband signals have been developed and improved to the point where transmission losses are less than 3 dB/km and bandwidth-length products are greater than 1 GHz-km for commercially produced fibers.[1,2] Similarly, research in integrated optics has led to the development of miniaturized broadband optical components (e.g., solid state lasers, couplers, modulators, and detectors) which provide fast

processing and input/output capabilities for use with optical fibers. To date, the bulk of research and development efforts in fiber optic technology has been directed towards communications applications. Other important potential uses of this technology in signal processing and sensing areas have been realized only recently. At present, fiber optic sensors are being developed for sensing a variety of physical parameters such as strain, acoustic pressures, magnetic fields, temperature, acceleration, and rate of rotation.

Fiber optic sensors have some general inherent advantages over conventional methods because the fiber is typically made of silica or plastic. This type of sensor has negligible electromagnetic interference susceptibility, can be used in explosive or high voltage environments, and can be integrated into conducting or non-conducting materials to measure signals in real-time (e.g., in-flight measurements of strain in aircraft wings).

The most sensitive fiber sensors employ a Mach-Zehnder interferometric approach wherein the optical phase shift induced in the sensing arm by external signals is compared with the optical phase shift in a reference arm. Both optical and microwave interferometers have been conceived and will be presented in this section.

The optical interferometer is shown in Figure 1. Here the optical source is operated in the CW mode. The optical signal is split via a one-to-two fiber coupler into a reference arm and a sensing arm. The outputs are then recombined and detected by a photodiode. Changes in the fiber's physical length and index of refraction due to external forces affect the optical propagation speed. Provided the optical source is coherent, this difference in propagation speed between the reference and sensing signals creates a relative phase shift which, in turn, produces an interference pattern at the input to the photodiode. If only a narrow portion of the interference pattern is sensed, any changes, for example, due to variations in stress-strain can be detected as changes in the detected voltage signal. For lasers operating in the visible or near IR region, this stress sensor is highly sensitive because a 2π phase shift requires an optical path length difference of only 600 to 1300 nm. On the basis of this technique, strain sensitivities of less than 0.4×10^{-6} have been reported in the literature.[3]

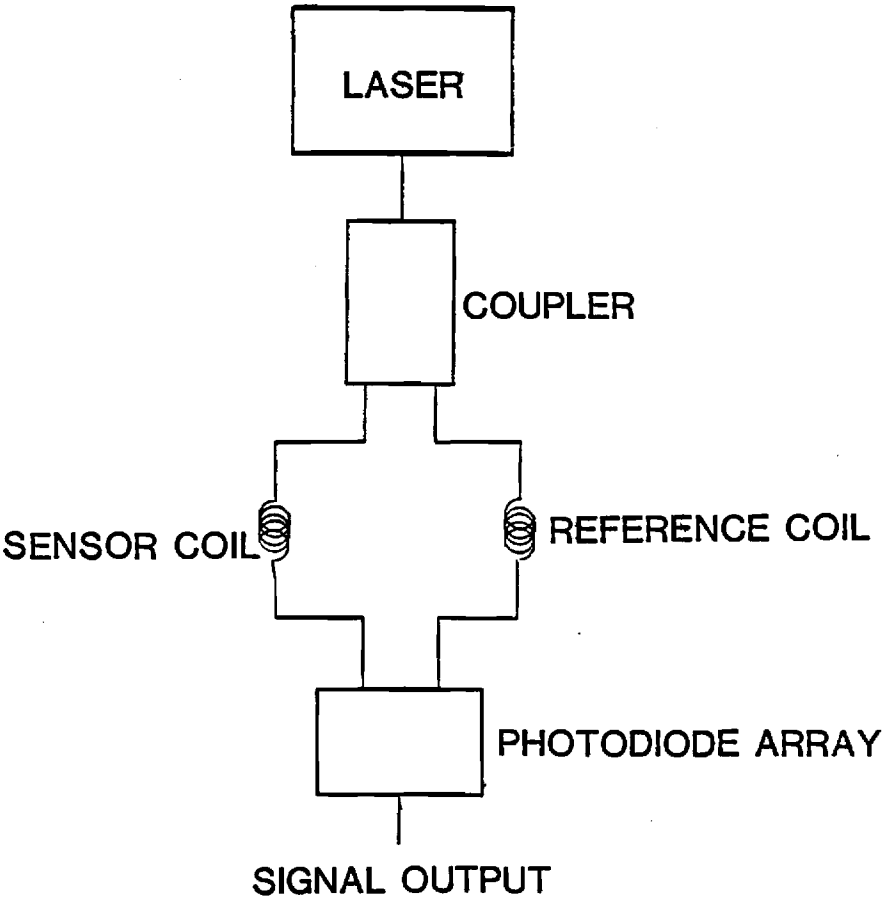

Figure 1. Simplified block diagram of an optical interferometer using fiber optics.

The RF interferometer, an alternate concept, does not require a coherent optical source nor a single mode fiber (see Figure 2). In this case, the output intensity of the source is modulated with CW RF signal, i.e., the optical frequency acts as a carrier. The modulated optical signal is routed through a sensing fiber. The RF is redetected with an intensity sensitive photodiode and combined with the reference signal in a mixer. The output voltage of the mixer is sensitive to the RF phase shift between the reference and sensor signals.

The RF interferometric method is potentially inexpensive to implement because of the use of light emitting diodes (LED). Unfortunately, the highest modulation frequency for LEDs is on the order of 10^8 Hz. In contrast, optical frequencies are six orders of magnitude greater, or typically in the 10^{14} Hz region. As a result, the maximum sensitivity of the RF interferometer is expected to be orders of magnitude less than that of the optical interferometer. But, because the RF interferometer is operated in a CW mode, a very narrow filter placed about the center of the modulation frequency can remove much of the unwanted noise in the circuit and in effect increase the sensitivity of this type of sensor. Recent experiments have demonstrated a strain sensitivity, ε, of 7×10^{-4} using a total fiber length, L, of 1 m, a modulation frequency of 1 GHz, and a bandwidth of 100 MHz.

In its simplest configuration (as shown in Figure 2), the RF interferometric sensor can produce spurious signals since a mixer is sensitive to amplitude as well as phase differences at its input terminals. Thus, changes in the fiber's speckle pattern due to fiber displacement or vibrations can be converted into voltage oscillations at misaligned fiber-fiber connections (i.e., modal noise) and transferred through the system to the mixer output. Modal noise oscillations can be removed by splitting the reference and sensor signals into two equal components and introducing a 90^o phase shift in one sensor arm, as shown in Figure 3. The output voltages of the two mixers, Q and I, are now proportional to $A_S A_R \cos \phi$ and $A_S A_R \sin \phi$, respectively, where A_S and A_R are the amplitudes of the sensor and reference signals, respectively, and ϕ is the phase angle between the two signals. Hence, the phase difference, ϕ, is given by

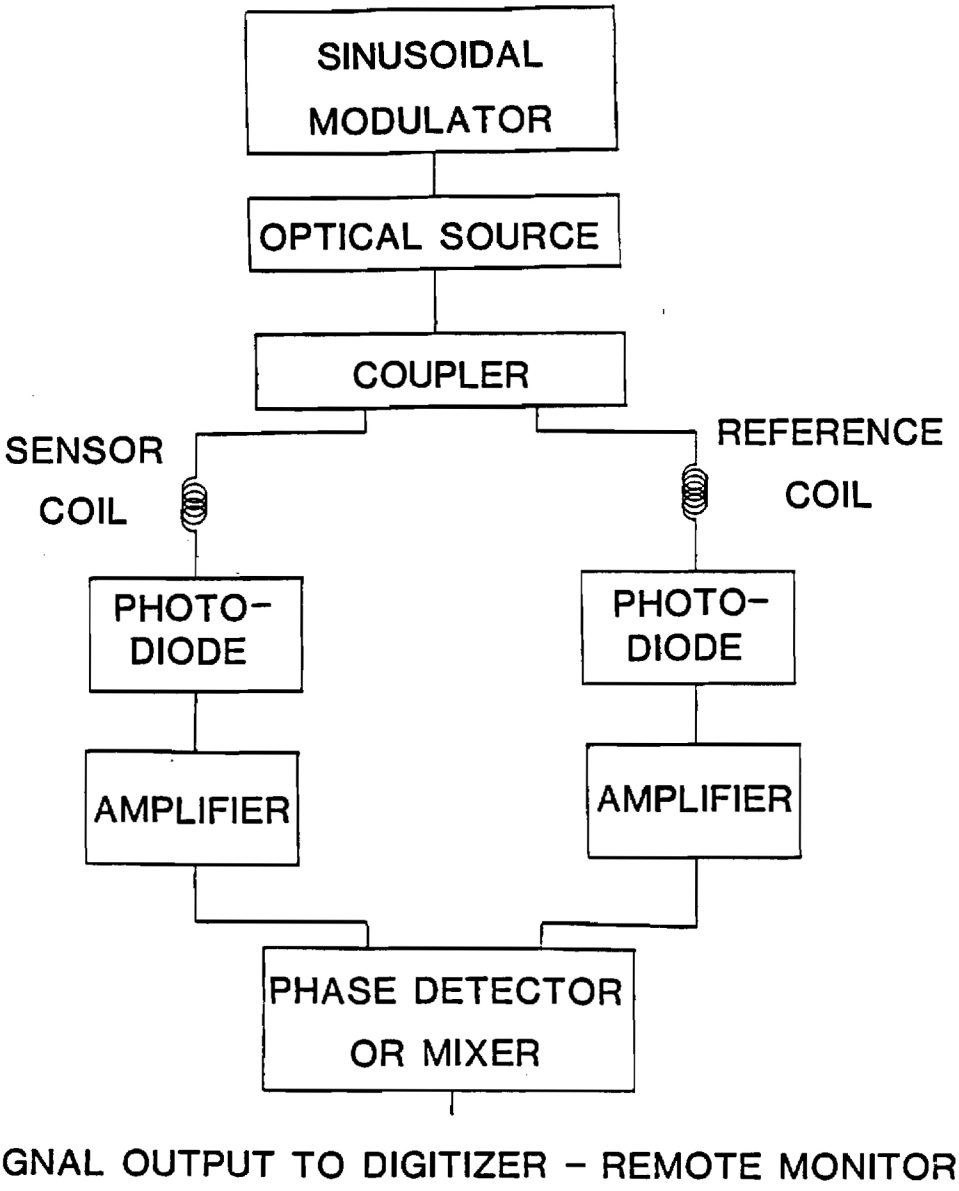

Figure 2. Simplified block diagram of a fiber optic RF interferometer.

$$\phi = \arctan (Q/I). \qquad (1.1)$$

Any changes in the amplitudes of the mixer input signals (e.g., due to modal noise) will appear equally in amplitude in the Q and I components and, thus, will not affect θ in Equation 1.1.

The analysis presented in this report is based on the sensor configuration of Figure 3. In Section 2, the signal-to-noise ratio of the system is calculated and used in Section 3 to derive the sensitivity of the system to a small phase change, $\Delta\phi$. $\Delta\phi$, in turn, is translated into a minimum strain sensitivity. These calculations involve two optical sources: the light emitting diode (LED) and the injection laser diode (ILD). A comparison of measured and predicted phase shifts is also included in Section 3. Section 4 concludes the report with an analysis of the system's sensitivity to temperature and pressure changes.

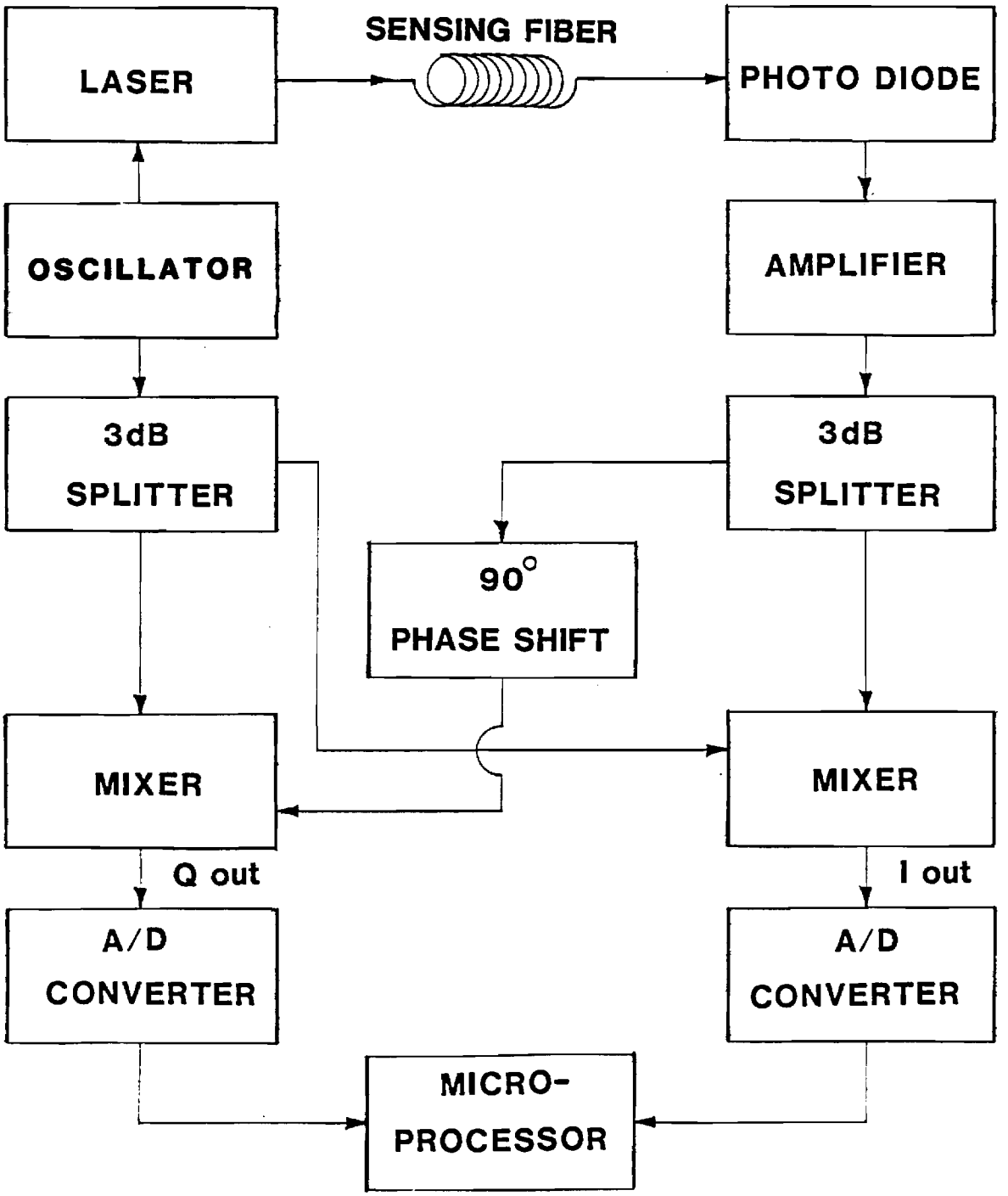

Figure 3. Block diagram of a practical RF fiber optic interferometer.

THIS PAGE IS LEFT INTENTIONALLY BLANK

SECTION 2
SIGNAL-TO-NOISE RATIO ANALYSIS

2.1 INTRODUCTION

The approach taken in this analysis was to compute the signal-to-noise ratio (SNR) at the mixer outputs of the RF interferometric sensor for a CW signal and a monomode fiber. These calculations are straightforward to implement. The computations were then refined to include dispersion effects in a multimode fiber and the fact that the RF may be a pulse modulated RF signal rather than a CW signal. This section is, therefore, divided into several parts. Sections 2.2 through 2.5 discuss: (1) SNR calculations for a system with a monomode fiber, a CW signal, and an ILD; (2) SNR calculations for a multimode fiber system with a CW signal and an ILD; (3) SNR calculations for a multimode fiber system with a pulsed signal and an ILD; and (4) validation of calculated SNR with measured values. Section 2.6 deals with SNR calculations where the optical source is an LED.

2.2 DERIVATION OF SNR FOR A SYSTEM WITH MONOMODE FIBER-CW SIGNAL - ILD

2.2.1 DERIVATION OF SIGNAL POWER

Consider the fiber optic sensor sketched in Figure 3. The laser diode oscillates at a single optical frequency, ω, and the light output is modulated by an RF CW signal with frequency, Ω, and RF bandwidth, F_B. The optical fiber has a loss of α (dB/km) and is L (km) long. The detector is an avalanche photodiode (APD) followed by an amplifier. The output is delivered into a 50 ohm load. The signal's frequency and RF bandwidth are assumed to be well within the bandwidths of the fiber, APD, and amplifier. An examination of commercial products shows that monomode fiber length-bandwidth products can be as high as hundreds of GHz-km. Laser bandwidths are typically greater than or equal to 1 GHz; the bandwidth of the APD can be as high as 20 GHz, and the bandwidths of amplifiers can be greater than 3.5 GHz. Thus, if the RF frequency and RF bandwidth are $<$ 1 GHz, the above assumptions are well justified.

The modulated light output from the laser diode is assumed to be a CW sinusoidal signal at frequency , with a modulation depth m. The optical power fed into the fiber is then

$$P_{in}(t) = P(1 + m \cos \Omega t) + S(t) \qquad (2.1)$$

where P is the average optical power and S(t) is the spontaneous emission noise generated by the laser.

The magnitude and spectral characteristics of this noise are quite complicated and have been investigated by several authors (4, 5). Figure 4 (from Reference 5) illustrates the spectral properties of laser noise for various laser operating parameters. P_{n2} is defined as the laser operating current divided by the laser current threshold. The operating currents can be related to laser output power and plotted against the photon noise values. This has been done in Figure 5 which shows the low frequency (< 1 GHz) relative photon noise per 1 Hz bandwidth as a function of laser output power. Relative photon noise is defined as the ratio $< | N_p |^2 > /N_{PL}^2$ where $< | N_p | >$ is the average number of noise photons in a bandwidth of 1 Hz, and N_{PL} is the number of photons in the lasing mode. The mean source laser noise power (S^2) at a specified laser output power is now easily obtained by multiplying $< | N_p |^2 > /N_{PL}^2$ by the square of the laser output power.

Propagation through a fiber of length L subjects $P_{in}(t)$ to an attenuation factor of $10^{-L/10}$; hence, the optical output power is

$$P_{out}(t) = 10^{-L/10} P_{in}(t) \qquad (2.2)$$

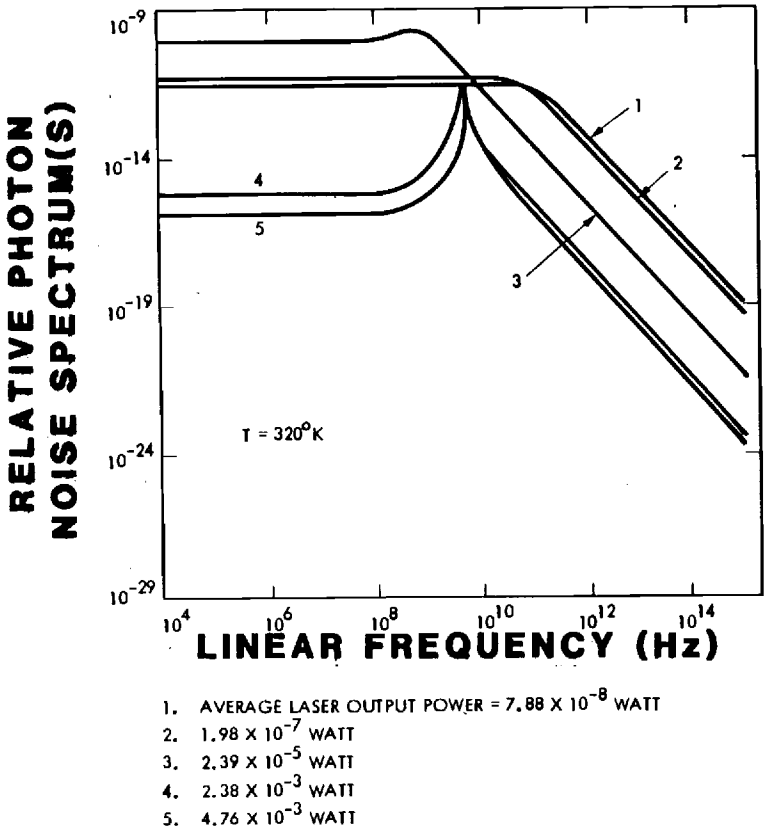

Figure 4. Relative photon noise spectrum.

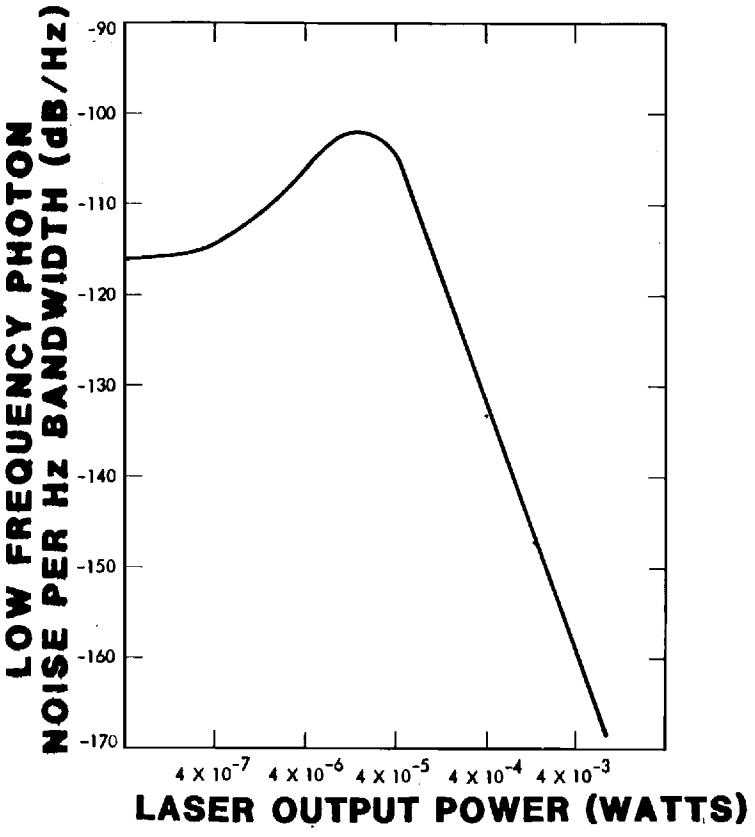

Figure 5. Low frequency (<1GHz) relative photon noise per 1 Hz bandwidth as a funciton of laser output power.

The current generated by the APD is proportional to the incident optical power (lumping splicing and insertion losses into the attenuation term) and is given by

$$i(t) = \lfloor (GPe\eta 2\pi)/(h\omega) \rfloor \quad P_{out}(t) \tag{2.3}$$

where G and η are the avalanche gain and the internal quantum efficiency of the APD, respectively, h is Planck's constant, ω is the optical frequency, and e is the electronic charge. Using Equation (2.2) we have

$$i(t) = \lfloor (GPe\eta 2\pi)/(h\omega) \rfloor (1 + m \cos \Omega t)\ 10^{-\alpha L/10}$$

$$+ \quad \lfloor (Ge\eta 2\pi)/(h\omega) \rfloor S(t)\ 10^{-\alpha\ L/10} \ . \tag{2.4}$$

The first term in Equation (2.4) represents the signal current. The second term is the laser noise current, which will be considered separately.

The total current i(t) is then passed through an amplifier which has bandwidth $\Delta\nu$ and current gain G_A. The power gain of the amplifier is G_A^2. The signal current at the amplifier output port can be rewritten to include the amplifier current gain G_A

$$i_S(t) = ((G_A G\ \ Pe\eta 2\pi)/(h\omega))\ (m \cos \Omega t)\ 10^{-\alpha L/10} \tag{2.5}$$

where the DC signal term $((GPe\eta 2\pi)/(h\omega))\ 10^{-\alpha L/10}$ in Equation (2.4) disappears because the amplifier is assumed to be AC coupled to the APD. The average electrical signal power is given by

$$\langle P_s \rangle = \langle i_s^2 \rangle R$$

where R represents the 50 ohm load, and $< i_s^2(t) >$ is defined by

$$< i_s^2 > = \frac{1}{T} \int_{-T/2}^{+T/2} i_S^2(t)\, dt$$

or

$$< i_s^2 > = 0.5 \left((G_A G P e \eta 2\pi m)/(h\omega)\right)^2 10^{-\alpha L/5} \qquad (2.6)$$

2.2.2 DERIVATION OF NOISE POWER

We will now consider four independent noise sources in the fiber link. These are: the dark current, laser noise, shot noise, and thermal noise.[6]

The shot noise current has a mean square value of[6]

$$\overline{i_N^2}_{\text{shot}} = 2e\bar{I}\Delta\nu \qquad (2.7)$$

where $\bar{I}$ is the average amplified current given by

$$\bar{I} = \lfloor (G_A G e \eta 2\pi)/(h\omega) \rfloor (P 10^{-\alpha L/10}) + G_A i_d \qquad (2.8)$$

and i_d is the dark current of the APD.

Combining Equations (2.7) and (2.8) yields the shot noise current generated in the APD by the optical DC bias term

$$i_{N_{SHOT}}^2 = 2e \left((G_A 2\pi G e \eta)/(h\omega)\right) (P\ 10^{-\alpha L/10})\Delta\nu \qquad (2.9)$$

The shot noise current due to the dark current has a mean square value

$$i_{N\ \text{dark current}}^2 = 2G_A e i_d \Delta\nu \qquad (2.10)$$

Background light entering the APD in a closed fiber optic system was assumed to be negligible.

The thermal noise current has a mean square value given by

$$i^2_{N_{thermal}} = G_A^2(4\ KTN_F/R_L)\Delta\nu \tag{2.11}$$

where N_F is the noise figure of the amplifier, R_L is the load resistance (50 Ω), k is the Boltzmann constant, and T is the equivalent absolute temperature of the system (including the noise temperature of the amplifier).

The laser noise S(t) is attenuated in passing through the fiber and generates a mean square noise current at the amplifier output equal to

$$i^2_{N_{laser}} = ((G_A Ge\eta 2\pi)/(h\omega))^2 < S^2 > \ 10^{-\alpha L/5}\ \Delta\nu, \tag{2.12}$$

which takes into account the amplifier power gain and bandwidth.

Thus, the total noise power is

$$\overline{i^2_N} = \overline{i^2_{N_{shot}}} + \overline{i^2_{N_{thermal}}} + \overline{i^2_{N_{laser}}} + \overline{i^2_{N_{dark\ current}}} =$$

$$2eG_A((Ge\eta 2\pi)/h\omega))\ (P10^{-\alpha\ L/10})\ \Delta\nu + 2eG_A i_d\Delta\nu + \tag{2.13}$$

$$G_A^2\ (4KTN_F/R_L)\ \Delta\nu + ((G_A Ge\eta\ 2\pi)/(h\omega))^2 < S >^2 10^{-\alpha L/5}\ \Delta\nu$$

The signal-to-noise ratio is

$$S/N = < i_S^2 > R/(\overline{i^2_N}\ R) = < i_S^2 > /\overline{i^2_N}$$

or

$$S/N = 0.5\ ((G_A GPe\eta m2\pi)/(h\omega))^2\ 10^{-\alpha L/5}\ )/\ \overline{i^2_N} \tag{2.14}$$

where $\overline{i_N^2}$ is given by Equation (2.13). Equation (2.14) is the SNR for a monomode fiber link with a CW signal.

But the actual desired SNR is obtained at the output of the mixer which follows the amplifier stage. A typical mixer multiplies the two inputs (i.e., f_1 and f_2) and generates an output at $f_1 - f_2$ and $f_1 + f_2$. Since in this case f_1 is equal to f_2 the output appears at DC and at $2f_1$ (or 2 f_2).

The $2f_1$ component is filtered out (see Section 3), whereas the energy of interest at DC is passed. Thus, the signal as well as the noise voltage from the fiber link is reduced by a factor of two (the power is decreased by a factor of four). In addition, the mixer generates its own thermal noise given by

$$\overline{i_{N_{\text{thermal-mixer}}}^2} = (4KTN_F/R_L)\Delta\nu \tag{2.15}$$

where N_F is the noise figure of the mixer. By incorporating the thermal noise term of the mixer and the reduction factor into Equation (2.14) the final desired expression for the SNR is

$$S/N = \frac{0.25(0.5)((G_A G P e \eta m 2\pi)/(h\omega))^2 10^{-\alpha L/5}))}{(i_N^2)\ 0.25 + i_{N_{\text{thermal-mixer}}}^2} \tag{2.16}$$

2.2.3 NUMERICAL ESTIMATIONS

In this section, the contributions of the four noise terms will be estimated.

Typical parameters for a silicon avalanche photodiode are: G = 100, η = 0.6, and i_d = 16 nA. The values of the constants are:

$h = 6.626 \times 10^{-34}$ J-sec, $e = 1.6021 \times 10^{-19}$ C,
$\omega = 2.216 \times 10^{+15}$ Hz, and

$k = 1.3805 \times 10^{-23}$ J/°C

Hence, $(Ge\eta 2\pi)/h\omega$ = 41.1 ampere per watt at the wavelength of GaAs laser diodes (850 nm).

The DC bias power, P, coupled from the laser diode into the optical fiber is approximately 3.0 mW. Hence, the shot noise contribution is

$$2e((G_A Ge\eta 2\pi)/(h\omega))P10^{-\alpha L/10} = 3.9X10^{-20} G_A 10^{-\alpha L/10}$$

The dark current contribution is

$$2ei_d G_A = 5.1 \times 10^{-27} G_A.$$

Assuming an ambient temperature of 300 K and a noise figure, N_F, of 6 dB, the thermal noise contribution of the amplifier is

$$G_A^2(4KTN_F/R_L) = 1.3 \times 10^{-21} G_A^2$$

and that of the mixer (N_F = 5 dB) is

$$4KTN_F/R_L = 1.047 \times 10^{-21}$$

The laser noise power is determined by specifying the average laser output power in Figure 5 and multiplying the square of that quantity by its corresponding relative photon noise ratio. Given an average optical output of 3.0 mW from the laser diode, the mean square laser noise power is approximately $< S^2 >$ = 7.2 X 10^{-21} watt^2 per Hz. The optical noise power launched into the fiber is about 33% of $< S^2 >$, or 2.4 x 10^{-21} watt^2 per Hz. Hence, the electrical mean square noise current at the amplifier output is

$$((G_A Ge\eta 2\pi)/(h\omega))^2 < S^2 > 10^{-\alpha L/5} =$$

$$4.1 \times 10^{-18} \; 10^{-\alpha L/5} \; G_A^2$$

The electrical signal contribution is

$$(0.25)(0.5)((Ge\eta 2\pi Pm))/(h\omega)^2 10^{-\alpha L/5}\ G_A^2 =$$

$$5.25 \times 10^{-5}\ m^2\ 10^{-\alpha L/5}\ \ G_A^2$$

Thus, the signal-to-noise ratio is

$$S/N = (Am^2\ 10^{-\alpha L/5}\ G_A^2\ )/\lfloor 0.25\ (BG_A\ 10^{-\alpha L/10}) + CG_A + G_A{}^2 D + G_A{}^2 E\ 10^{-\alpha L/5})\ \Delta\upsilon + F\Delta\upsilon \rfloor$$

where

$A = 5.25 \times 10^{-5}$	(signal)
$B = 3.9 \times 10^{-20}$	(shot noise)
$C = 5.1 \times 10^{-27}$	(dark current noise)
$D = 1.3 \times 10^{-21}$	(thermal noise, amplifier)
$E = 4.1 \times 10^{-18}$	(laser noise)
$F = 1.1 \times 10^{-21}$	(thermal noise, mixer)

Equation (2.17) is the principal result. The contributions of the various noises as a function of fiber length-attenuation product are shown in Figure 6. If the attenuation is 4 dB/km, then the x-axis will be scaled in km. Furthermore, for a fiber loss of 4 dB/km, laser noise dominates for $L < 4$ km, and the signal-to-noise ratio is approximately constant,

$$S/N \simeq (Am^2)/(0.25E\ \Delta\nu) = 5.1 \times 10^{13}/\Delta\nu \qquad (2.18)$$

where m, the modulation index, was chosen to be 1.

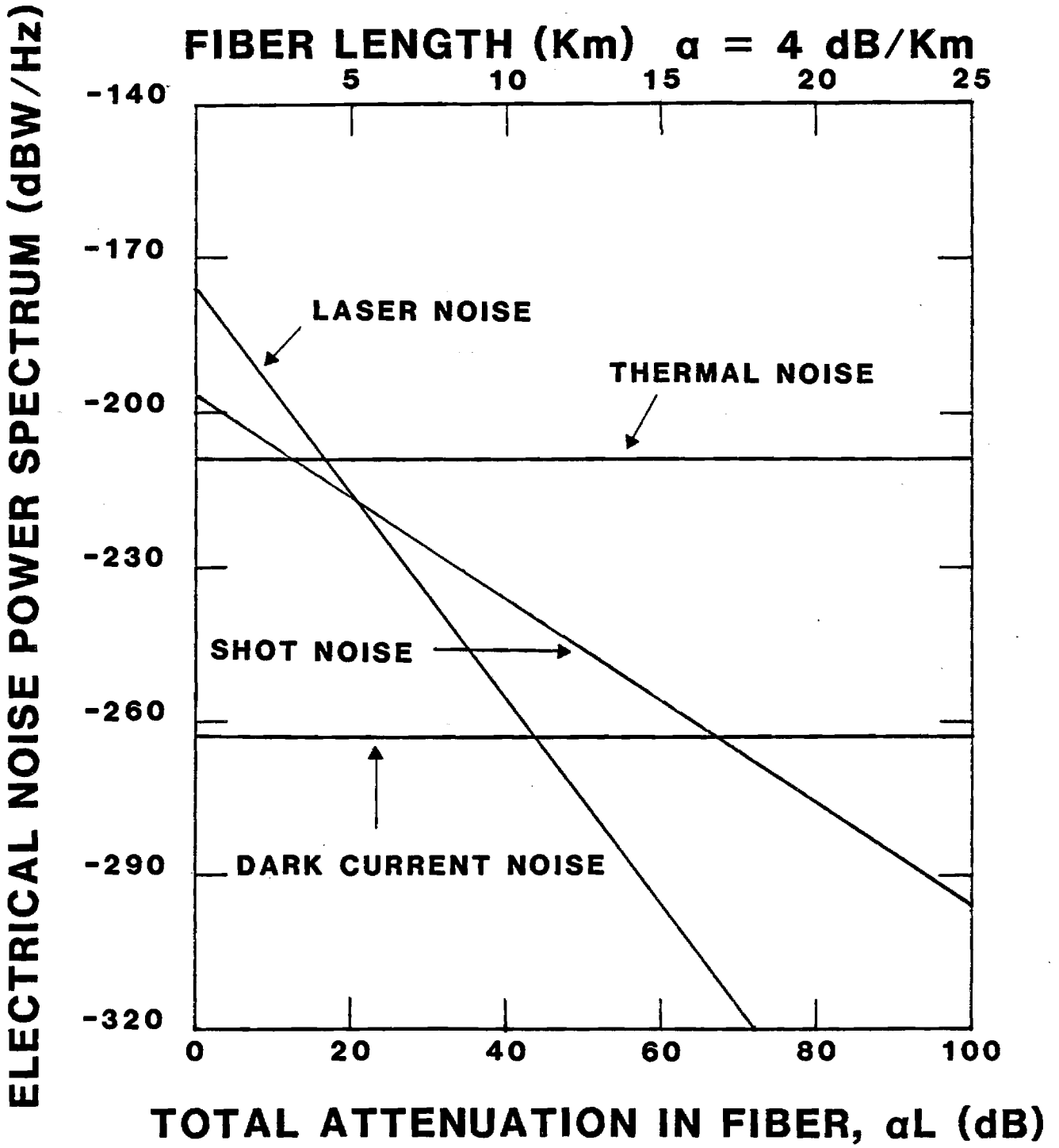

Figure 6. Noise power as a function of total attenuation in fiber. Amplifier gain, G_A is 1. System bandwidth $\Delta\upsilon$, is 1 Hz.

Beyond 4 km, the SNR is fiber length dependent, because the dominant noise in this region (i.e., thermal noise) is independent of αL, whereas the signal continues to decrease with αL.
Hence, the SNR is given by

$$S/N = (Am^2\ 10^{-\alpha L/5}\ G_A^{\ 2})/((0.25G_A^2\ D\Delta\nu) + F\Delta\nu)$$

Since $G_A^{\ 2} >> 1$, the term $F\Delta\nu$ is negligible and

$$S/N = (1.6 \times 10^{17}\ m^2\ 10^{-\alpha L/5})/\Delta\nu$$

The SNR for $\alpha L >$ 15 dB is linear with respect to αL as indicated in Figure 7.

2.3 DERIVATION OF SNR FOR A SYSTEM WITH MULTIMODE FIBER-CW SIGNAL-ILD

In previous calculations, it was assumed that the carrier signal falls within the transmission bandwidth of the optical fiber. The bandwidth-length product for single-mode fibers can be as high as 100 GHz-km (assuming a single mode laser source), while the bandwidth-length product for multimode fibers is commonly in the range of 1 GHz-km. Thus, a 1 GHz RF modulation signal lies comfortably within the bandwidth of a single mode 2 km fiber link, but not a 2 km multimode fiber link. This effect will now be included and its consequences will be examined.

The bandwidth-limiting factor in multimode fibers is intermodal dispersion. Multimode fibers support a large number (several hundred) of transverse optical modes due to their relatively large size. These transverse modes, each carrying a sinusoidal modulation, travel down the fiber at different group velocities. Hence, the received signal is a sum of sinusoids of different phases. The result is a lowering of the modulation depth as compared with that at the input where each mode carries modulation with the same phase (Apendix A).

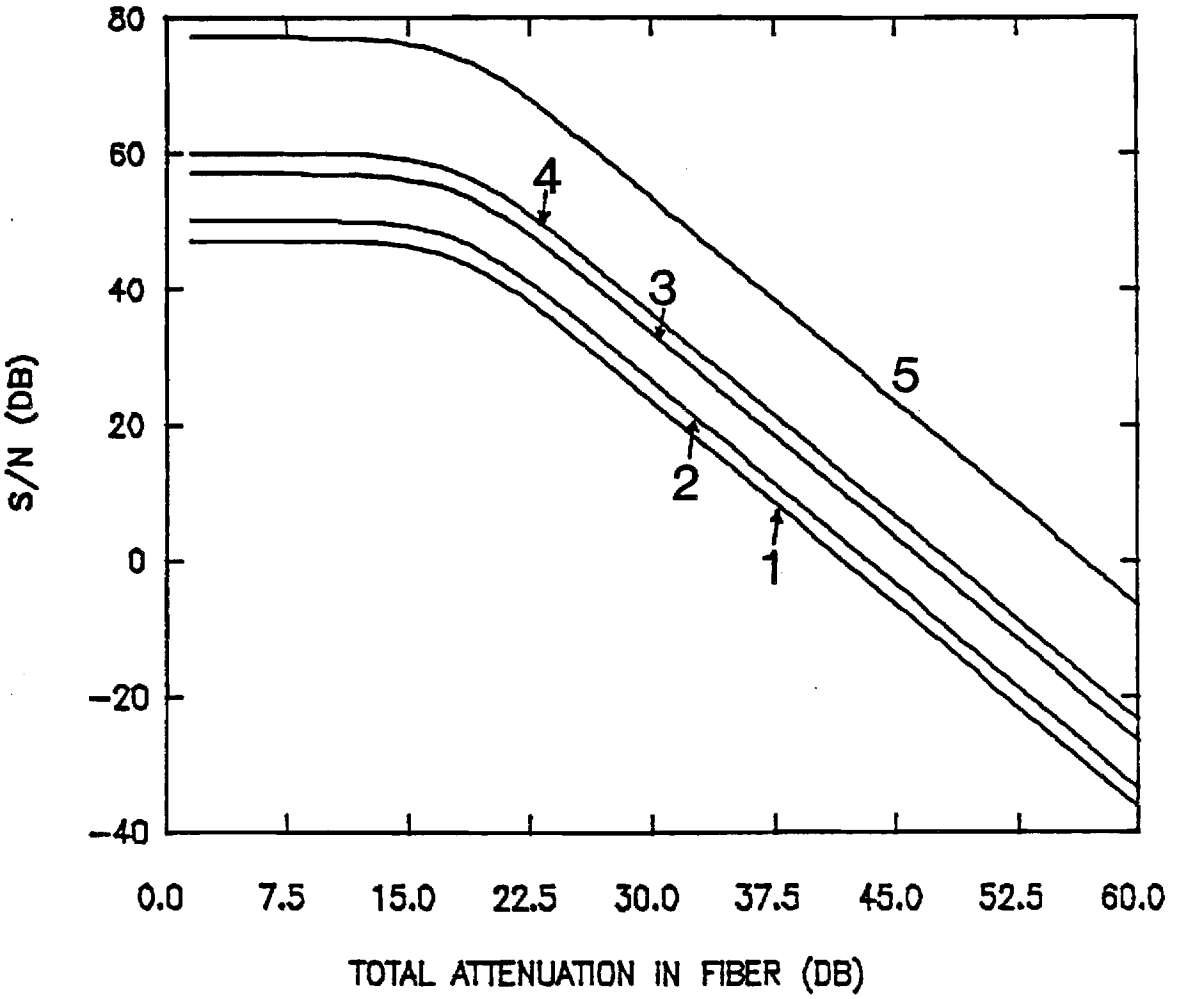

Figure 7. Signal-to-noise ratio as a function of total attenuation in a monomode fiber optic link for various system bandwidths. The bandwidth is: (1) 1 GHz, (2) 500 MHz, (3) 100 MHz, (4) 50 MHz, (5) 1 MHz.

The amount of intermodal dispersion in a multimode fiber is usually specified in time-spread/km. When an optical impulse is fed into the fiber, the output can be approximated by a Gaussian pulse with pulse-width increasing linearly with fiber length[7]. Thus, the impulse response of the fiber is

$$g(t) = (1/\ (\gamma L\sqrt{\pi}\ ))\ \exp(-t^2/(\gamma^2 L^2)) \tag{2.19}$$

where the intermodal dispersion constant (γ) is measured in ns/km, and L is the total length of the fiber in km. The factor $1/(\gamma L\sqrt{\pi})$ is a normalization constant required for power conservation.

The response of the fiber due to an arbitrary input is given by the convolution integral

$$P_{out}\ (\tau) = \int_{-\infty}^{\infty} P_{in}(t + \tau)g(t)dt \tag{2.20}$$

For a purely sinusoidal input with modulation depth m,

$$P_{in}(t) = P(1 + m \cos\ \Omega\ t),$$

the output is

$$P_{out}\ (t) = P\ (1 + m \exp\ (-\gamma L\Omega/2)^2 \cos\ \Omega t), \tag{2.21}$$

where t was substituted for the variable τ . Hence, the modulation depth is reduced to an effective value

$$m' = m \exp\ (-\gamma L\Omega/2)^2 \tag{2.22}$$

Details of this calculation are described in Appendix B.

According to Equation (2.17), the signal-to-noise ratio is proportional to m^2. It follows that the SNR decreases as $\exp\ (-\gamma^2 L^2 \Omega^2/2)$. This effect was included in Figure 8 for two modulation frequencies. The effect is a sharp reduction in SNR once the modulation frequency falls outside the fiber

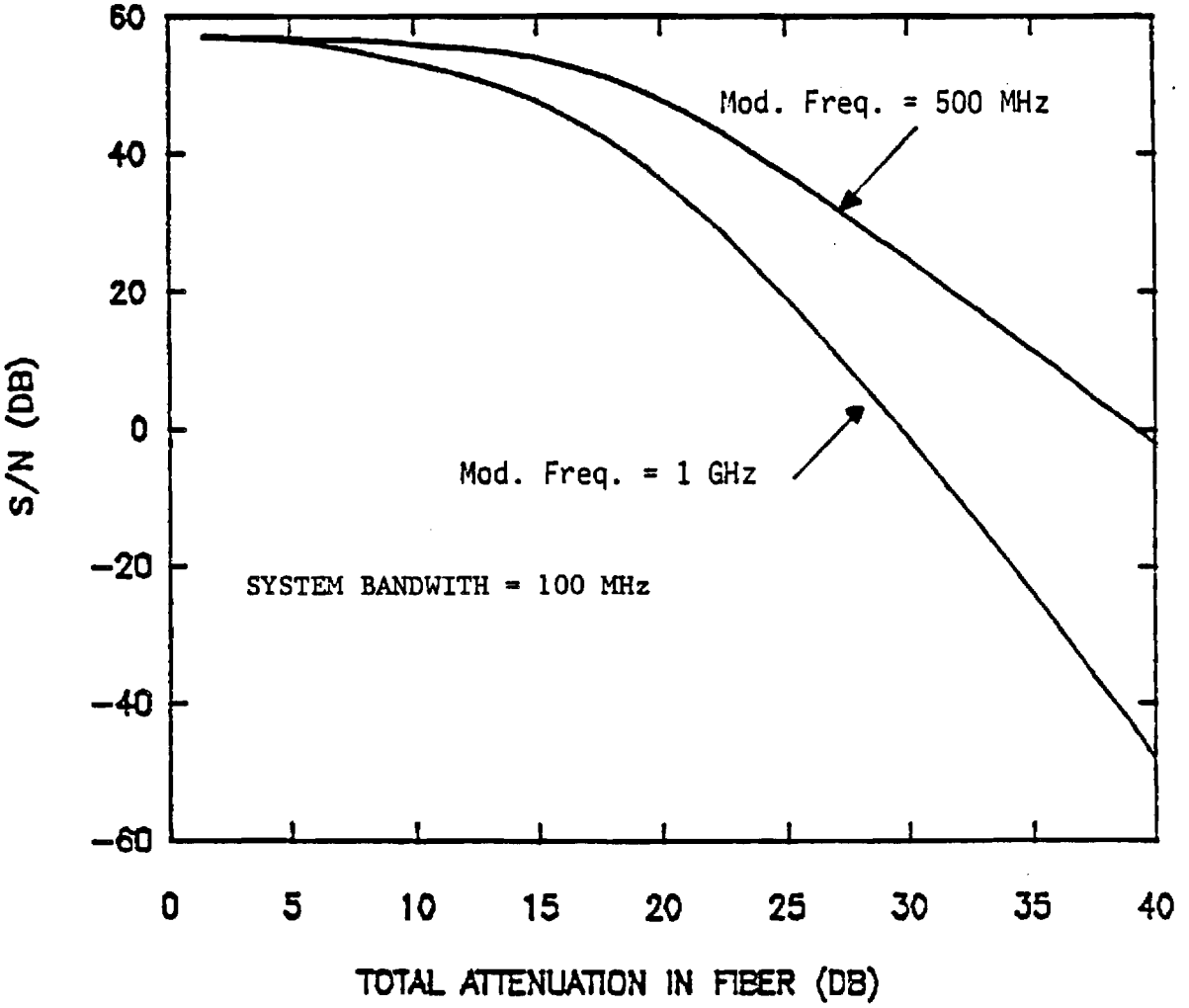

Figure 8. Signal-to-noise ratio versus total attenuation in a multimode fiber optic link.

bandwidth. As long as this is not the case, the difference between single mode and multimode fibers is minimal. For a 100 m multimode fiber, this requirement is satisfied if the modulation frequency is equal to or less than 1 GHz.

2.4 SNR CALCULATIONS OF A SYSTEM WITH MULTIMODE FIBER - PULSED SIGNAL - ILD

This section describes the interaction of a pulsed optical signal with the response function of a multimode fiber as a function of fiber length and pulse width of the input signal. Details of the calculations are given in Appendix C.

In previous sections the RF input signal was assumed to be a continuous sinusoidal signal of frequency Ω with a fixed modulation index m, i.e.,

$$P_{in}(t) = P(1 + m \cos \Omega t)$$

In this section, the RF signal is not continuous, but assumes a pulse shape with a Gaussian envelope. The optical signal power launched into the multimode fiber is given by

$$P_{in}(t) = P(1 + m\, e^{\beta t^2} \cos \Omega t) \tag{2.23}$$

where β is related to the standard deviation of the input pulse. The output power is given by the convolution of $P_{in}(t)$ with the impulse response function of the fiber (Equation (2.19)). Hence P_{out} can be written as

$$P_{out}(\tau) = (P/(\gamma L\sqrt{\pi}) \int_{-\infty}^{\infty} [1 + m \exp(\beta(t - \tau)^2)$$

$$\cos \Omega (t - \tau)] \exp(-t^2/(\gamma^2 L^2)) dt \tag{2.24}$$

The solution to the integral is

$$P_{out}(t) = P(1 + m' e^{-\beta' t^2} \cos \Omega' t) \tag{2.25}$$

where

$$m' = m \exp\left((-\Omega^2 \gamma^2 L^2)/(4\gamma^2 L^2 \beta + 4) \sqrt{\beta\gamma^2 L^2 + 1}\right.$$

$$\Omega' = \Omega/(\beta\gamma^2 L^2 + 1)$$

$$\beta' = \beta/(\beta\gamma^2 L^2 + 1)$$

and t was replaced by τ .

Note that if $\beta\gamma^2 L^2 \ll 1$, Equation (2.25) reduces to Equation (2.23).

We will now address the magnitude of the term $\beta\gamma^2 L^2$. For a multimode fiber, at γ is equal to 0.2×10^{-9} s/km at 850 nm, and β is related to the standard deviation of the pulse according to Equation (2.26).

$$\beta = 1/2\sigma^2 \tag{2.26}$$

Assuming a minimum 10 nanosecond pulse width, i.e., $3\sigma = 10^{-8}$ s, we obtain $\sigma = 0.3 \times 10^{-8}$s and $\beta = 5.6 \times 10^{16} s^{-2}$

If L is $\leq$ 100 m, then

$$\beta\gamma^2 L^2 = 2.2 \times 10^{-5}$$

which is small compared to 1.0. Thus, β' becomes β in Equation (2.25) under these conditions.

2.5 MAXIMUM MEASURED SNR IN A MULTIMODE SYSTEM WITH CW SIGNAL AND ILD

The maximum SNR of the multimode fiber delay line is defined as the ratio of maximum to minimum detectable output power. The minimum detectable power for short fibers is obtained when the signal power is equal to the average laser noise power. Thus, the calculated maximum SNR is

$$SNR_C = \langle i_S^2 \rangle / \langle N^2_{LASER} \rangle \tag{2.27}$$

where $\langle i_S^2 \rangle$ is the maximum signal power. This calculated value is the maximum SNR at $\alpha L \leq 15$ dB which is 57 dB for a 100 MHz system bandwidth.

The measured maximum SNR can be derived from Figure 9 which shows the system's gain linearity. The B curve amplifier was limited to 500 MHz bandwidth. The A curve amplifier exceeded one gigahertz in bandwidth and had a smaller gain than the B amplifier. V_o is the output voltage and V_i is the input voltage. The range on the B curve extends from a minimum observable V_o of 0.0053 to a maximum V_o of 4.0 volts. The measured value is

$$SNR_M = 20 \log (V_{o\ MAX}/V_{o\ MIN})$$

$$SNR_M = 57 \text{ dB}$$

which is in good agreement with the calculated value.

2.6 DERIVATION OF SNR FOR A SYSTEM WITH AN LED SOURCE

A coherent optical source, such as an ILD, is not a requirement for proper operation of the RF interferometer since the output intensity of the source only acts as a carrier for the RF CW signal. Other sources, such as light emitting diodes (LEDs), are less expensive and more reliable. However, the highest modulation frequency for LEDs is about 250 MHz. In contrast, commercially available laser diodes can be modulated up to 6 GHz. Since the operating RF frequency is one parameter that controls system sensitivity, the choice between an LED or ILD is a function of economical considerations and maximum required

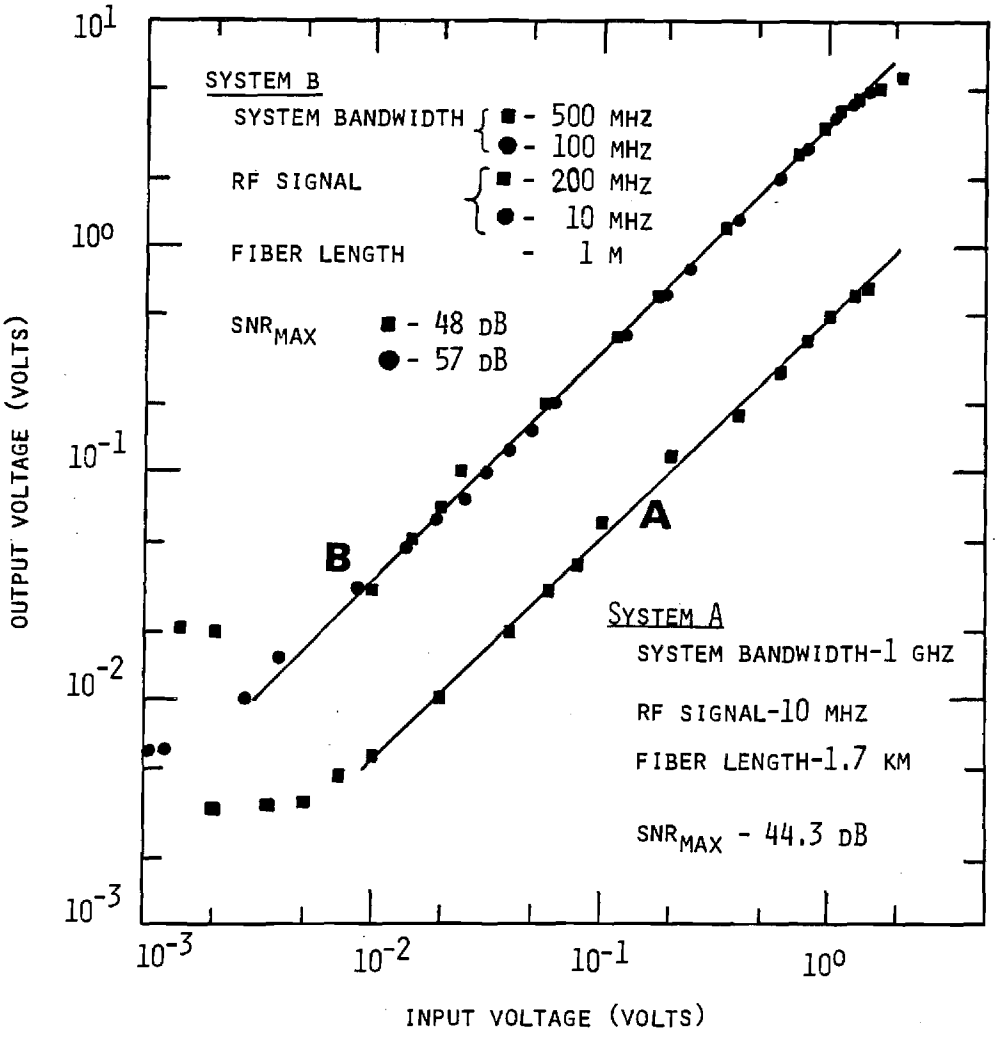

Figure 9. Peak to peak output voltage of multimode fiber optic transmission link versus peak to peak input voltage. System A had a lower gain than System B.

system sensitivity. This section will explore the LED's impact on the signal-to-noise ratio of the system.

Experimental evidence at Georgia Tech and at other institutions has shown that the dominant noise in an LED fiber link originates in the receiver circuitry (shot noise, thermal noise), not the LED. To include this fact in our analysis, we eliminated the optical source noise term, i.e., E was set to zero in Equation (2.17) and the source output power, P, was reduced to a value of 2.5 μW, which is typical for LEDs having wide bandwidth and long lifetimes. Figure 10 shows the SNR in dB for an LED system as a function of total attenuation. The plot is fiber length dependent and linear with respect to fiber attenuation, αL, since the thermal noise, a constant, is the dominant noise source. The length dependence is due to signal attenuation in the fiber. The values for C, D, and F in Equation 2.17 have not changed. E was set to zero. B was changed to 3.29×10^{-23} and A was changed to 1.32×10^{-9} because of the reduced LED output power (2.5×10^{-6} W). Thus, the SNR is given by

$$S/N = \frac{1.02 \times 10^{12}}{\Delta\nu} 10^{-\alpha L/5} \qquad (2.28)$$

Once again, m, the modulation index, was chosen to be 1. If $\Delta\nu$ is 1 MHz and L = 0, then the SNR is 1.02×10^{6} or 60 dB, as shown in Figure 10.

In the case of the strain sensor, an additional noise term, namely the thermal noise generated in the mixer, was taken into account. Furthermore, reduction in signal level by 3 dB due to the mixing action was also incorporated into the computer program. The net effect was to decrease the SNR by 6 dB.

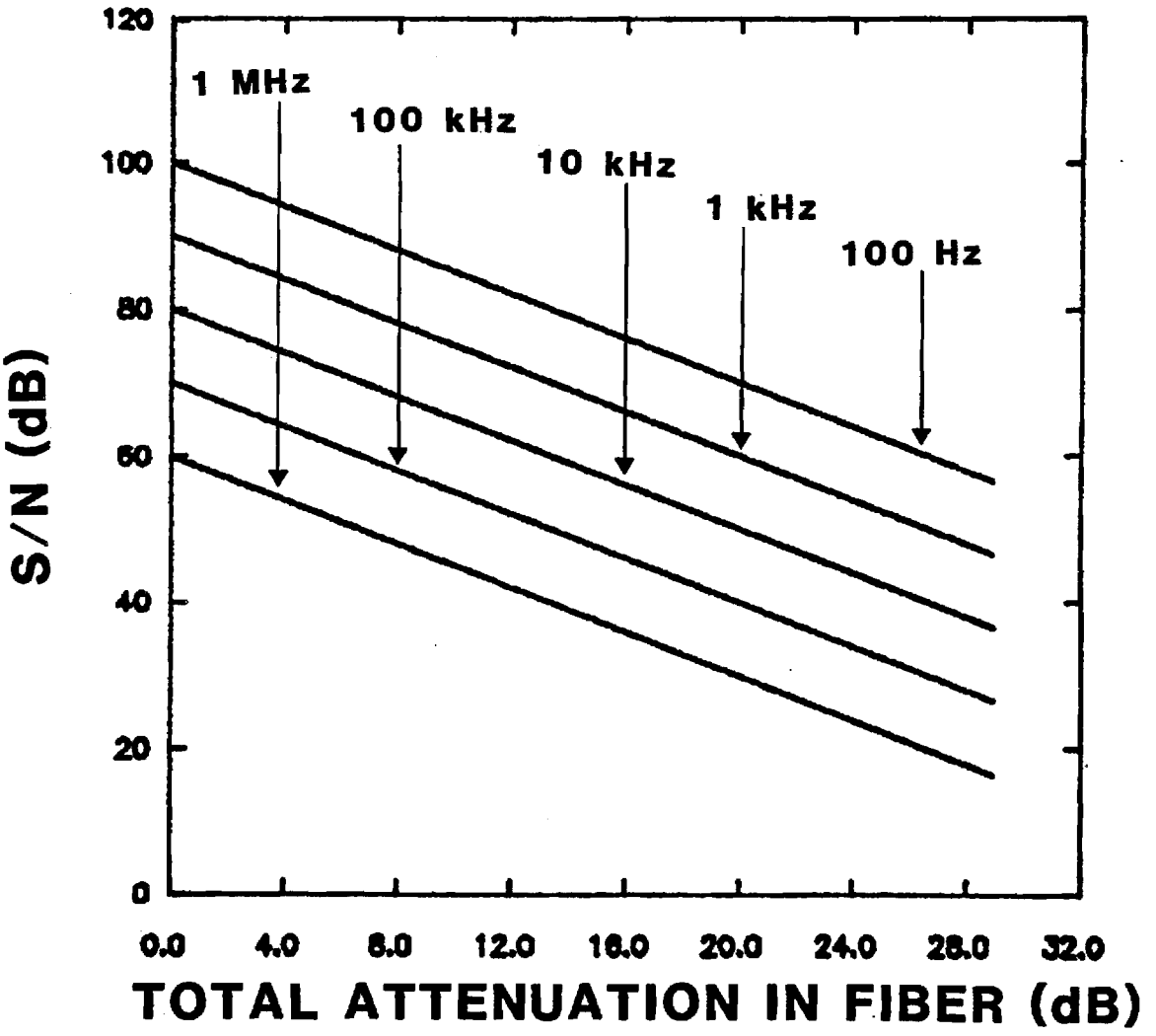

Figure 10. Signal-to-noise ratio as a function of total attenuation in a multimode fiber link for various system bandwidths. The optical source is an LED. The RF frequency was set at 100 MHz.

SECTION 3
SENSITIVITY ANALYSIS

3.1 MIXER TRANSFER FUNCTIONS

The general signal at the output of the strain sensor can be described by a single vector S where

$$S = A^2 e^{i\phi} \tag{3.1}$$

A^2 is the intensity of the signal, and ϕ is the absolute phase difference between the reference and the sensor signal. S can be separated into its vector components as

$$S = A^2 (\cos\phi + i \sin\phi), \tag{3.2}$$

where $A^2\cos\phi$ is referred to as the real, or in-phase (I), component and $A^2\sin\phi$ is known as the imaginary or quadrature (Q), component. The two components can be measured with I and Q mixers as shown in Figure 11.

The sensor signal input to the I mixer is $A_S\cos(\omega t - \phi)$ and the reference input signal is $A_R\cos\omega t$. ω is the oscillator frequency, A_S and A_R are the sensing and reference signal amplitudes, respectively, and ϕ is defined as before. The mixer multiplies the two signals together such that the product is

$$I = A_R\cos\omega t \cdot A_S\cos(\omega t - \phi) \tag{3.3}$$

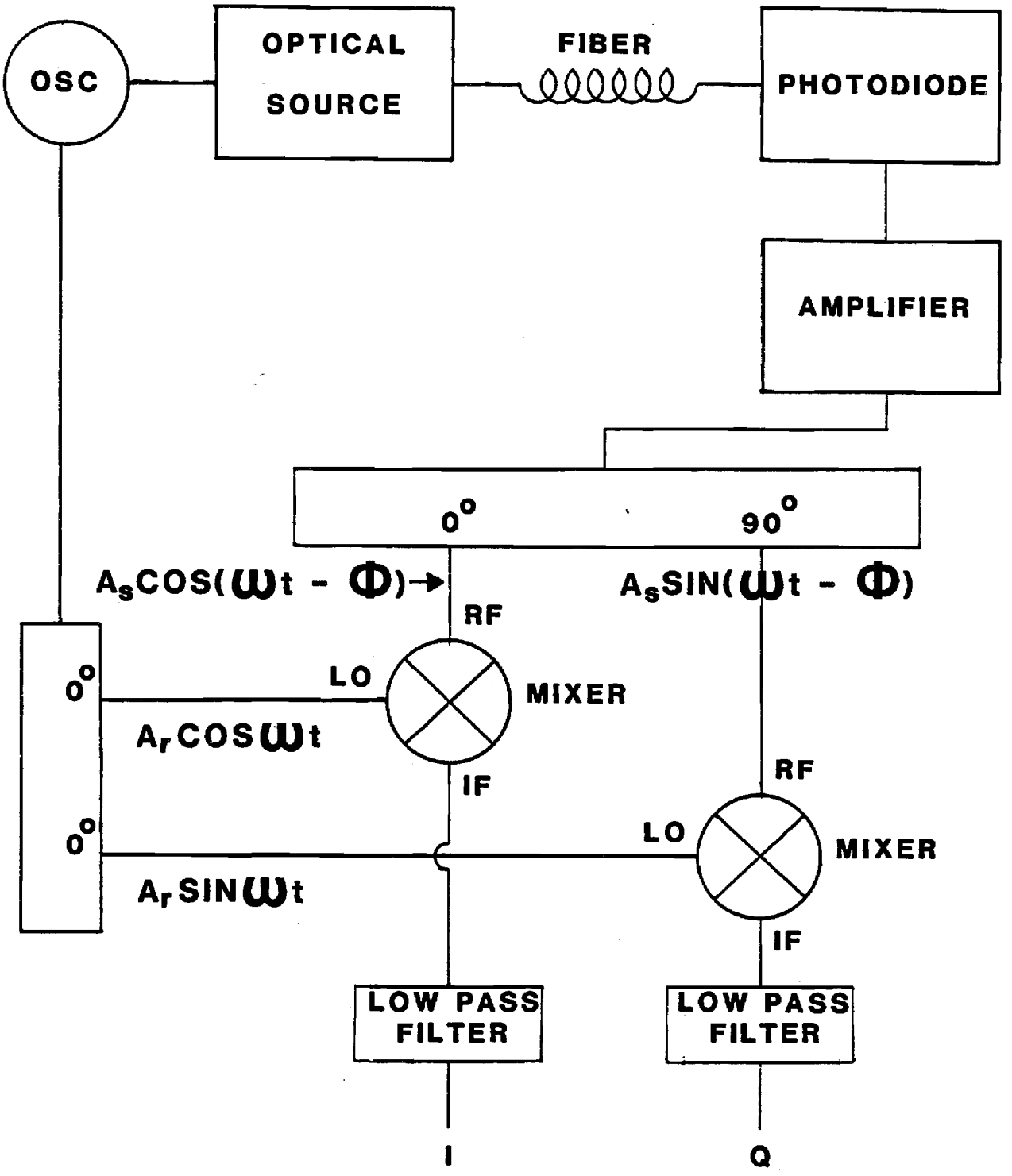

Figure 11. Block diagram of a practical fiber optic RF sensor.

Trigonometric expansion yields

$$I = A_R \cos\omega t \ (A_S \cos\omega t \cos\phi + A_S \sin\omega t \sin\phi)$$

or

$$I = A_R A_S \ (\cos^2\omega t \cos\phi + \cos\omega t \sin\omega t \sin\phi),$$

but $\cos^2\omega t = (1 + \cos 2\omega t)/2$,

and $\cos\omega t \sin\omega t = (\sin 2\omega t)/2$.

Substituting for $\cos^2\omega t$ and $\cos\omega t \sin\omega t$, we obtain

$$I = A_R A_S \left(\frac{\cos\phi}{2} + \frac{\cos 2\omega t \cos\phi}{2} + \frac{1}{2} \sin 2\omega t \sin\phi \right).$$

The terms containing $\cos 2\omega t$ and $\sin 2\omega t$ can be removed by routing the mixer output through a low pass filter.
Then

$$I = (A_R A_S \cos\phi)/2. \qquad (3.4)$$

Similarly, the output of the Q mixer is given by

$$Q = A_S \cos\omega t \cdot A_X \cos(\omega t - \phi + \pi/2) \qquad (3.5)$$

but

$$\cos(\omega t - \phi + \pi/2) = -\sin(\omega t - \phi)$$

Therefore

$$Q = A_R \cos\omega t \cdot A_S \sin(\omega t - \phi).$$

Expanding $\sin(\omega t - \phi)$, we obtain

$$Q = -A_R A_S \cos\omega t \, (\sin\omega t \cos\phi - \cos\omega t \sin\phi)$$

or

$$Q = -A_R A_S \, (\cos\omega t \sin\omega t \cos\phi - \cos^2\omega t \sin\phi),$$

and using the above relationships for $\cos^2\omega t$ and $\cos\omega t \sin\omega t$ we obtain

$$Q = -A_R A_S \left(\frac{\sin 2\omega t}{2} \cos\phi - \frac{\sin\phi}{2} - \frac{\cos 2\omega t}{2} \sin\phi\right).$$

Again, a low pass filter will remove all terms containing $2\omega t$.
Then

$$Q = (A_R A_S \sin\phi)/2. \tag{3.6}$$

The relationship of the I and Q components is shown in Figure 12. In practice, at any instant in time, I and Q are fluctuating quantities due to noise contamination. This noise is added to I and Q as ΔI and ΔQ to form the noise vector S_N as shown in Figure 13. The vectorial addition of S_N and S generates a new vector R and an uncertainty in ϕ, which is $\Delta\phi$. Figure 13 clearly shows that the value of $\Delta\phi$ depends only on the relative magnitudes of S_N and S (i.e., SNR) and the orientation of S_N; it does not depend on the orientation of S itself. In the following sections, the dependence of $\Delta\phi$ on SNR and the orientation of S_N will be explored, and a mathematical expression relating $\Delta\phi$ to SNR will be derived.

3.2 MINIMUM OBSERVABLE PHASE SHIFT

The phase shift due to noise (see Figure 13) at an arbitrary phase ϕ is

$$\tan(\phi + \Delta\phi) = Q/I = \frac{Q_o + \Delta Q}{I_o + \Delta I}. \tag{3.7}$$

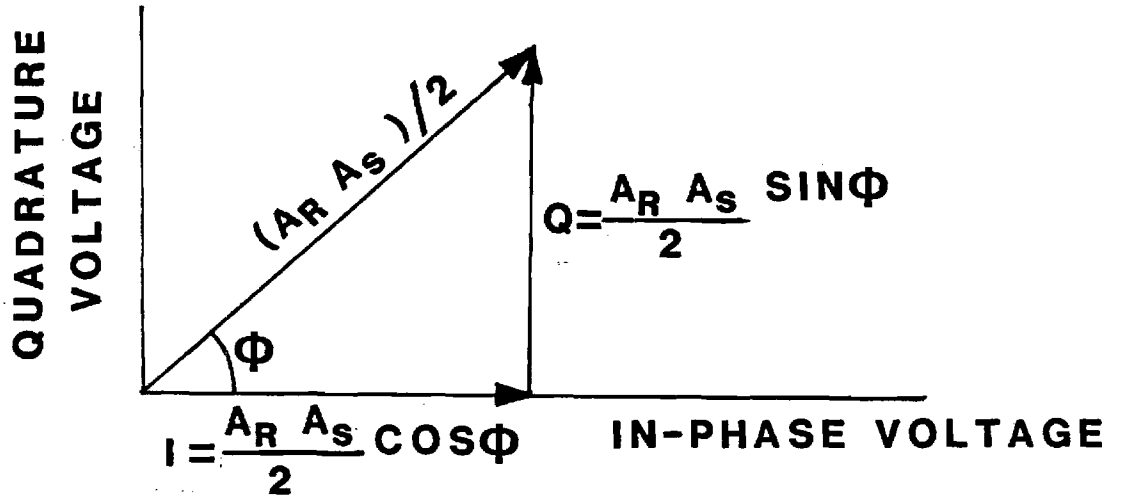

Figure 12. Relationship between I and Q components.

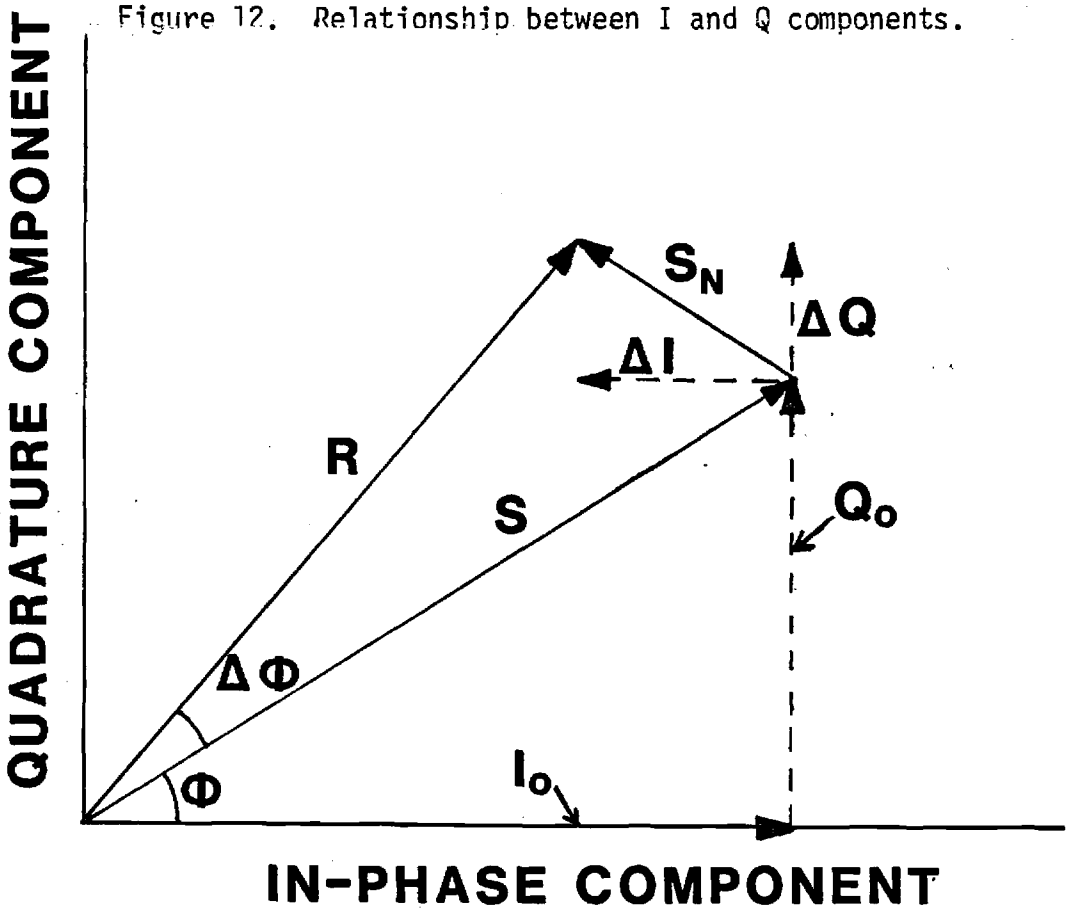

Figure 13. Relationship between the quantities S, S_N, R, and $\Delta\phi$.

Solving for $\Delta\phi$ we obtain

$$\Delta\phi = \arctan\left(\frac{Q_o + \Delta Q}{I_o + \Delta I}\right) - \arctan\left(\frac{Q_o}{I_o}\right)$$

Without loss of generality, this expression can be simplified by setting $\phi = 0$ (since, from Figure 13, $\Delta\phi$ does not depend on ϕ) which sets $Q_o = 0$ and $\arctan(Q_o/I_o) = 0$.

Then

$$\Delta\phi = \arctan\left(\frac{\Delta Q}{I_o + \Delta I}\right) \tag{3.8}$$

or

$$\Delta\phi = \arctan\left(\frac{\Delta Q/\Delta I}{I_o/\Delta I + 1}\right) \tag{3.9}$$

Figure 14 shows the $Q_o = 0$ situation. Represented are the component I_o, the noise vector S_N with an instantaneous magnitude $A_R A_n/2$ and instantaneous phase value ϕ_n, and the phase uncertainty $\Delta\phi$. Since ϕ can assume any value with equal probablity, its value was chosen to maximize $\Delta\phi$. This situation occurs only if the vectors R and S_N form a right angle. The following relationships are obtained from Figure 14.

$$\Delta Q/\Delta I = -\tan\phi \tag{3.10}$$

$$I_o/\Delta I = \frac{-(A_R A_S \cos\phi)}{2} \Big/ \frac{(A_R A_N \cos\phi_n)}{2}$$

or

$$I_o/\Delta I = \frac{A_R A_S}{2} \Big/ \left(\frac{A_R A_N}{2} \cos\phi_n\right). \tag{3.11}$$

Substitution of Equations (3.10) and (3.11) into Equation (3.9) yields

$$\Delta\phi = \arctan\left\{\frac{\tan\phi_n}{\left[\left(\frac{A_R A_S}{2}\right)/\left(\left(\frac{A_R A_N}{2}\right)\cos\phi_n\right)\right] - 1}\right\}. \tag{3.12}$$

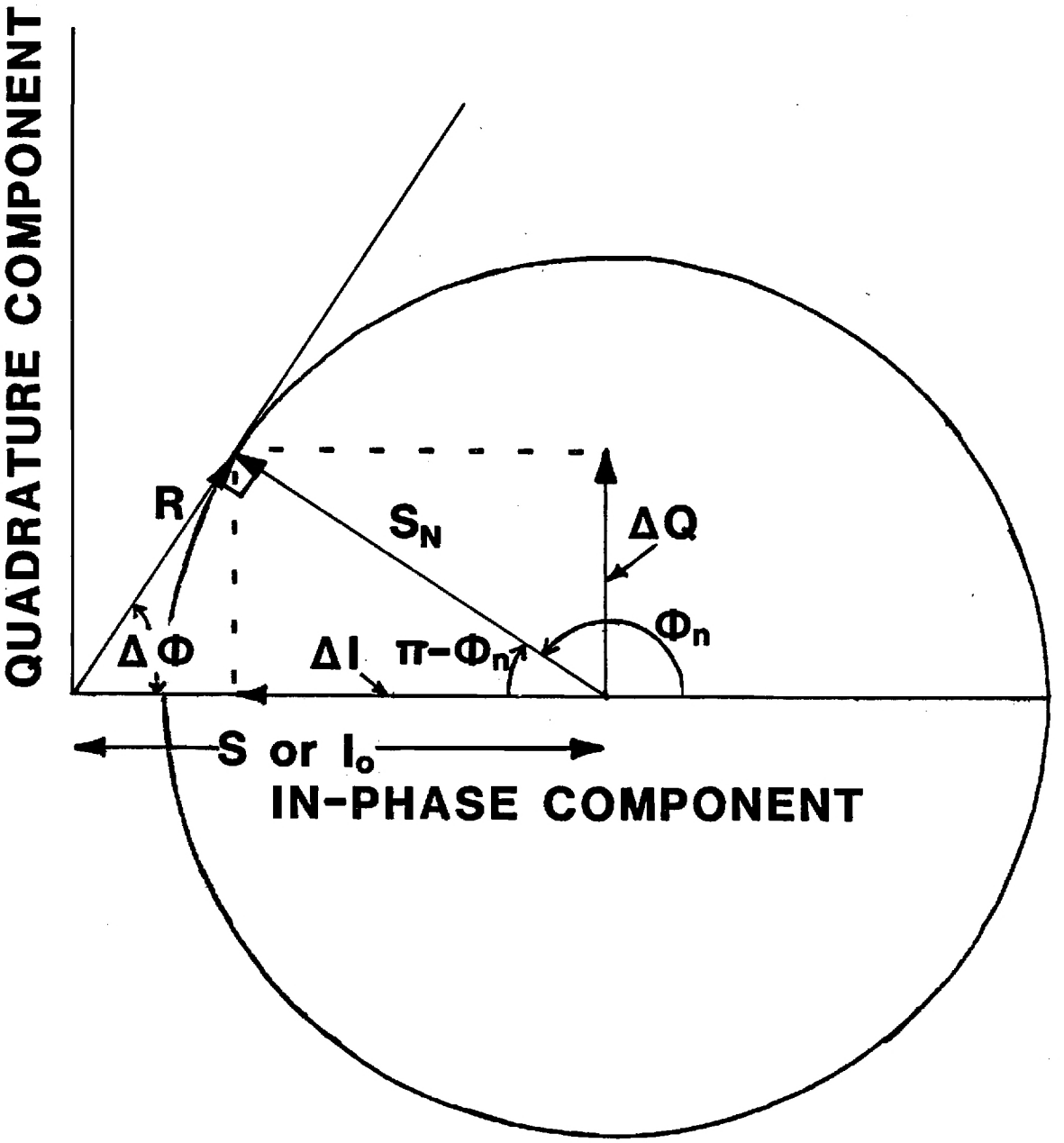

Figure 14. Relationship between observable phase shift due to noise, $\Delta\Phi$, and phase noise vector, S_N.

ϕ_n is determined by setting

$$\cos(\pi - \phi_n) = \frac{A_R A_N}{2} / I_o = \left(\frac{A_R A_N}{2}\right) / \left(\frac{A_R A_S}{2} \cos\phi\right),$$

but $\phi = 0$, so $\cos \phi = 1$,

and $\cos(\pi - \phi_n) = \cos\phi_n$.

Thus

$$\cos\phi_n = - \frac{A_R A_N}{2} / \frac{A_R A_S}{2} = -A_N/A_S, \tag{3.13}$$

and

$$\tan \phi_n = \tan(\arccos(- A_N/A_S)), \tag{3.14}$$

The substitution of $\tan \phi_n$ and $\cos \phi_n$ into Equation (3.12) yields

$$\Delta\phi = \arctan\left\{\frac{\tan (\arccos(-A_N/A_S))}{- (A_S^2/A_N^2) - 1}\right\} . \tag{3.15}$$

Note that $A_R/2$ does not appear in Equation (3.15). This fact merely confirms that $A_R/2$ is a scaling factor that is applied to both the signal and the noise level; therefore, it does not affect $\Delta\phi$. $A_R/2$ is henceforth set equal to 1 to simplify the mathematics. Hence, the magnitude of the noise vector is given by A_N. To arrive at the desired expression that relates $\Delta\phi_{min}$ to SNR the ratio A_S/A_N must be converted to a signal-to-noise ratio, and $\Delta\phi$ must be related to the minimum observable phase shift $\Delta\phi_{min}$.

Consider Figure 15, which shows two signal vectors S and S' and two noise vectors S_N and S'_N. In general, S_N and S'_N can assume any orientation ϕ_n, and their magnitudes are random variables each having a Gaussian probability density function with a non-zero mean μ and a standard deviation σ. Thus, the tips of the resultant vector R and R' are distributed inside two rotationally

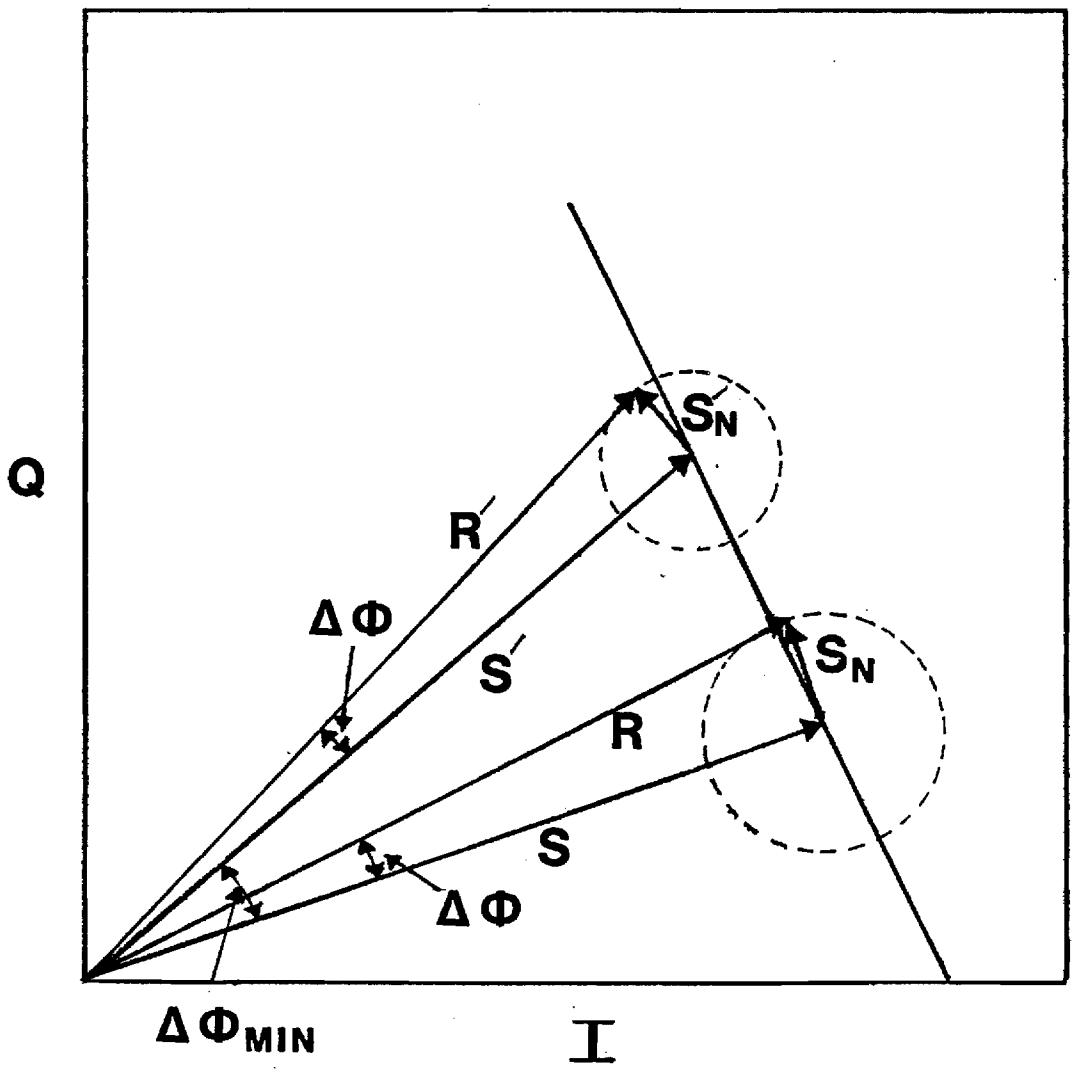

Figure 15. Relationship between minimum observable phase shift, $\Delta\phi_{MIN}$, and phase shift due to noise, $\Delta\phi$

symmetric, two-dimensional, Gaussian probability density functions having two different means μ and μ', but they will have the same standard deviation σ if the I and Q channels are assumed to be balanced with respect to maximum output voltage. The line L connecting the vectors S and S' represents a one-dimensional cut through the two-dimensional Gaussian distributions, as shown in Figure 16. The horizontal axis denotes distance along L. Each distribution in Figure 16 consists of noise vectors that are aligned with L but have magnitudes A_N that vary according to a Gaussian function. Now, the minimum observable phase shift ϕ_{min} is defined as a change in phase between S and S' such that the separation between the two Gaussians in Figure 16 yields a probability of true phase detection (PD) of nearly 1.0 and a probability of false phase detection due to noise (probability of false alarm, PFA) of 10^{-6}. With these imposed conditions, the separation between the means of the Gaussian probability functions was found to be 9.4 σ in Appendix D. The discrimination threshold was placed at the intersection of the two Gaussians, which is its optimal position.

According to Figure 15, $\Delta\phi$ can be determined mathematically via Equation (3.16),

$$\Delta\phi_{min} = \Delta\phi\Big|_{A_N = 9.4\sigma} \tag{3.16}$$

where $\Delta\phi$ is evaluated by setting A_N equal to 9.4 σ. In other words, the minimum observable phase shift can be determined if the length of line L joining S and S' is replaced by a noise vector with amplitude A_N equal to 9.4σ.

We will now show that σ is related to the RMS noise amplitude. Consider, for example, a sample distribution of A_N. An approximation of the standard deviation of that distribution is given [8] by

$$\sigma = \sqrt{\frac{\sum_i (X_i - \mu)^2}{n - 1}} \tag{3.17}$$

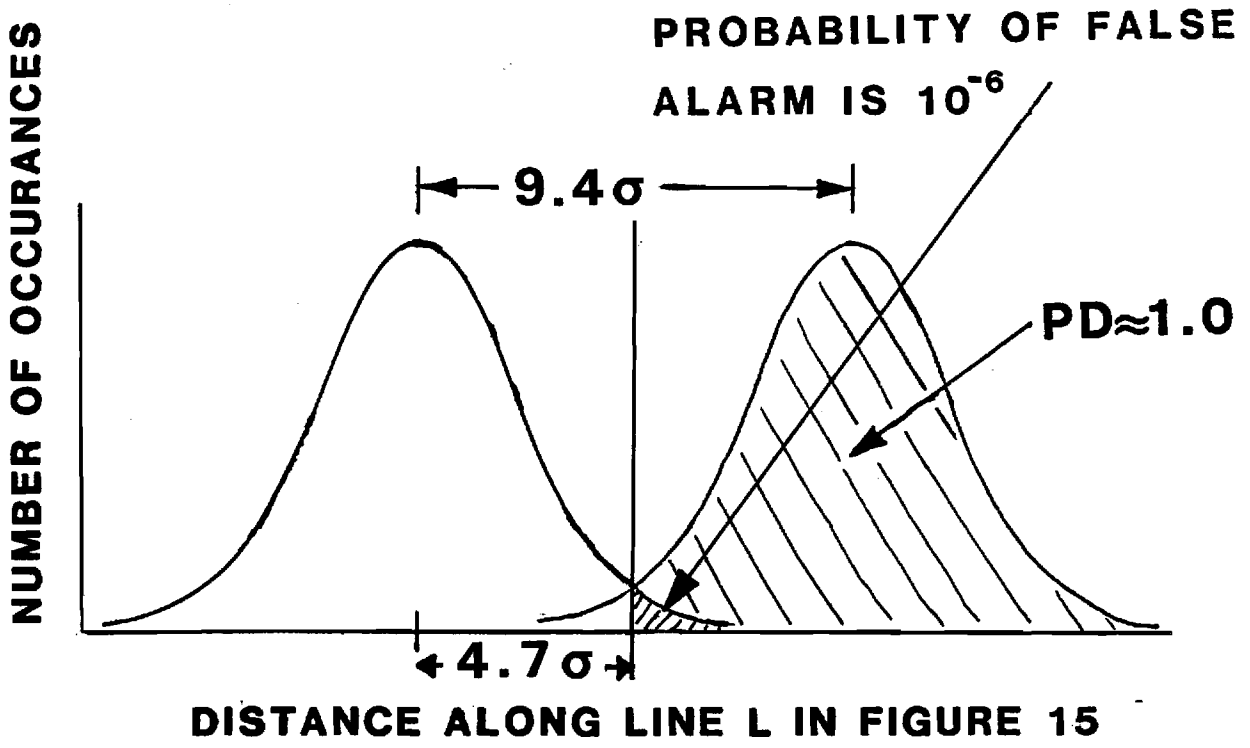

Figure 16. Definition of probability of detecting a false phase shift or false alarm (PFA) and probability of detecting a true phase shift (PD).

where the X_i's are the sampled A_N ($A_{N_i} = \sqrt{\Delta I_i^2 + \Delta Q_i^2}$), μ is the mean, and n is the number of samples. For large n (n>100), Equation (3.17) reduces to

$$\sigma = \sqrt{\sum_i \frac{(X_i^2 - \mu)}{n}}$$

which is identical to the definition of the root mean square amplitude, A_{RMS}. The ratio A_S/A_N can now be written as

$$A_S/A_N = A_S/9.4\sigma = A_S/(9.4\ A_{N-RMS}) \tag{3.19}$$

where A_{N-RMS} is the RMS noise amplitude and A_S is the peak signal amplitude. A_S/A_N can be written in terms of the SNR by converting A_S to an RMS value as follows

$$A_{S-RMS} = \frac{A_S}{\sqrt{2}} \tag{3.20}$$

Substituting Equation (3.20) into Equation (3.19), we obtain

$$A_S/A_N = \frac{\sqrt{2}\ A_{S-RMS}}{9.4\ A_{N-RMS}}$$

But A_{S-RMS}/A_{N-RMS} is defined as the square root of the signal-to-noise ratio (SNR). Therefore, A_S/A_N can be rewritten as

$$A_S/A_N = \frac{\sqrt{2}}{9.4}\sqrt{SNR} = 0.15045\ \sqrt{SNR} \tag{3.21}$$

Equation (3.21) is substituted into Equation (3.15) to obtain the desired expression for $\Delta\phi_{min}$.

$$\Delta\phi_{min} = \arctan \left[\frac{\tan\left(\arccos\left(-6.6468/\sqrt{SNR}\right)\right)}{-0.02263\ SNR - 1}\right] \tag{3.22}$$

3.3 MINIMUM OBSERVABLE STRAIN SENSITIVITY

Butter and Hocker[3] reported for their experiment a phase shift $\Delta\phi$ per unit strain per unit fiber length as

$$\frac{\Delta\phi}{\varepsilon L} = 1.2 \times 10^{7} \text{ rad/m.} \tag{3.23}$$

Their measurements were taken at an optical wavelength of

$$\lambda_{op} = 0.63 \times 10^{-6} \text{ m .}$$

Interpolation to wavelengths other than 0.63×10^{-6} m yields the expression

$$\frac{\Delta\phi}{\varepsilon L} = 1.2 \times 10^{7} \ \frac{\lambda_{op}}{\lambda_{RF}}$$

or

$$\frac{\Delta\phi}{\varepsilon L} = 1.2 \times 10^{7} \ \left(\frac{\lambda_{op}}{c}\right) F \tag{3.24}$$

where F is the system operating frequency and c is the speed of light. Substituting for c and λ_{op}, we obtain

$$\frac{\Delta\phi}{\varepsilon L} = (2.52 \times 10^{-8} \text{ rad})\ F.$$

The minimum observable strain ε_{min} is then defined as

$$\varepsilon_{min} = \frac{\Delta\phi_{min}}{L(2.52 \times 10^{-8} F)}. \tag{3.25}$$

3.4 ESTIMATED DYNAMIC RANGE

The estimated dynamic range is defined as

$$DR = \frac{\varepsilon_{MAX}}{\varepsilon_{MIN}} \tag{3.26}$$

where ε_{MAX} is defined in this report as the strain on the fiber with a 100,000 PSI pull. Strain, in general, is defined as

$$\varepsilon = \frac{F/A}{Y} \tag{3.27}$$

where F/A is the force per unit area exerted on the fiber (i.e., 100,000 PSI) and Y is Young's modulus for a quartz fiber; $Y = 8.12 \times 10^6$ PSI. Thus,

$$\varepsilon_{MAX} = \frac{10 \times 10^4}{8.12 \times 10^6} = 1.23 \times 10^{-2}$$

and the estimated dynamic range is

$$DR = 1.23 \text{ X } 10^{-2} / \varepsilon_{Min}. \tag{3.28}$$

3.5 TEMPERATURE SENSITIVITY

The absolute phase ϕ of a signal that exits a sensing fiber of length L is

$$\phi = 2\pi L/\lambda' \tag{3.29}$$

where λ' is the wavelength of the signal within the fiber. It is known that $\lambda' F = c/n$, where F is the optical frequency, n is the index of refraction, and c is the speed of light. Thus, $n\lambda' F = c = F\lambda$

or $\lambda' n = \lambda$

or $\lambda' = \lambda/n,$ (3.30)

which says that the wavelength of the RF modulation in free space, λ, is related to the wavelength within the fiber, λ', according to $\lambda' = \lambda/n$. Substituting for λ' in Equation (3.29) we obtain

$$\phi = (2\pi nL)/\lambda. \tag{3.31}$$

The change in phase with respect to temperature, $\partial\phi/\partial T$, is

$$\frac{\partial\phi}{\partial T} = \frac{2\pi}{\lambda}\left(\frac{\partial n}{\partial T}L + n\frac{\partial L}{\partial T}\right), \tag{3.32}$$

but

$$\frac{\partial L}{\partial T} = \alpha L$$

where α is the linear thermal coefficient of expansion. Substituting αL for $\partial L/\partial T$, we obtain

$$\frac{\partial\phi}{\partial T} = \frac{2\pi}{\lambda}\left(\frac{\partial n}{\partial T}L + n\alpha L\right)$$

or

$$\frac{\partial \phi}{\partial T} = \frac{2\pi L}{\lambda} \left(\frac{\partial n}{\partial T} + n\alpha\right). \tag{3.33}$$

The values of $\partial n/\partial T$ and α were reported in the literature for silica fibers.[9] These are

$$\alpha = 8 \times 10^{-7}/^{\circ}C$$

and

$$\frac{\partial n}{\partial T} = 10^{-5}$$

Thus,

$$\frac{\partial n}{\partial T} + n\alpha = 1.12 \times 10^{-5} \tag{3.34}$$

was assumed to be 1.48. Substituting Equation (3.34) into Equation (3.35), we obtain

$$\frac{\partial \phi}{\partial T} = (7.037 \times 10^{-5} L)/\lambda \ . \tag{3.35}$$

Solving for $\Delta\phi$, we obtain the final expression

$$\Delta\phi = (2.1096 \times 10^{-13} LF)\Delta T \tag{3.36}$$

where λ was replaced by F/c and the partials $\partial\phi$ and ∂T were replaced by the approximations $\Delta\phi$ and ΔT. F is the RF frequency in sec^{-1}, and L is the fiber length in meters.

3.6 PRESSURE SENSITIVITY

The derivation of the pressure sensitivity follows a mathematical procedure similar to that developed in Section 3.5. We start with Equation (3.31) and differentiate ϕ with respect to the pressure p, which yields

$$\frac{\partial \phi}{\partial P} = \frac{2\pi L}{\lambda} \left(\frac{\partial n}{\partial P} + \frac{n}{L} \frac{\partial L}{\partial P}\right). \tag{3.37}$$

The term in the brackets is constant for bare fused silica fibers, and its value is given[10] by

$$2\pi \left(\frac{\partial n}{\partial \pi} + \frac{n}{L} \frac{\partial L}{\partial P}\right) = 2.26 \times 10^{-11} \quad /(\text{dyne/cm}^2). \tag{3.38}$$

Substituting Equation (3.38) into Equation (3.37) and replacing λ by F/c, we obtain the final expression for the change in phase, $\Delta\phi$, due to a change in pressure, Δp. The partial $\partial\phi/\partial p$ was replaced by an approximation $\Delta\phi/\Delta p$.

$$\Delta\phi = 7.5385 \times 10^{-20} L \, \Delta P \, \frac{\text{rad-cm}^2}{\text{m-dyne}} \tag{3.39}$$

or

$$\Delta\phi = 7.638 \times 10^{-14} LF \, \Delta P \, \frac{\text{rad}}{\text{m-atm}}$$

3.7 COMPARISONS BETWEEN PREDICTED AND MEASURED PHASE SHIFTS

Georgia Tech fabricated a laboratory model of the strain sensor (using only one mixer) and initiated preliminary measurements. Figure 17 shows the sensor output in millivolts as a function of fiber displacement. The parameters of the system were as follows: modulation frequency was 1 GHz, fiber length was 1 m,

and RF bandwidth was 100 MHz. Although the trend of the graph is linear, the sensor output does exhibit oscillations due to modal noise. It should be emphasized that modal noise is associated only with optically coherent sources such as laser diodes. Modal noise and, thus, voltage oscillations are nonexistent in systems using LED sources or the I, Q detection scheme suggested in this report. As a result of using only one mixer with an optically coherent source, the minimum strain sensitivity ($\Delta\varepsilon_{min} = \pm 4 \times 10^{-4}$) determined from these measurements is a worst case example.

In this section, the predicted phase shift will be derived in two ways: (1) by using the Hocker Equation (3) with the relevant frequency and the measured strain sensitivity extracted from Figure 17, and (2) by using Equation (3.22) in this report.

The predicted phase shift using Hocker's equation is

$$\frac{\Delta\phi_H}{\varepsilon L} = 1.2 \times 10^7 \text{ rad/m at } \lambda = 630 \times 10^{-9} \text{m},$$

but the required phase shift at $\lambda = 0.3$ m (modulation frequency is 1 GHz) is

$$\frac{\Delta\phi_H}{\varepsilon L} = \frac{630 \times 10^{-9} \text{m}}{0.3 \text{ m}} (1.2 \times 10^7 \text{ rad/m})$$

or

$$\frac{\Delta\phi_H}{\varepsilon L} = 25.2 \text{ rad/m}.$$

The absolute phase shift sensitivity is, thus, given by

$$\Delta\phi_H = (25.2 \text{ rad/m}) \varepsilon L. \tag{3.40}$$

$\varepsilon = \pm 3.5 \times 10^{-4}$ is derived from Figure 17, and L is set to 1 m. Substituting for ε and L in Equation (3.40), we obtain

$$\Delta\phi_H = (25.2 \text{ rad/m})(\pm 3.5 \times 10^{-4})(1 \text{ m})$$

or

$$\Delta\phi_H = \pm 0.00882 \text{ rad} = \pm 0.51^{\circ}. \tag{3.41}$$

The system bandwidth in this case was 100 MHz.

The predicted phase shift sensitivity using Equation (3.22) can be read from Figure 1-1-2 (see Section 3.8) and is given by

$$\Delta\phi_p = \pm 9.0 \times 10^{-3} \text{rad} = \pm 0.52^{\circ}. \tag{3.42}$$

As before, L was 1 m, F was 1 GHz, and was bandwidth the 100 MHz.

The actual measured phase shift sensitivity is $\Delta\phi_M$= (Min observed change in fiber length) (number of wavelengths in 1 m of fiber) ($\cdot 360^{\circ}$). The minimum observed change in 1 m of fiber is just the minimum observed strain sensivity from Figure 17. Thus, $\Delta\phi_M = \pm 3.5 \times 10^{-4} \times 5 \times 360^{\circ}$, or

$$\Delta\phi_M = \pm 0.63^{\circ}. \tag{3.43}$$

Note that the predicted and measured sensitivities are in good agreement. Also note that the predicted sensitivity, just as the measured sensitivities, represent worst case calculations and measurements. Therefore, actual sensitivities with an LED or ILD system are expected to better than the predictions.

3.8 ANALYTICAL RESULTS

Computer generated analytical results were compiled to serve as reference material and to enable predictions and comparisons of the sensor's sensitivity and performance under varying conditions. All results were packed into one section and divided into two groups to facilitate the comparison task. In group 1, the optical source was a laser diode; in group 2, the laser was replaced with an LED. Each group was further subdivided into four sets. Each set, in turn, consists of four plots showing, always in the same succession, the following four prameters: SNR; minimum phase sensitivity, $\Delta\phi$; minimum strain sensitivity, $\Delta\varepsilon$; and estimated dynamic range. These key parameters are plotted as functions of various other quantities. In set #1, the key parameters are plotted as a function of fiber length for five different system bandwidths. The modulation frequency remained constant at 1 GHz. In set #2, the key parameters were again plotted as a function of fiber length, but, in this case, for four different frequencies. The bandwidth remained constant at 1 kHz. In set #3, the key parameters were plotted as a function of frequency for five various fiber lengths. The bandwidth was set to 1 kHz. In set #4, the key parameters were plotted as a function of system pulse width for five various fiber lengths. The source in this case was operated in a pulsed, not CW, mode. The modulation frequency was set at 100 MHz. The pulse was modeled as a CW sinusoidal waveform with a rectangular envelope. In order not to distort the pulse shape and to maximize the signal-to-noise ratio, the output bandwidth of the system, BW, must be

$$BW = 0.75\ (1/PW) \tag{3.44}$$

where PW is the width of the pulse in the time domain. Equation (3.44) was incorporated into the computer program. Thus, pulse width was translated into bandwidth which, in turn, affected the key parameters.

The computer generated plots are attached to this section. The figure numbers differ from the conventional numbering system to facilitate a comparison

of the various results. Each number contains three digits separated by dashes. The first digit denotes group 1 or 2, i.e., it shows whether the plot was generated with an ILD or LED. The second digit refers to one of the four sets, and the third digit refers to the particular parameter of interest within each set. For example, the user may wish to compare the minimum observable phase shift as a function of modulation frequency for two different optical sources such as an ILD or LED. This is done simply by comparing Figure 1-3-2 with Figure 2-3-2.

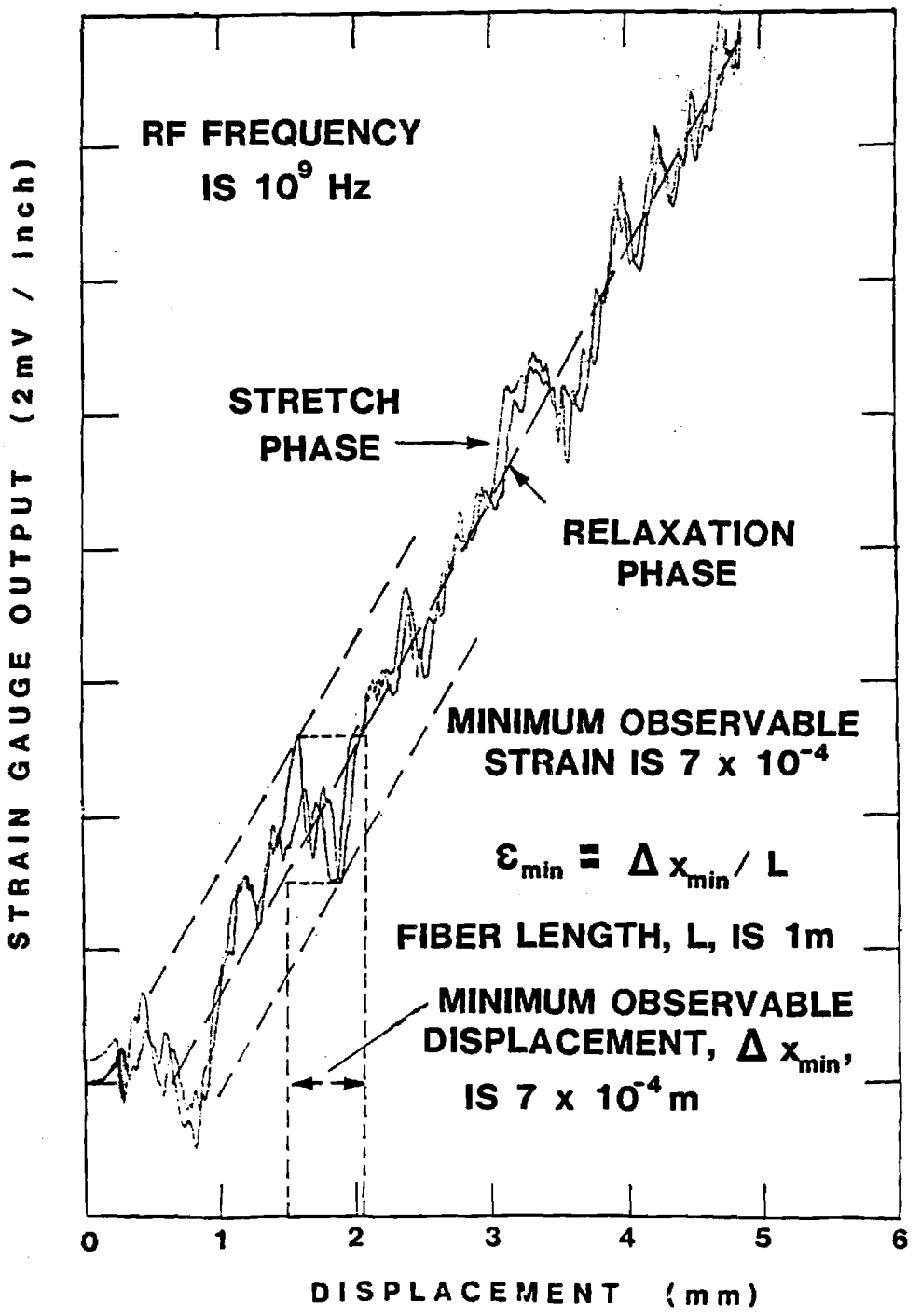

Figure 17. Mixer output as a function of fiber displacement. Bandwidth is 100 MHz. Fiber length is 1m. RF frequency is 1 GHz.

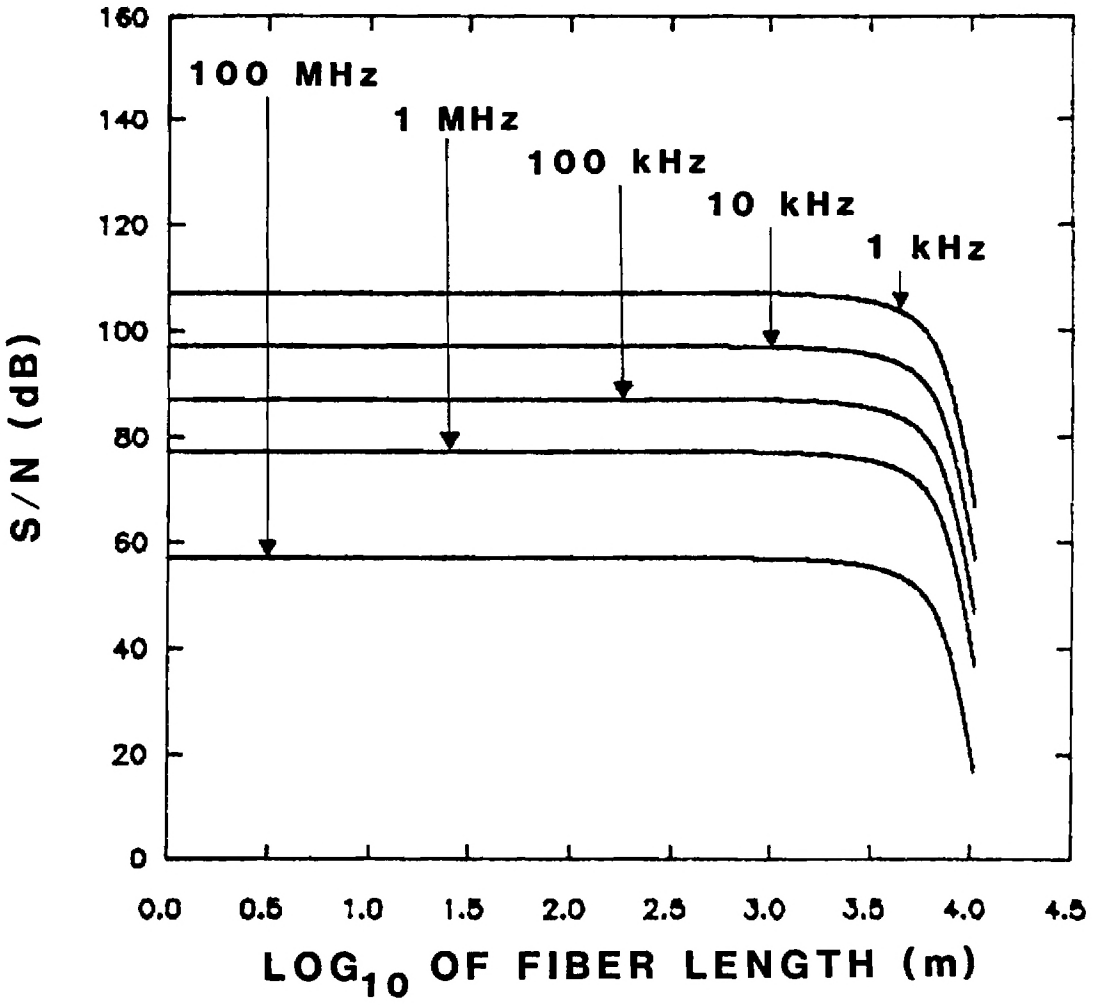

Figure 1-1-1. Signal-to-noise ratio as a function of fiber length for various bandwidths. RF frequency was set to 1 GHz. The optical source is a laser diode.

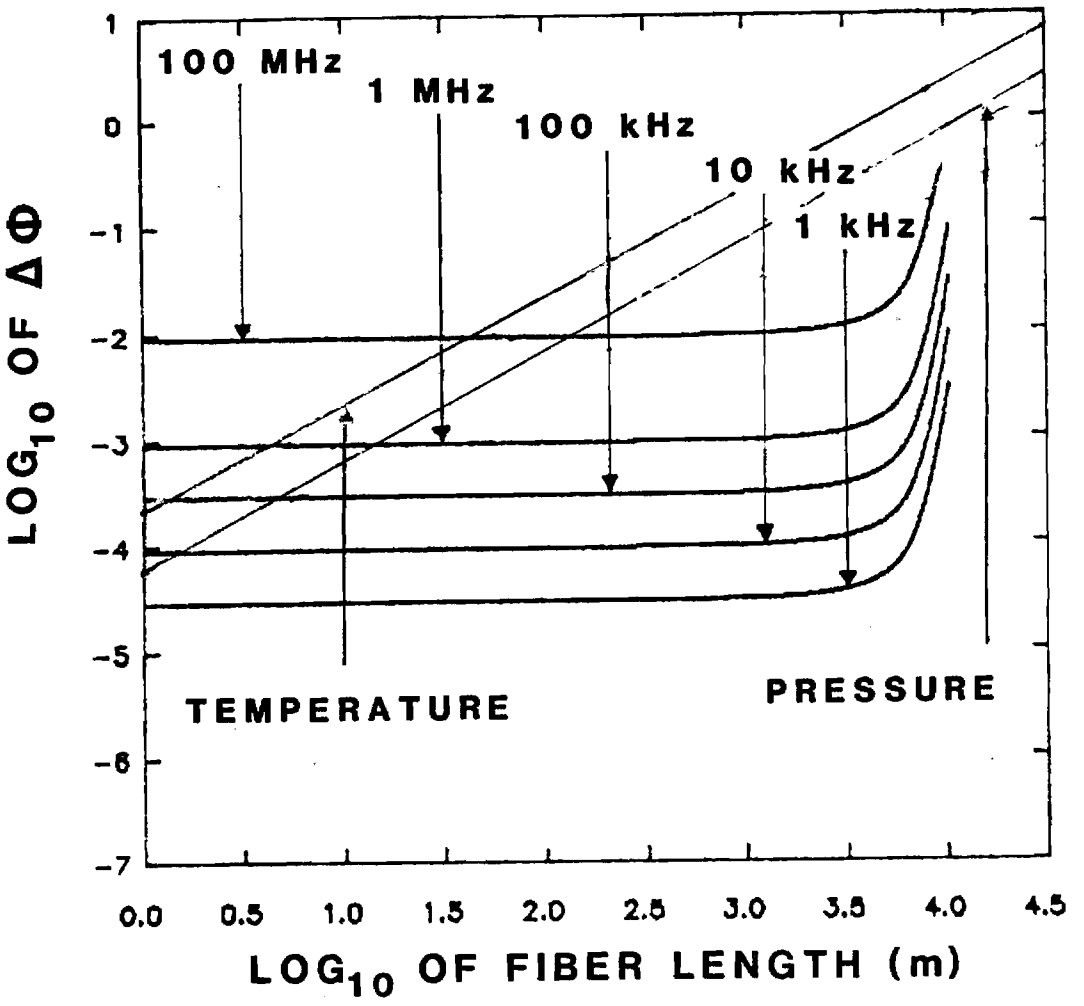

Figure 1-1-2. Minimum observable phase shift, $\Delta\Phi$, as a function of fiber length for various bandwidths. RF frequency was set to 1 GHz. The optical source is a laser diode. At 1 GHz the temperature sensitivity is 2.1096×10^{-4} rad/^{o}C-m and the pressure sensitivity is 7.638×10^{-5} rad/atm-m.

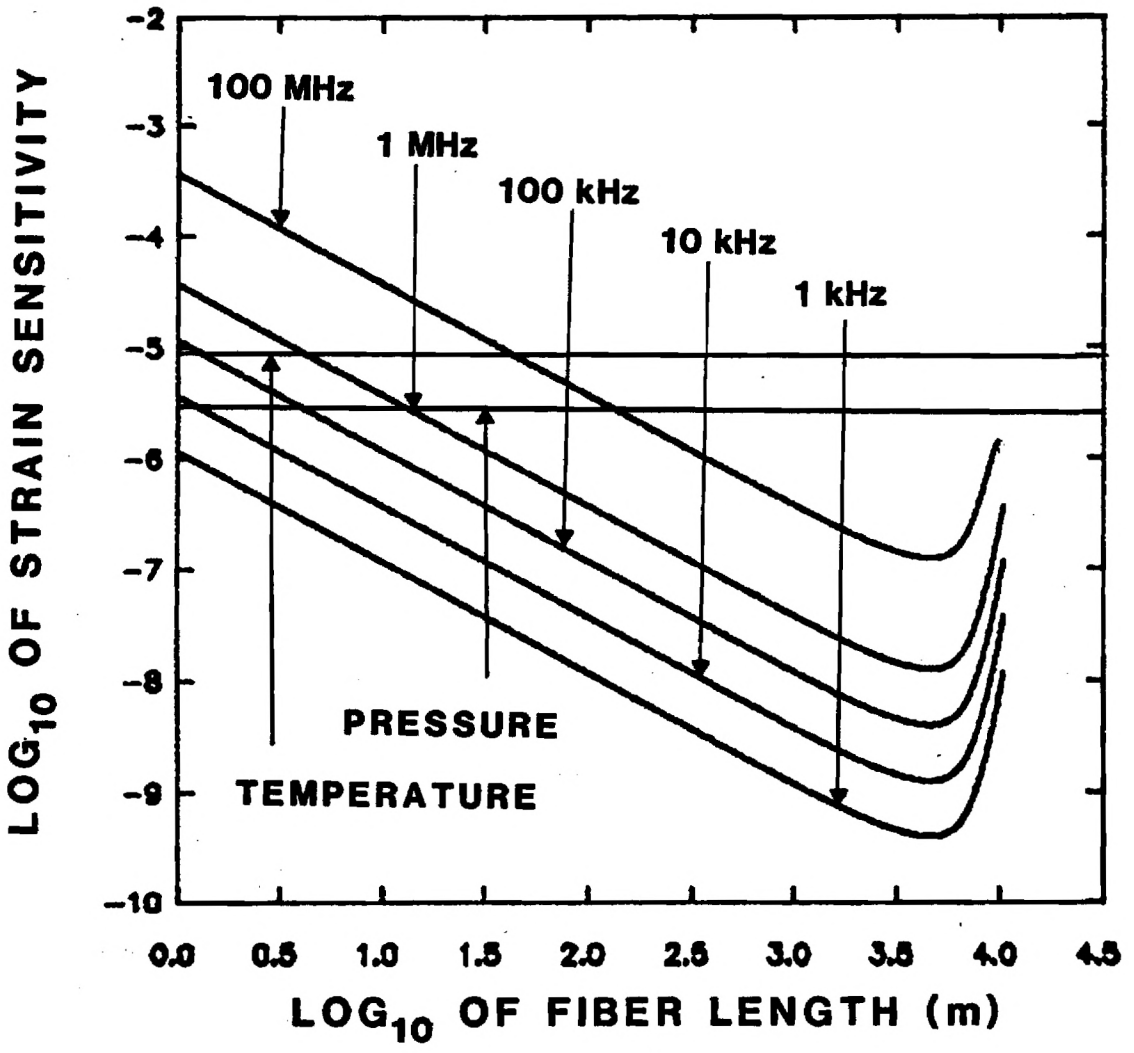

Figure 1-1-3. Minimum observable strain (strain sensitivity) as a function of fiber length for various bandwidths. RF frequency was set to 1 GHz. The optical source is a laser.

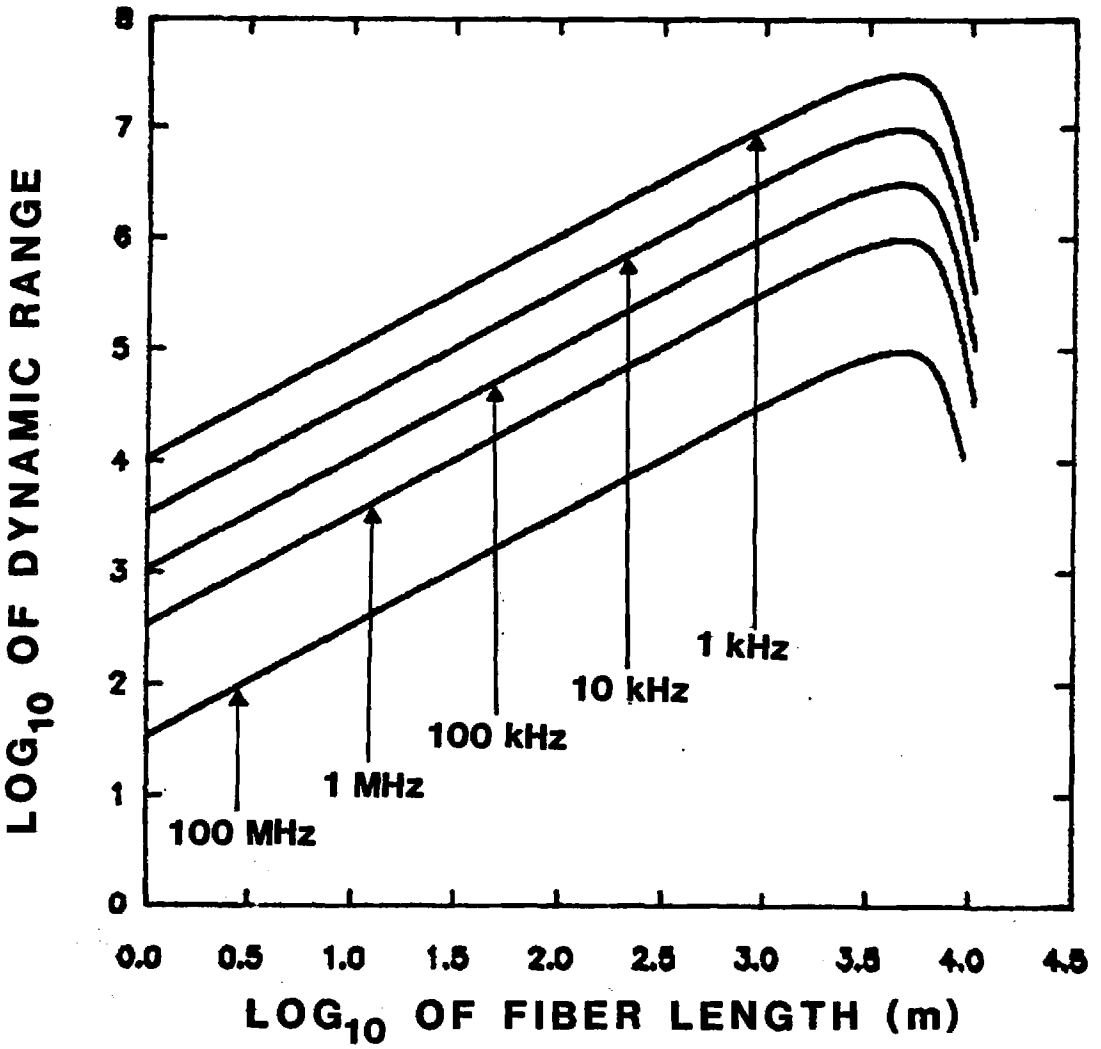

Figure 1-1-4. Expected dynamic range as a function of fiber length for various bandwidths. RF frequency was set to 1 GHz. The optical source is a laser. Maximum strain value is 1.23×10^{-2}. Minimum strain value is strain sensitivity.

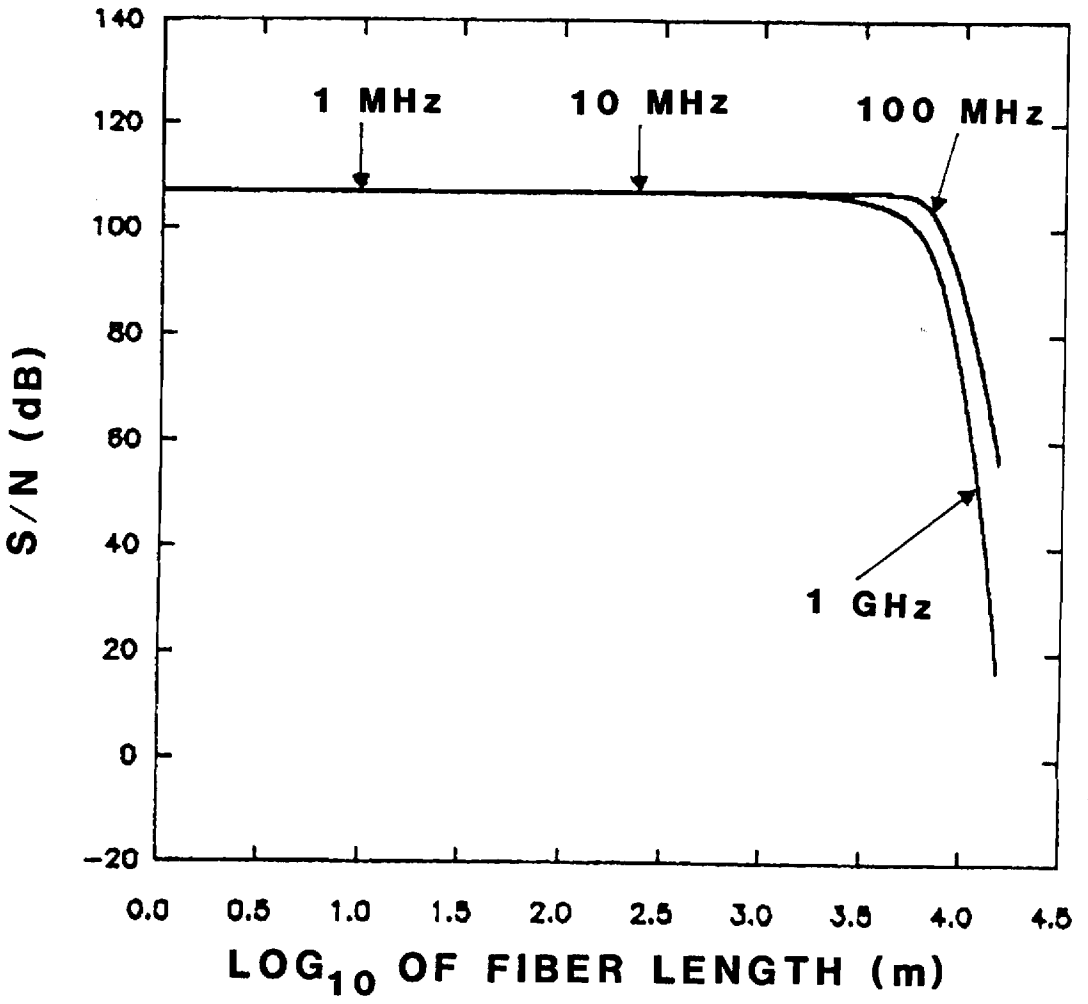

Figure 1-2-1. Signal-to-noise ratio as a function of fiber length for various RF frequencies. Bandwidth was set to 1 kHz. The optical source is a laser diode.

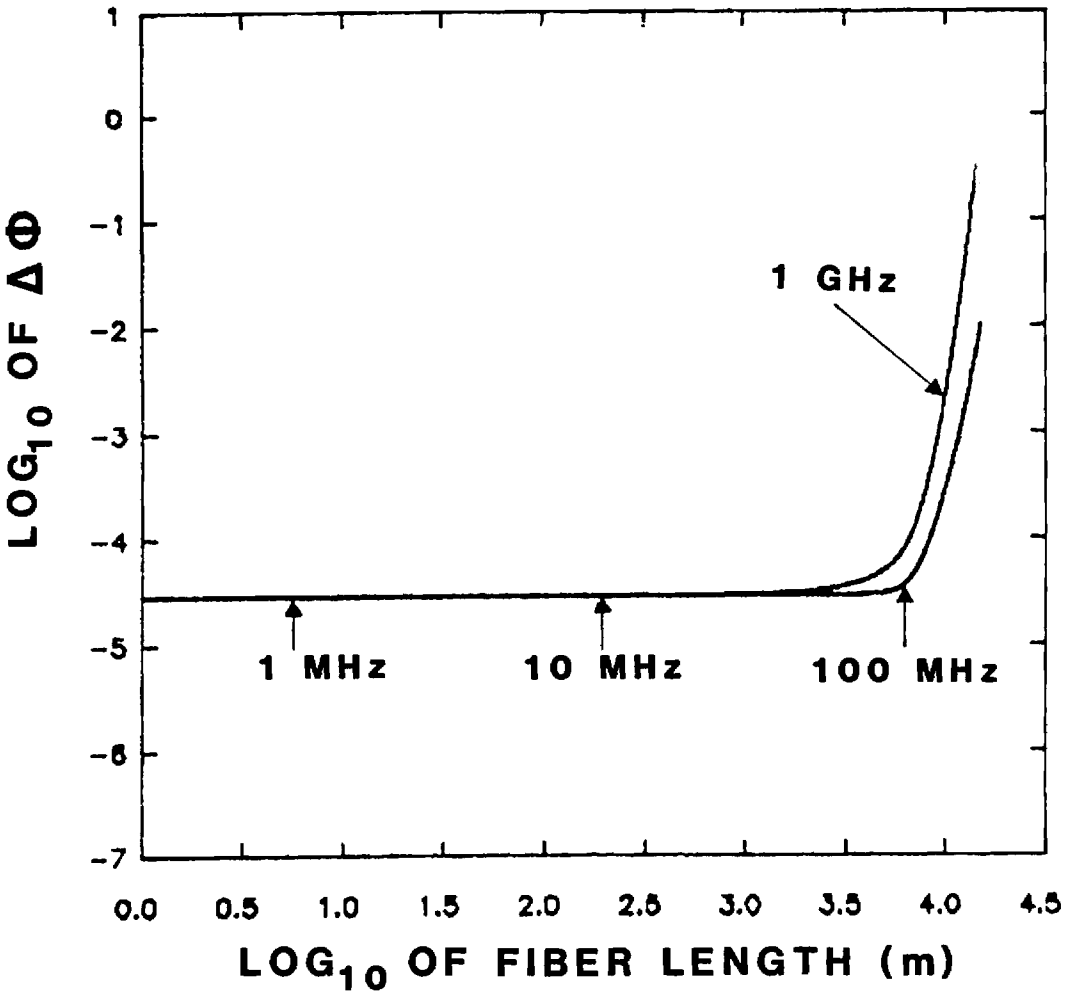

Figure 1-2-2. Minimum observable phase shift, $\Delta\Phi$, as a function of fiber length for various RF frequencies. Bandwidth was set to 1 kHz. The optical source is a laser diode.

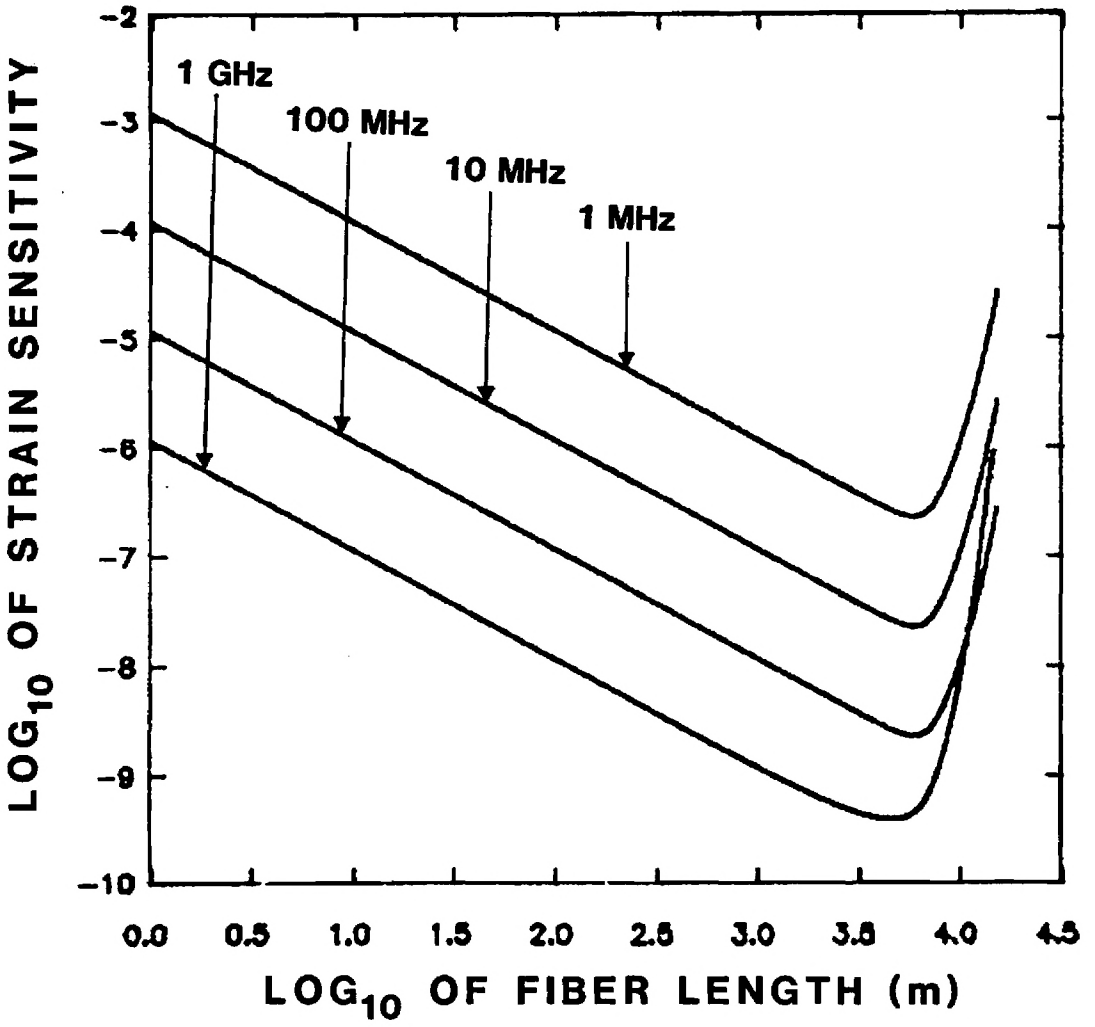

Figure 1-2-3. Minimum observable strain (strain sensitivity) as a function of fiber length for various RF frequencies. The bandwidth was set to 1 kHz. The optical source is a laser.

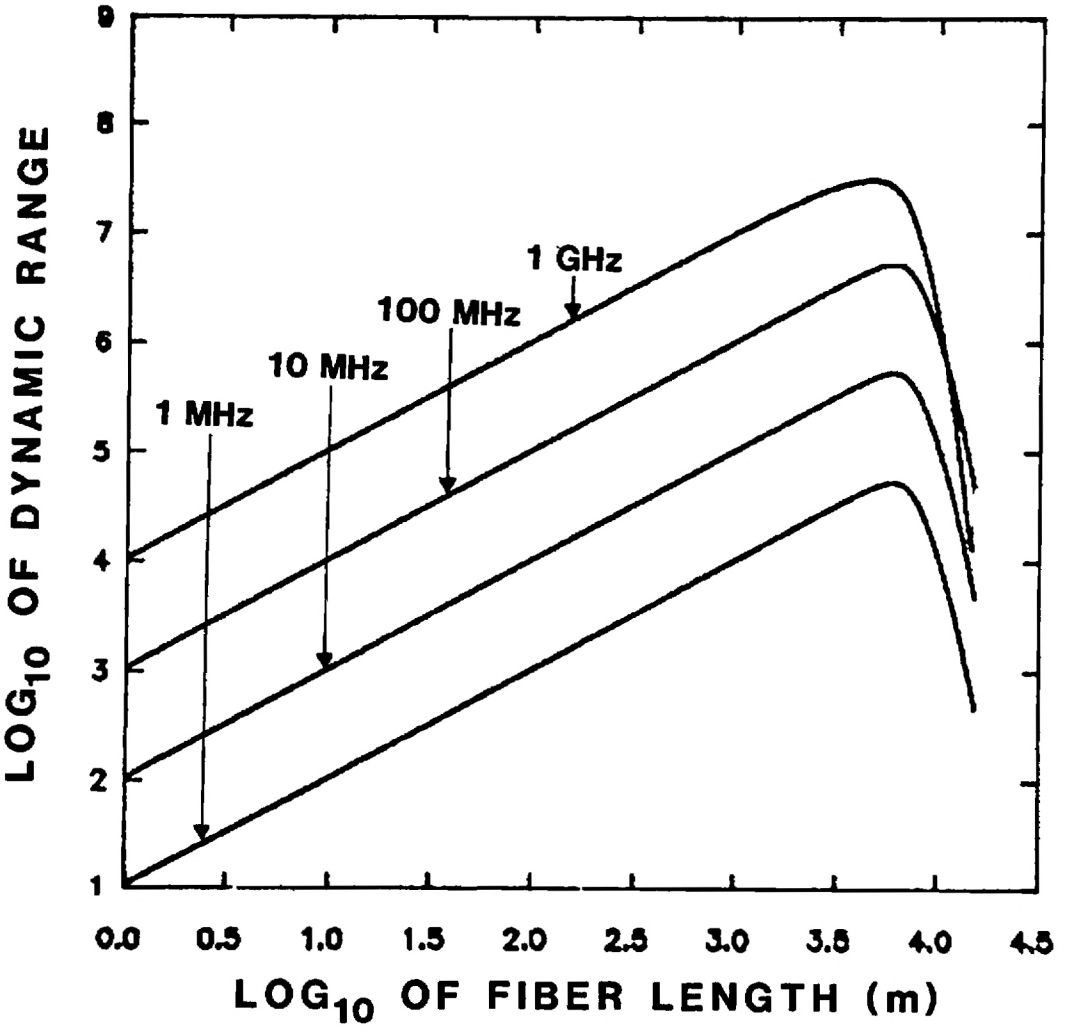

Figure 1-2-4. Expected dynamic range as a function of fiber length for various RF frequencies. Bandwidth was set to 1 kHz. The optical source is a laser. Maxiumum strain value is 1.23×10^{-2}. Minimum strain value is strain sensitivity.

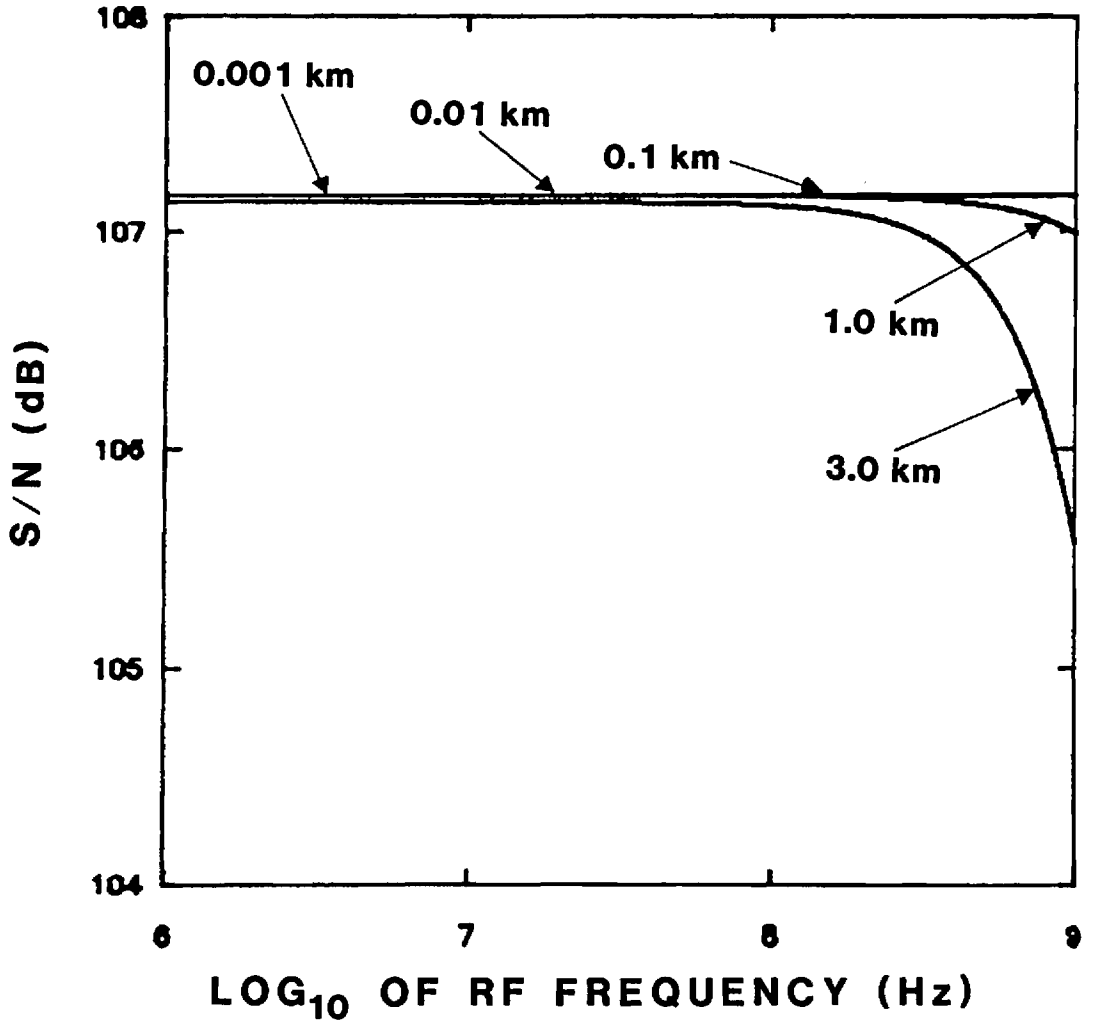

Figure 1-3-1. Signal-to-noise ratio as a function of RF frequency for various fiber lengths. Bandwidth was set to 1 kHz. The optical source is a laser.

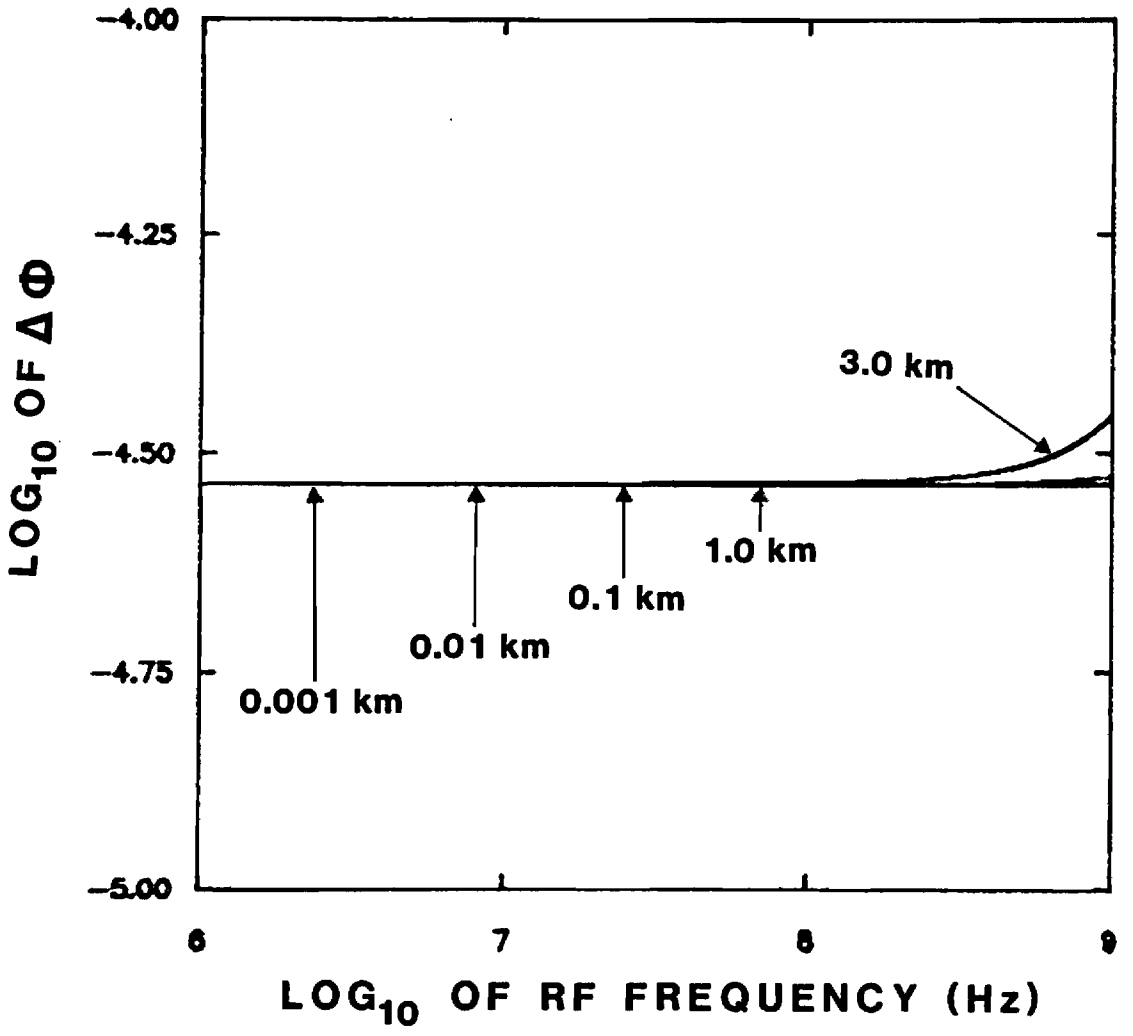

Figure 1-3-2. Minimum observable phase shift, $\Delta\Phi$, as a function of RF frequency for various fiber lengths. Bandwidth was set to 1 kHz. The optical source is a laser.

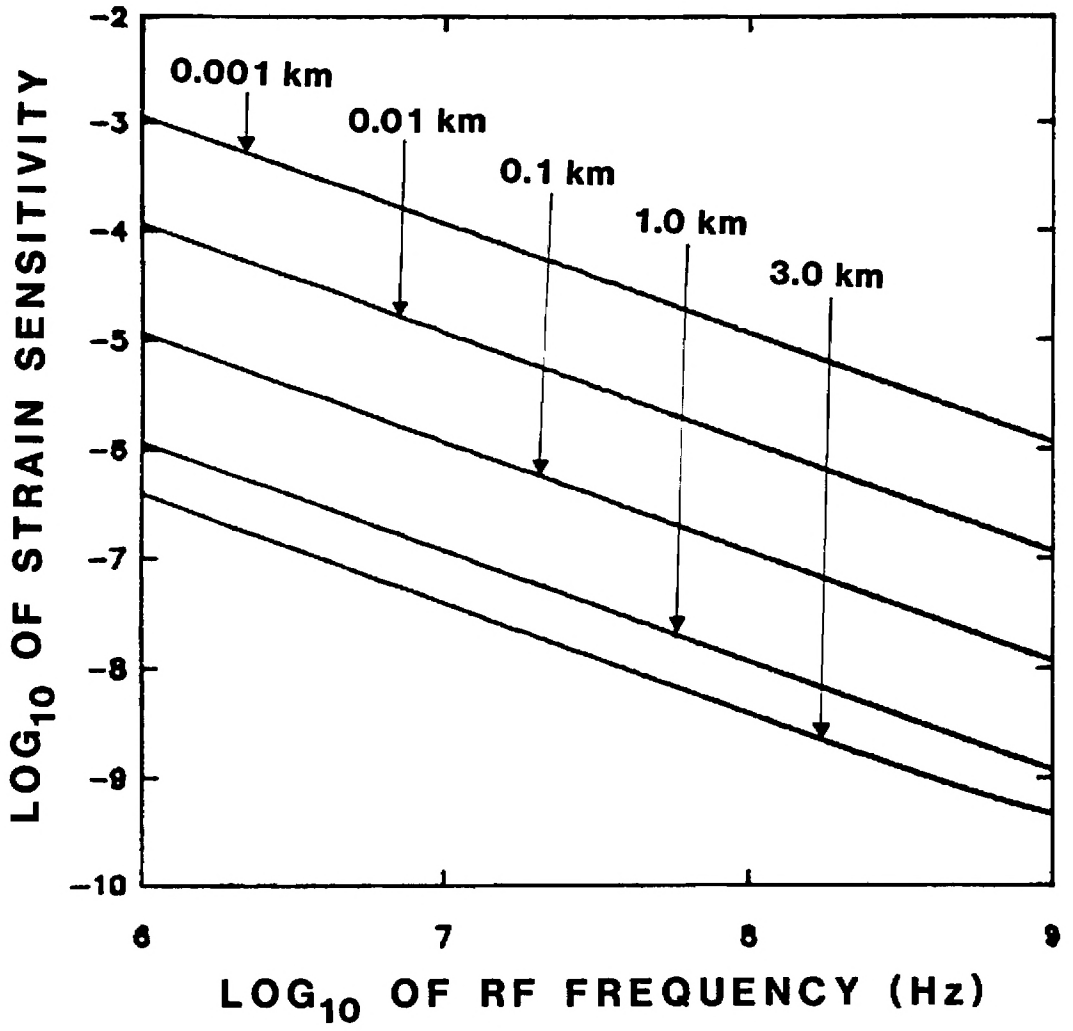

Figure 1-3-3. Minimum observable strain (strain sensitivity) as a function of RF frequency for various fiber lengths. Bandwidth was set to 1 kHz. The optical source is a laser.

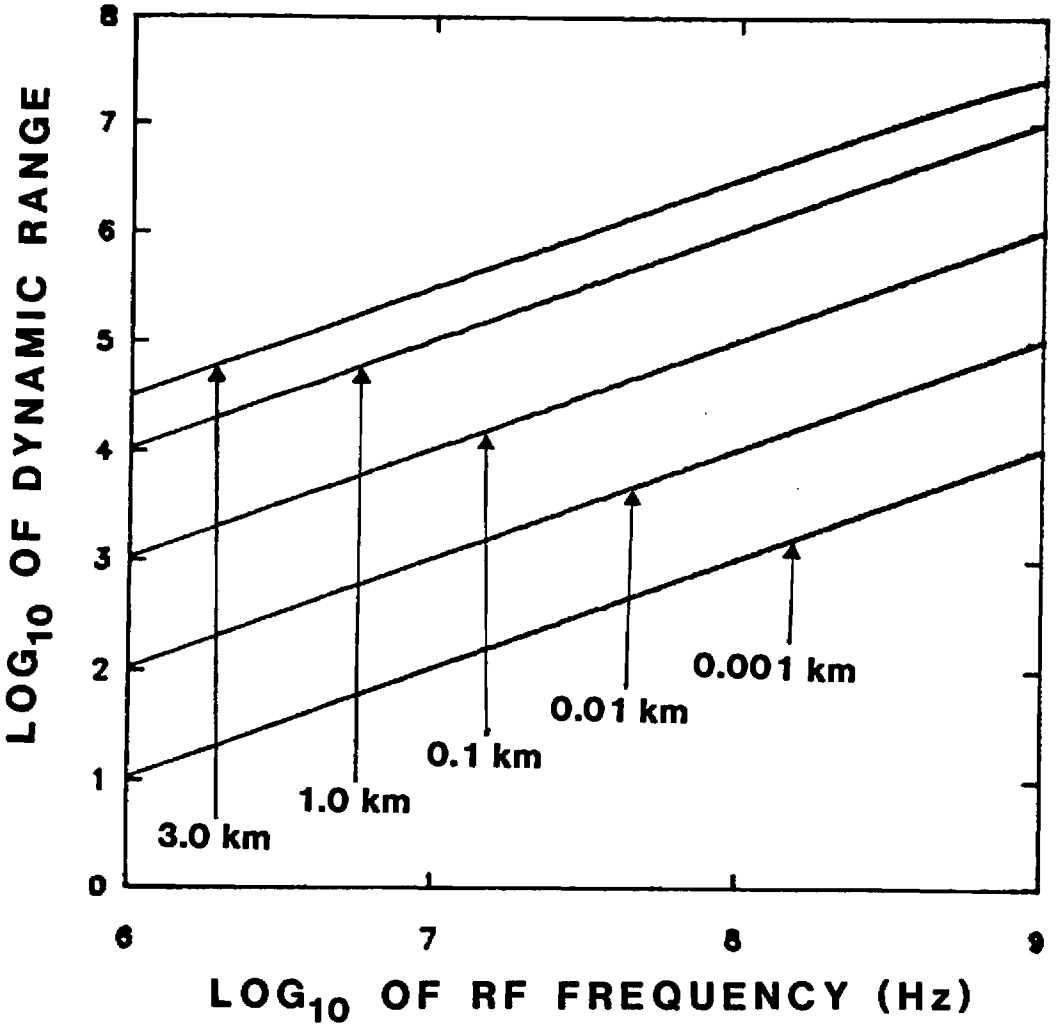

Figure 1-3-4. Expected dynamic range as a function of RF frequency for various fiber lengths. Bandwidth was set to 1 kHz. The optical source is a laser. Maximum strain value is 1.23×10^{-2}. Minimum strain value is strain sensitivity.

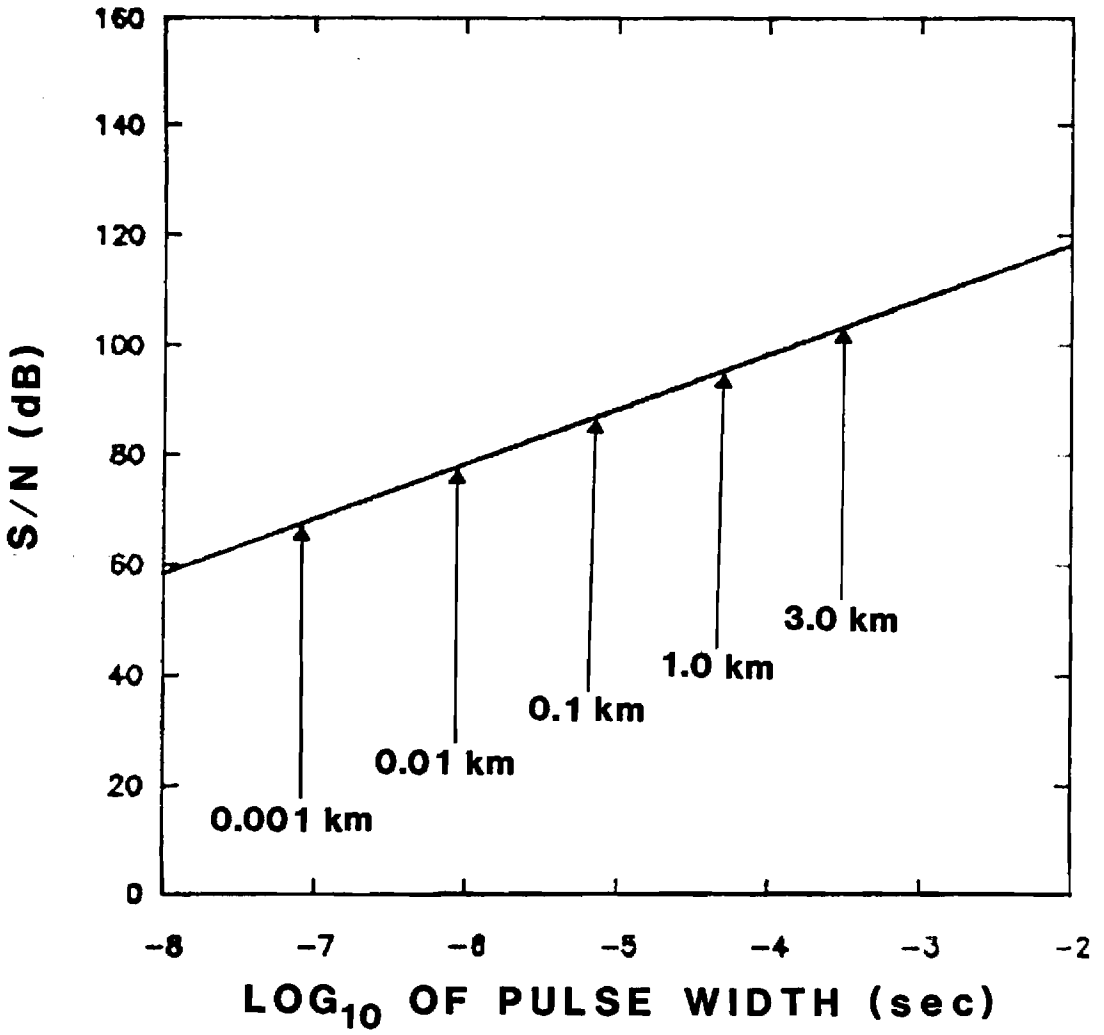

Figure 1-4-1. Signal-to-noise ratio as a function of pulse width for various fiber lengths. RF frequency was set to 100 MHz. The optical source is a laser.

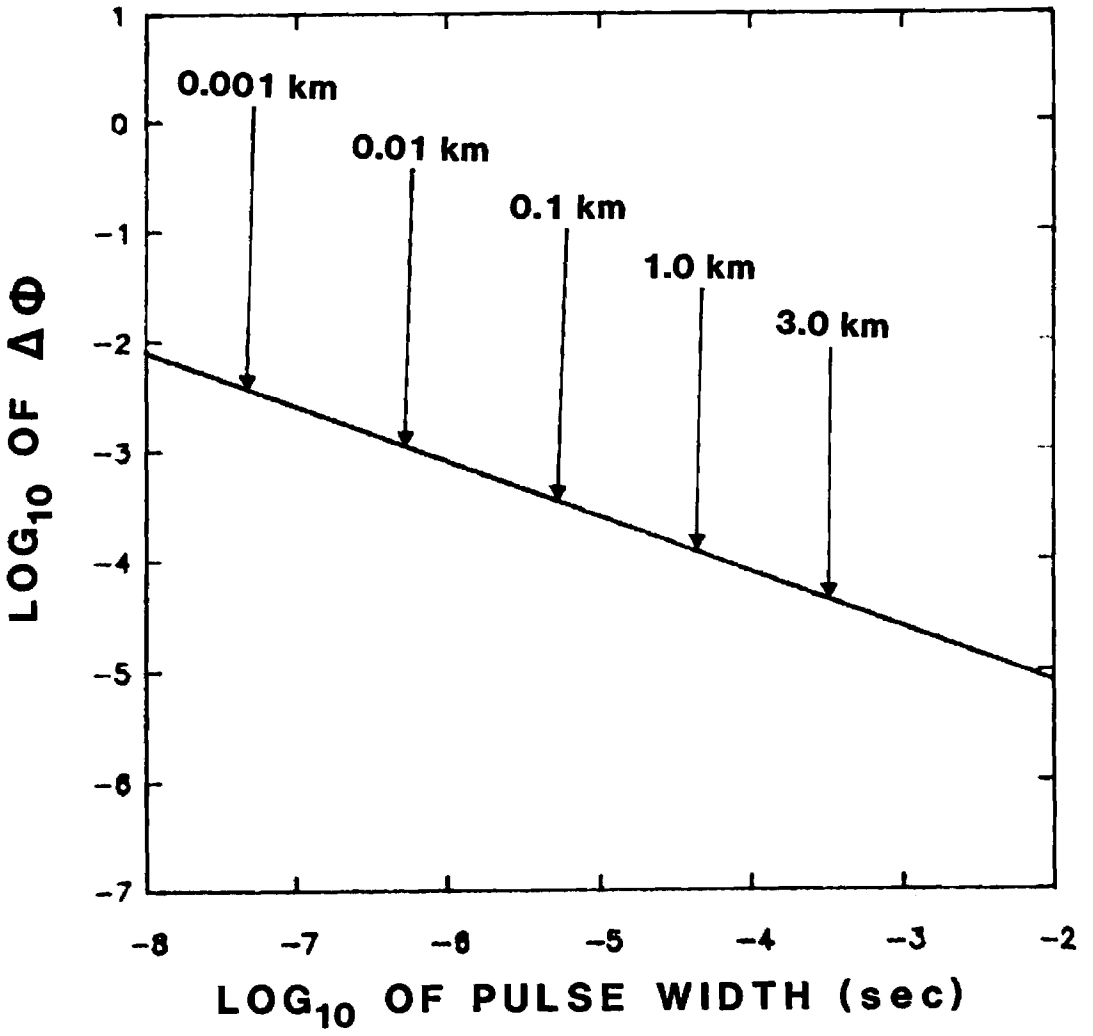

Figure 1-4-2. Minimum observable phase shift, $\Delta\Phi$, as a function of pulse width for various fiber lengths. RF frequency was set to 100 MHz. The optical source is a laser.

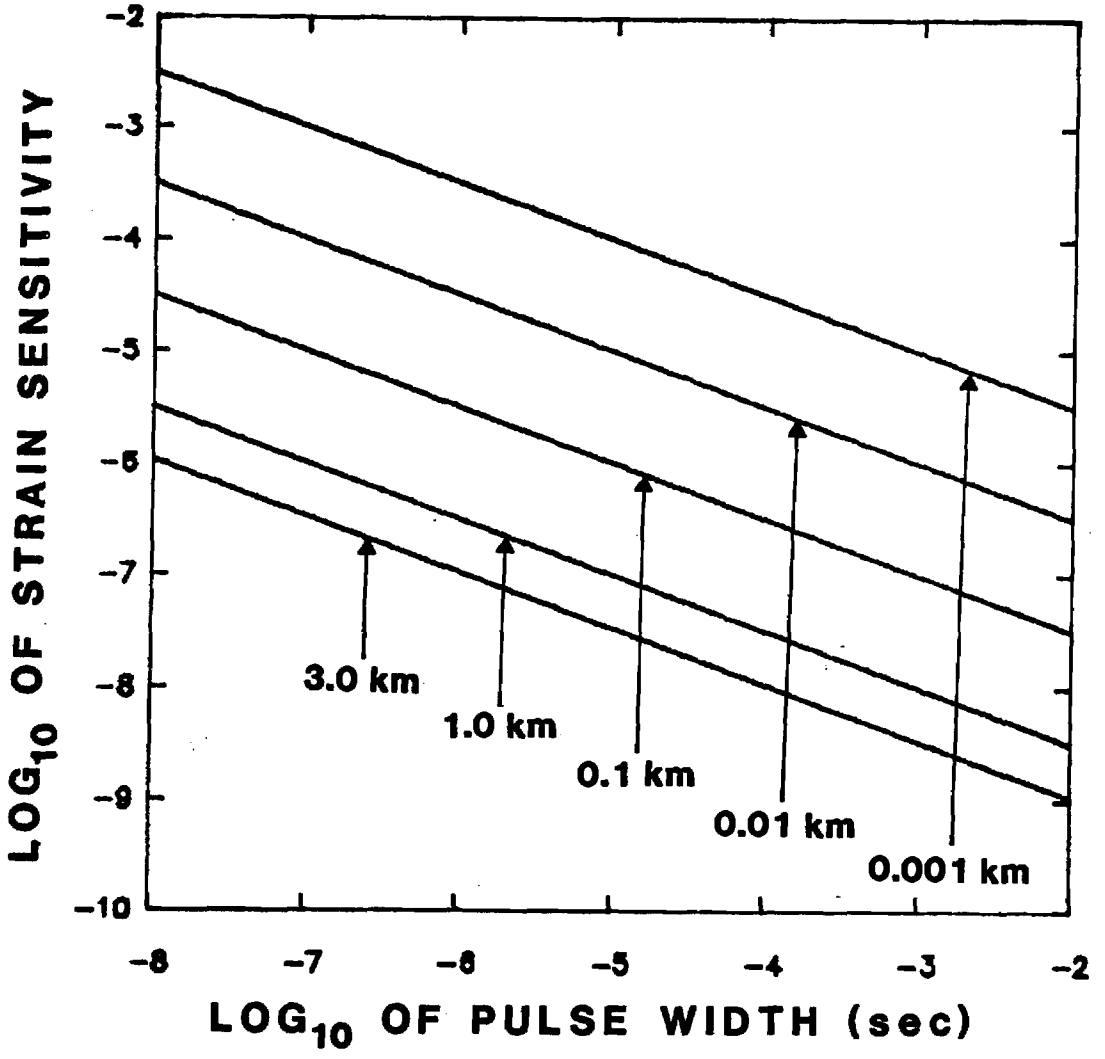

Figure 1-4-3. Minimum observable strain (strain sensitivity) as a function of pulse width for various fiber lengths. RF frequency was set to 100 MHz. The optical source is a laser.

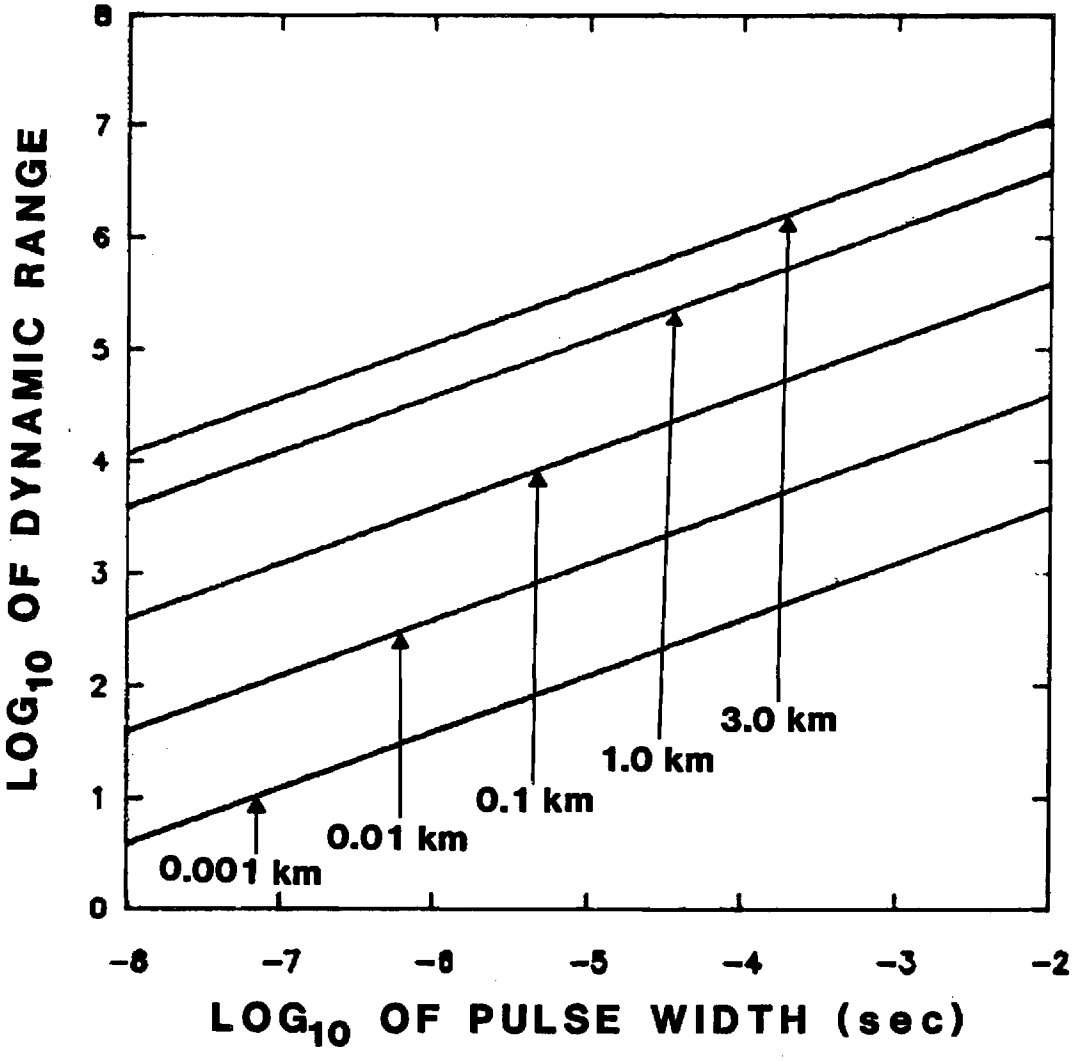

Figure 1-4-4. Expected dynamic range as a function of pulse width for various fiber lengths. RF frequency was set to 100 MHz. The optical source is a laser. Maximum strain value is 1.23×10^{-2}. Minimum strain value is strain sensitivity.

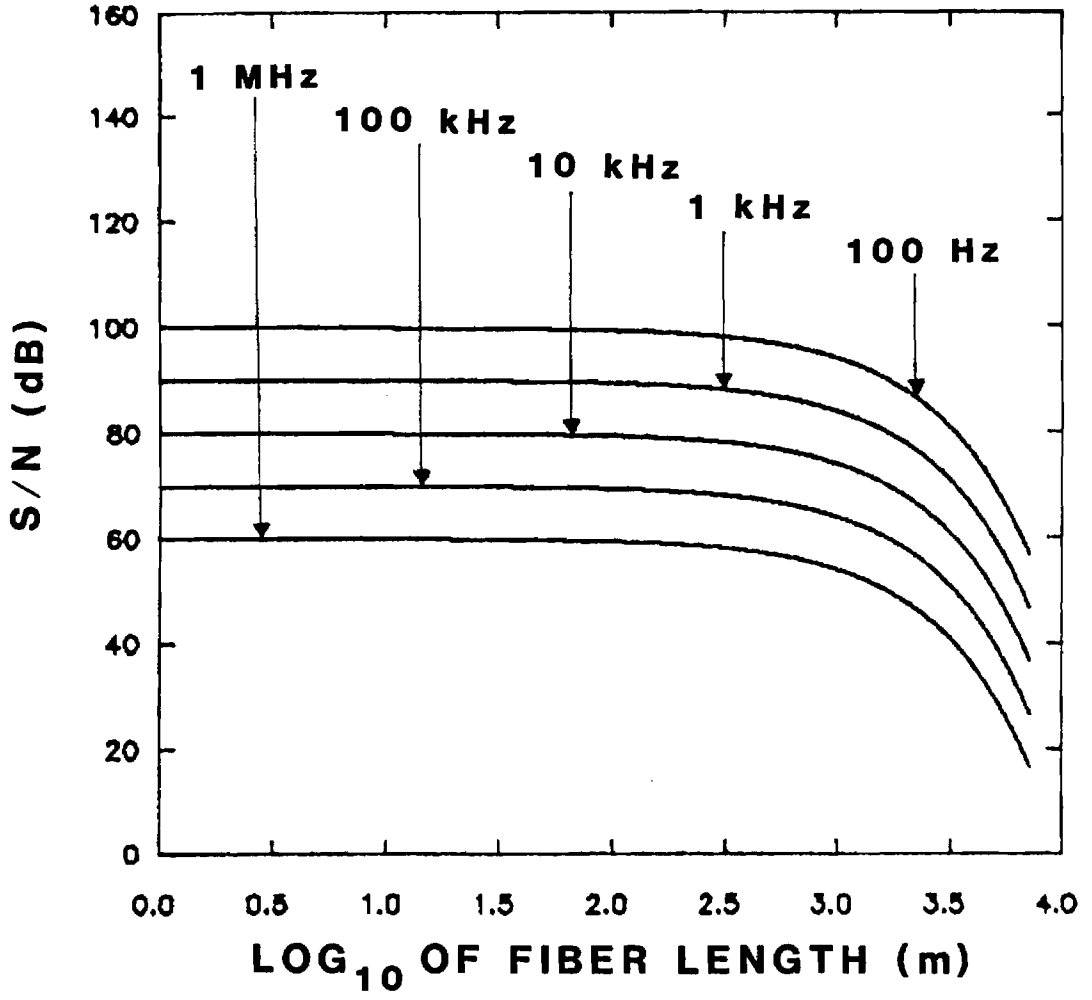

Figure 2-1-1. Signal-to-noise ratio as a function of fiber length for various bandwidths. RF frequency was set at 100 MHz. The optical source is an LED.

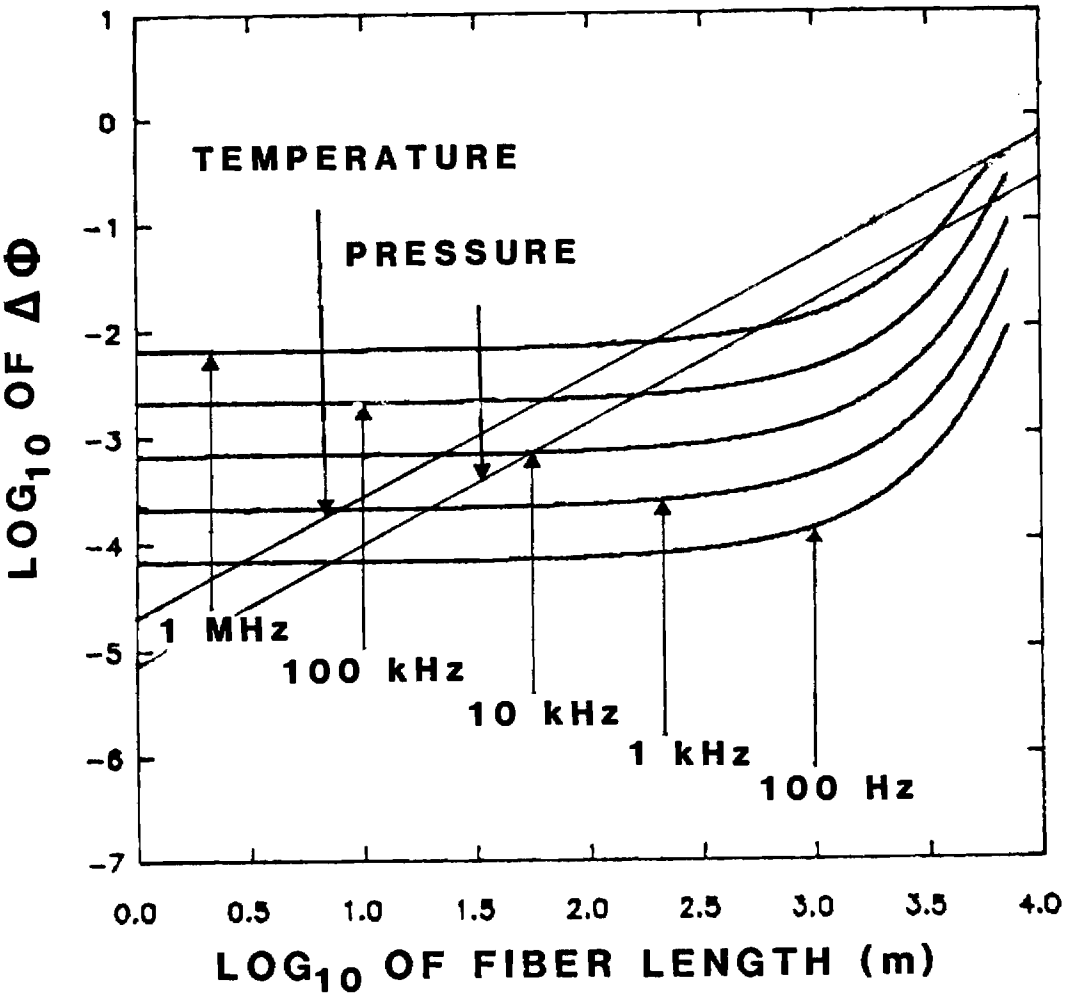

Figure 2-1-2. Minimum observable phase shift, $\Delta\Phi$, as a function of fiber length for various bandwidths. RF frequency was set to 100 MHz. The optical source is an LED. At 100 MHz the temperature sensitivity is 2.1096×10^{-5} rad/^{o}C-m and the pressure sensitivity is 7.638×10^{-6} rad/atm-m.

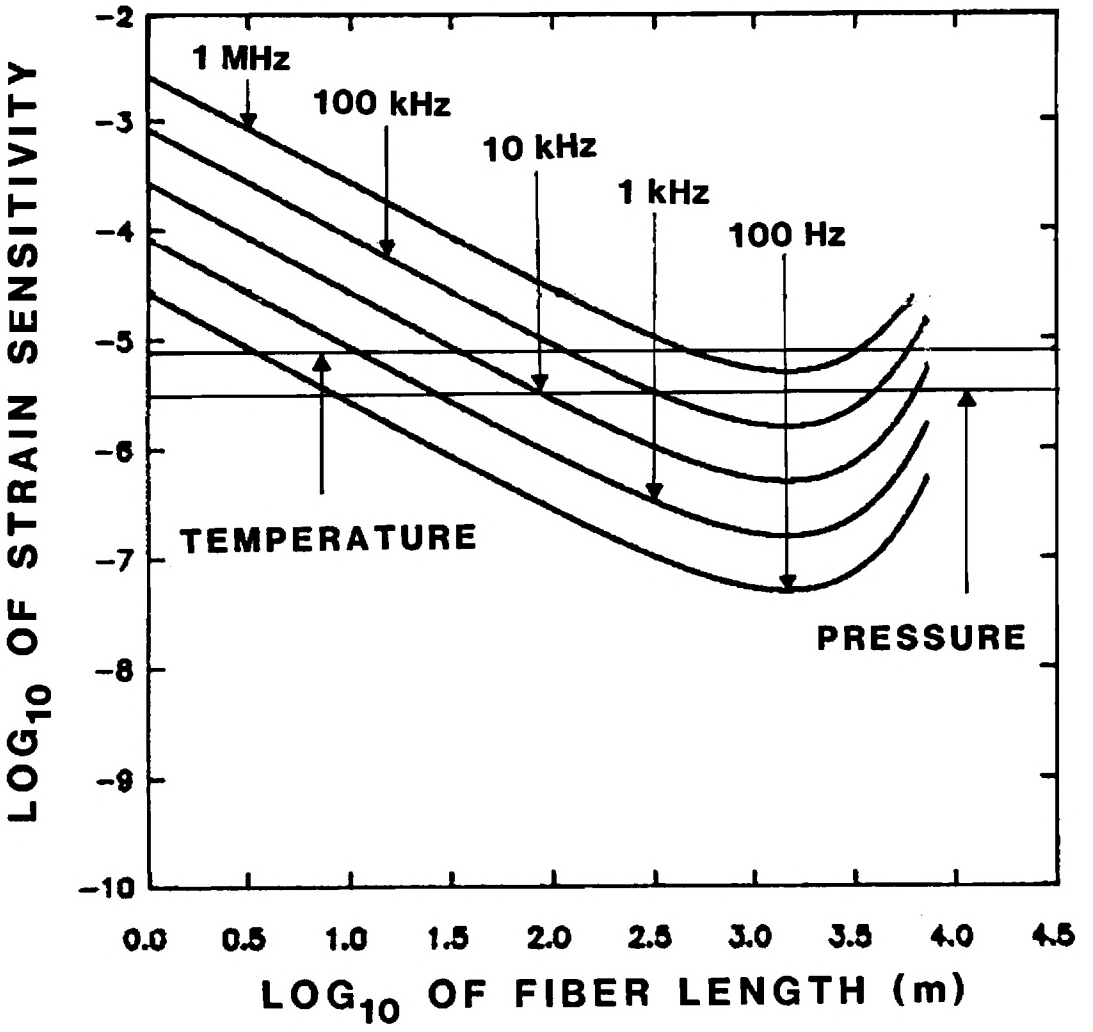

Figure 2-1-3. Minimum observable strain (strain sensitivity) as a function of fiber length for various bandwidths. RF frequency was set to 100 MHz. The optical source is an LED.

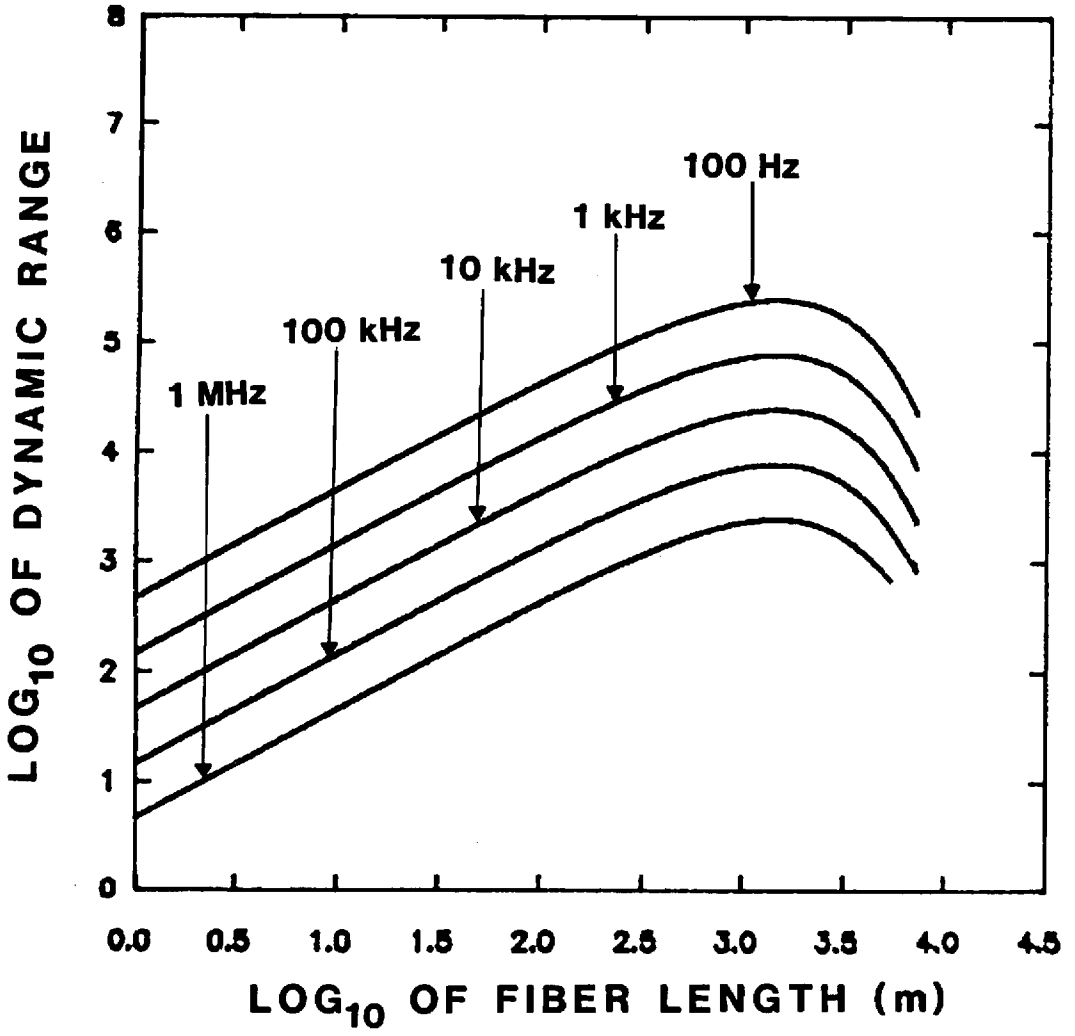

Figure 2-1-4. Expected dynamic range as a function of fiber length for various bandwidths. RF frequency was set to 100 MHz. The optical source is an LED. Maximum strain value is 1.23×10^{-2}. Minimum strain value is strain sensitivity.

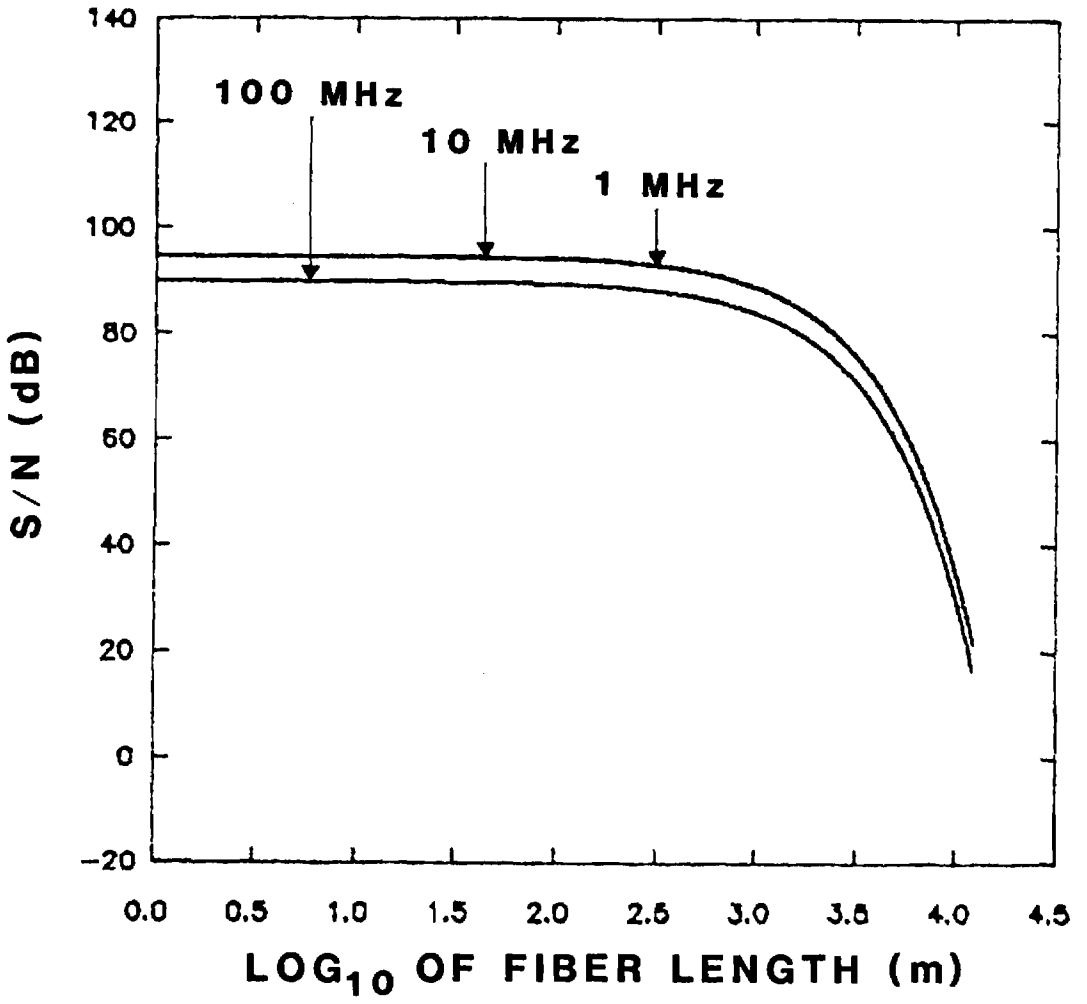

Figure 2-2-1. Signal-to-noise ratio as a function of fiber length for various RF frequencies. Bandwidth was set to 1 kHz. The optical source is an LED.

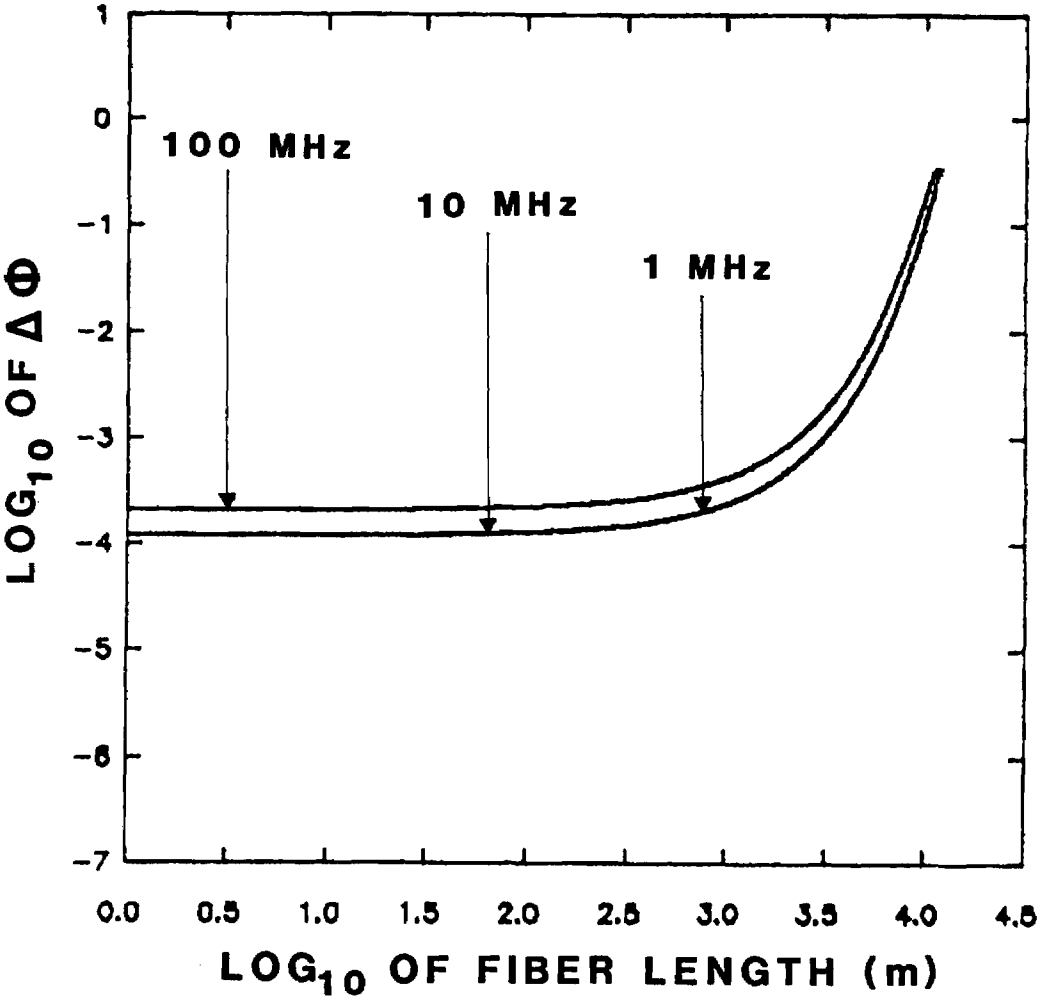

Figure 2-2-2. Minimum observable phase shift, $\Delta\Phi$, as a function of fiber length for various RF frequencies. Bandwidth was set to 1 kHz. The optical source is an LED.

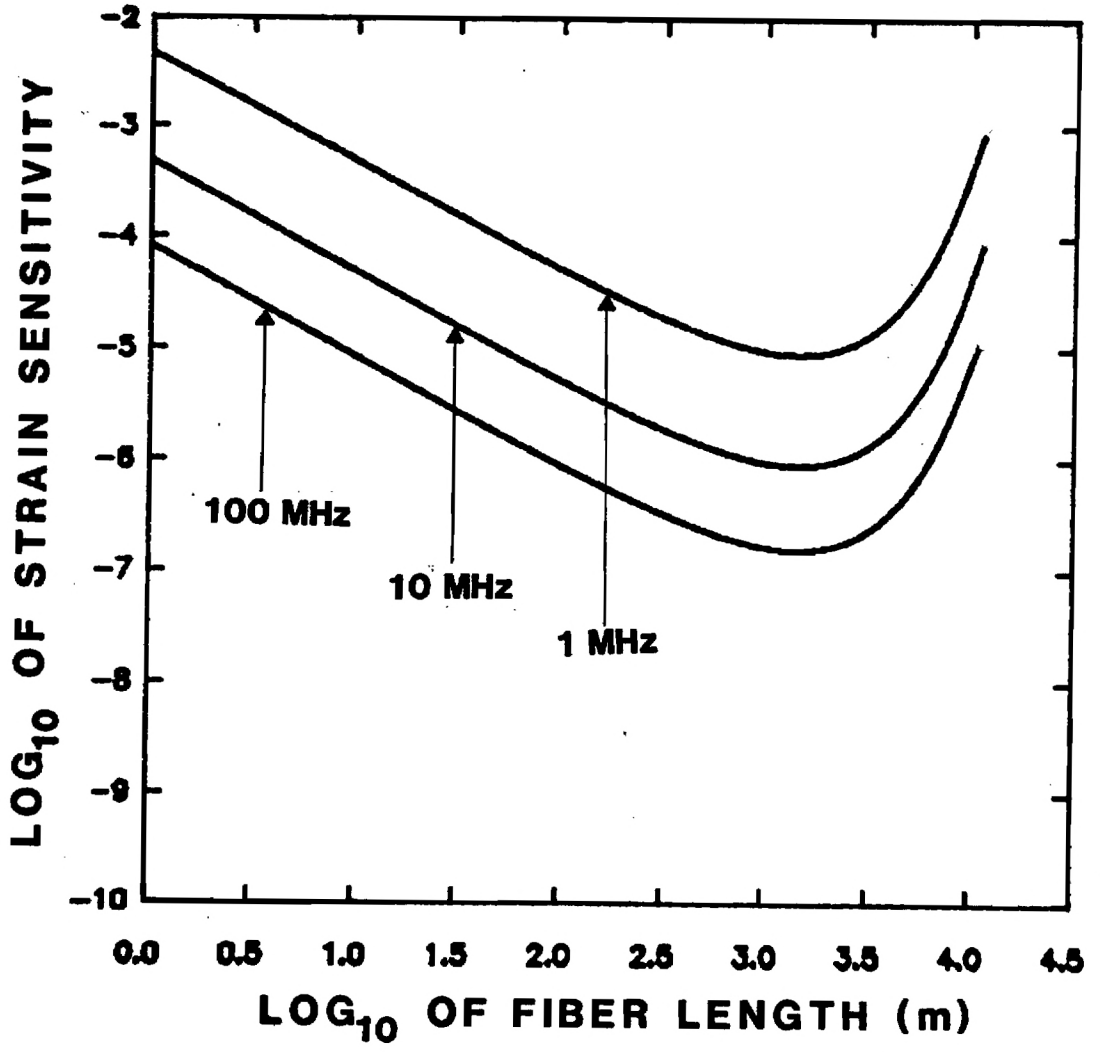

Figure 2-2-3. Minimum observable strain (strain sensitivity) as a function of fiber length for various RF frequencies. Bandwidth was set to 1 KHz. The optical source is an LED.

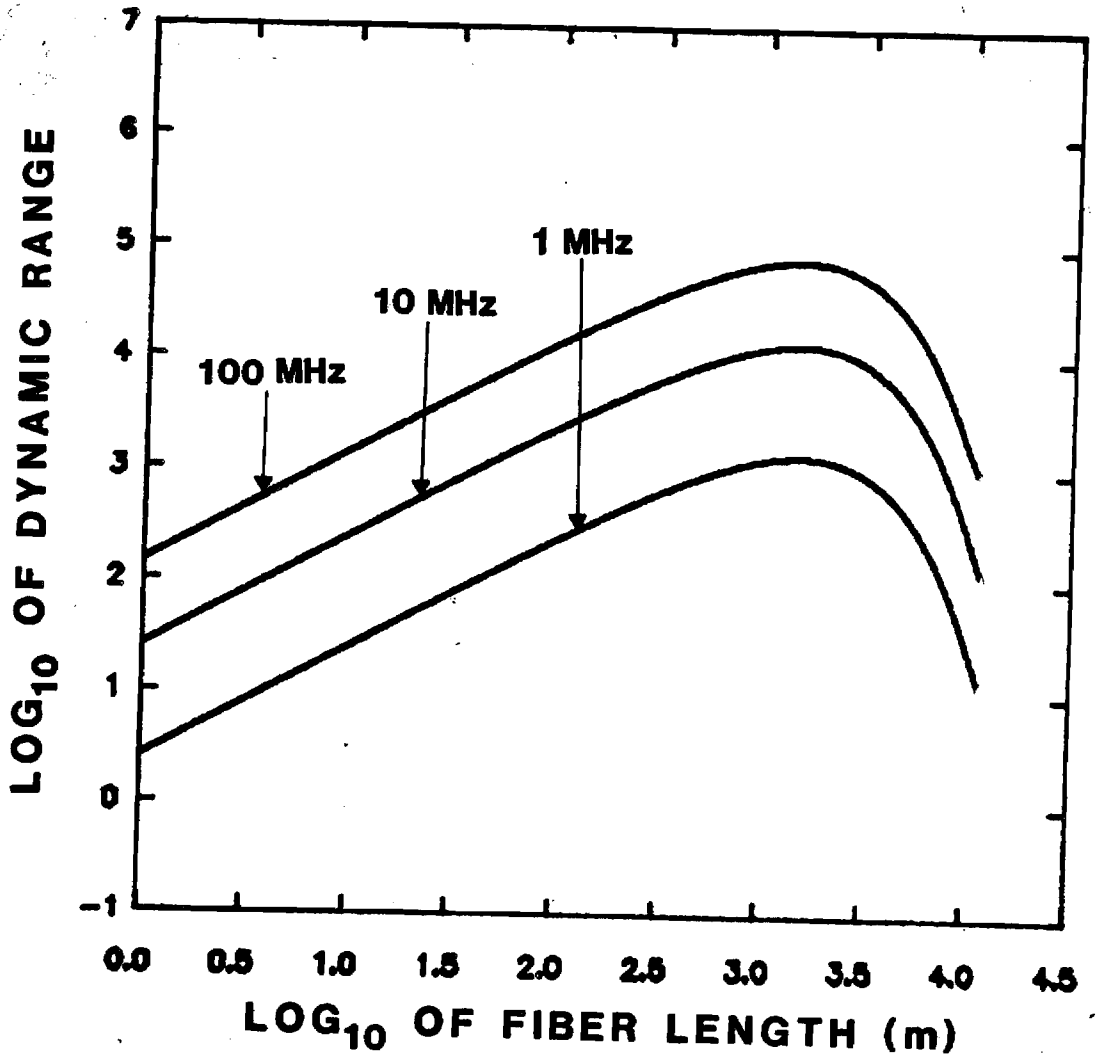

Figure 2-2-4. Expected dynamic range as a function of fiber length for various RF frequencies. Bandwidth was set to 1 kHz. The The optical source is an LED. Maximum strain value is 1.23×10^{-4}. Minimum strain value is strain sensitivity.

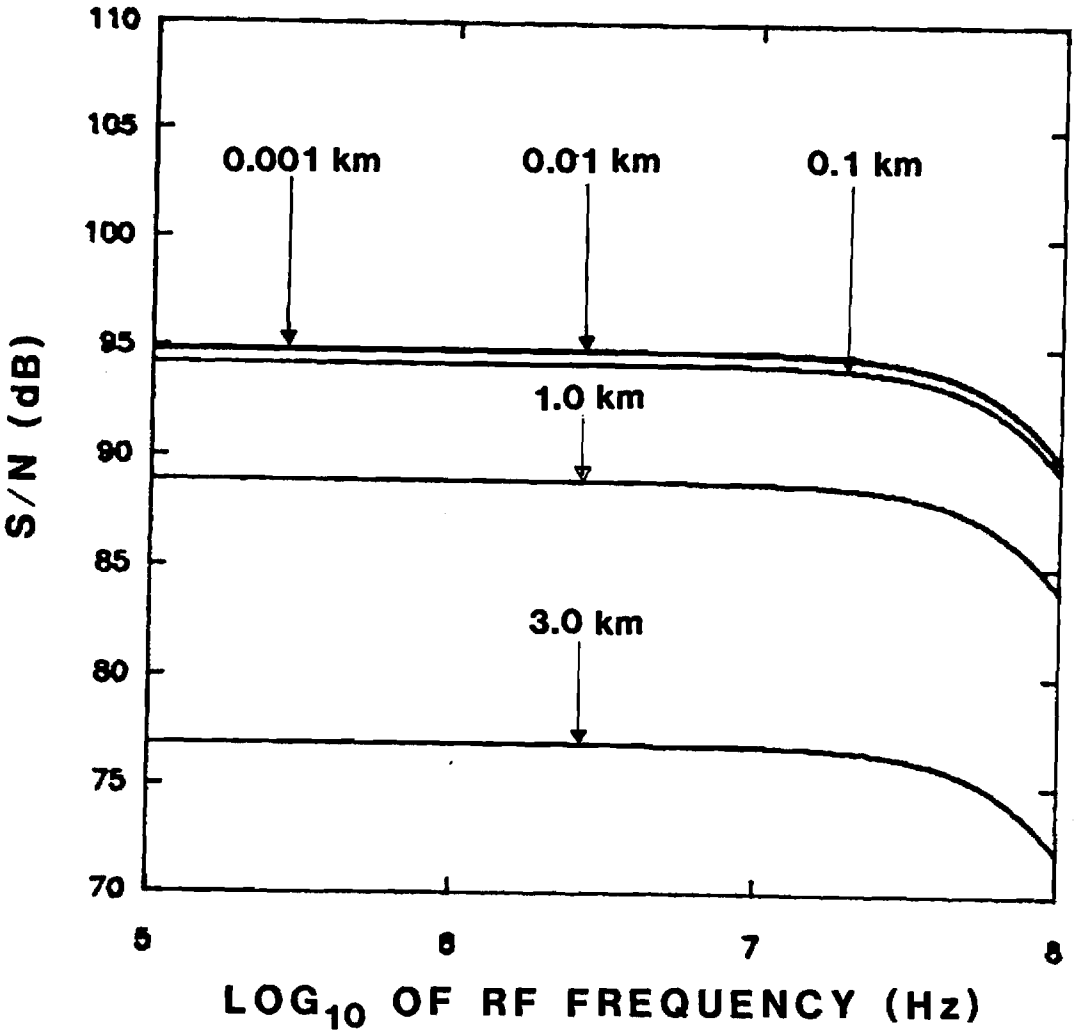

Figure 2-3-1. Signal-to-noise ratio as a function of RF frequency for various fiber lengths. Bandwidth was set to 1 kHz. The optical source is an LED.

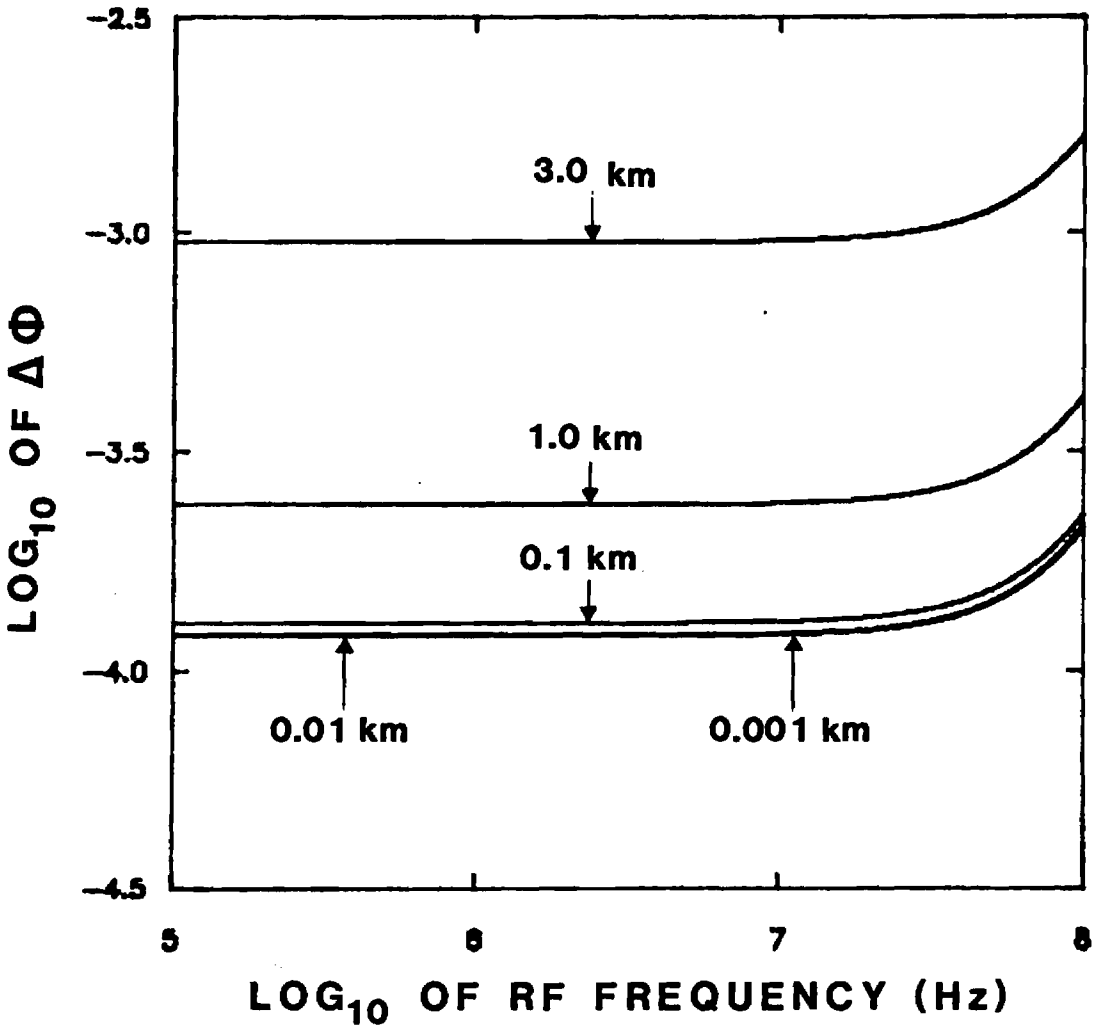

Figure 2-3-2. Minimum observable phase shift, $\Delta\Phi$, as a function of RF frequency for various fiber lengths. Bandwidth was set to 1 kHz. The optical source is an LED.

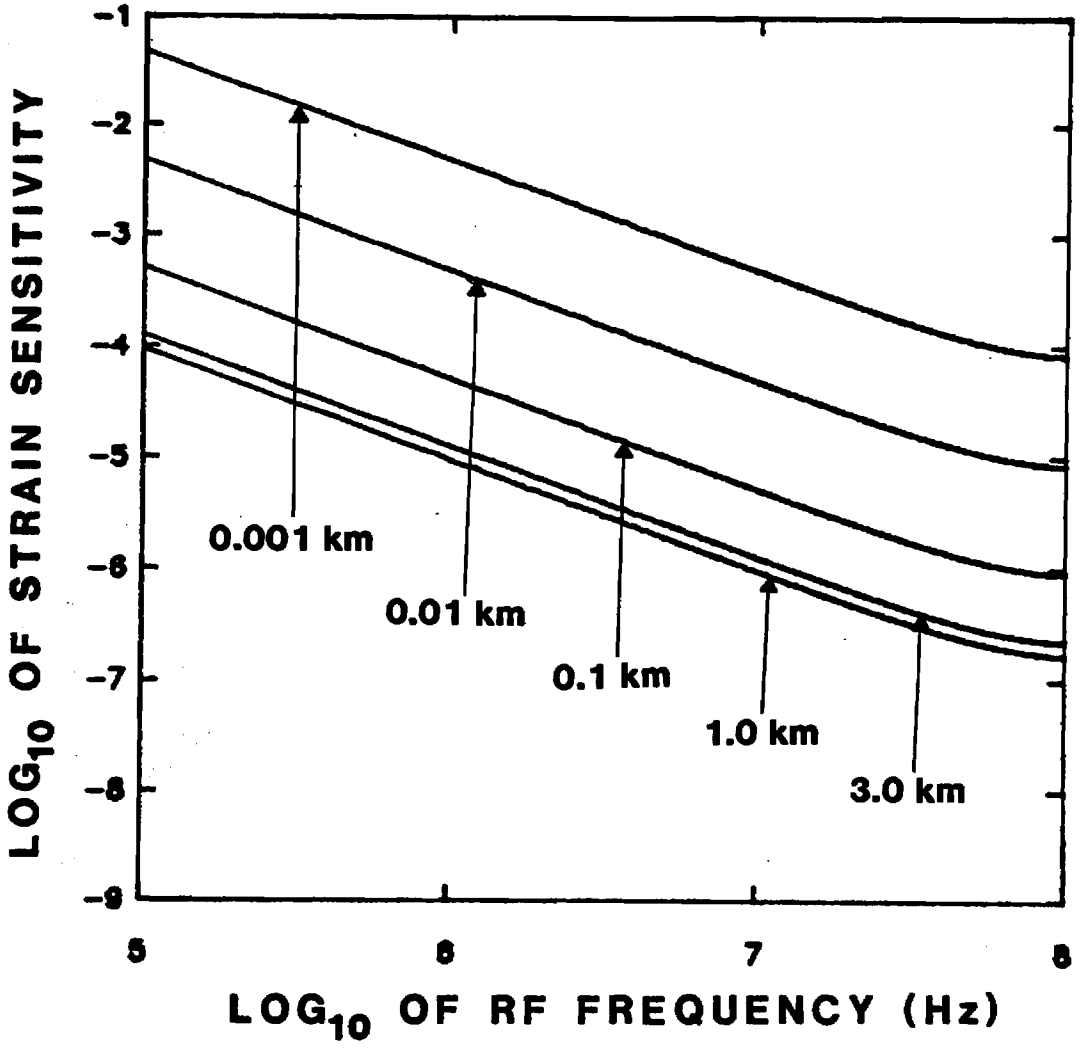

Figure 2-3-3. Minimum observable strain (strain sensitivity) as a function of RF frequency for various fiber lengths. Bandwidth was set to 1 kHz. The optical source is an LED.

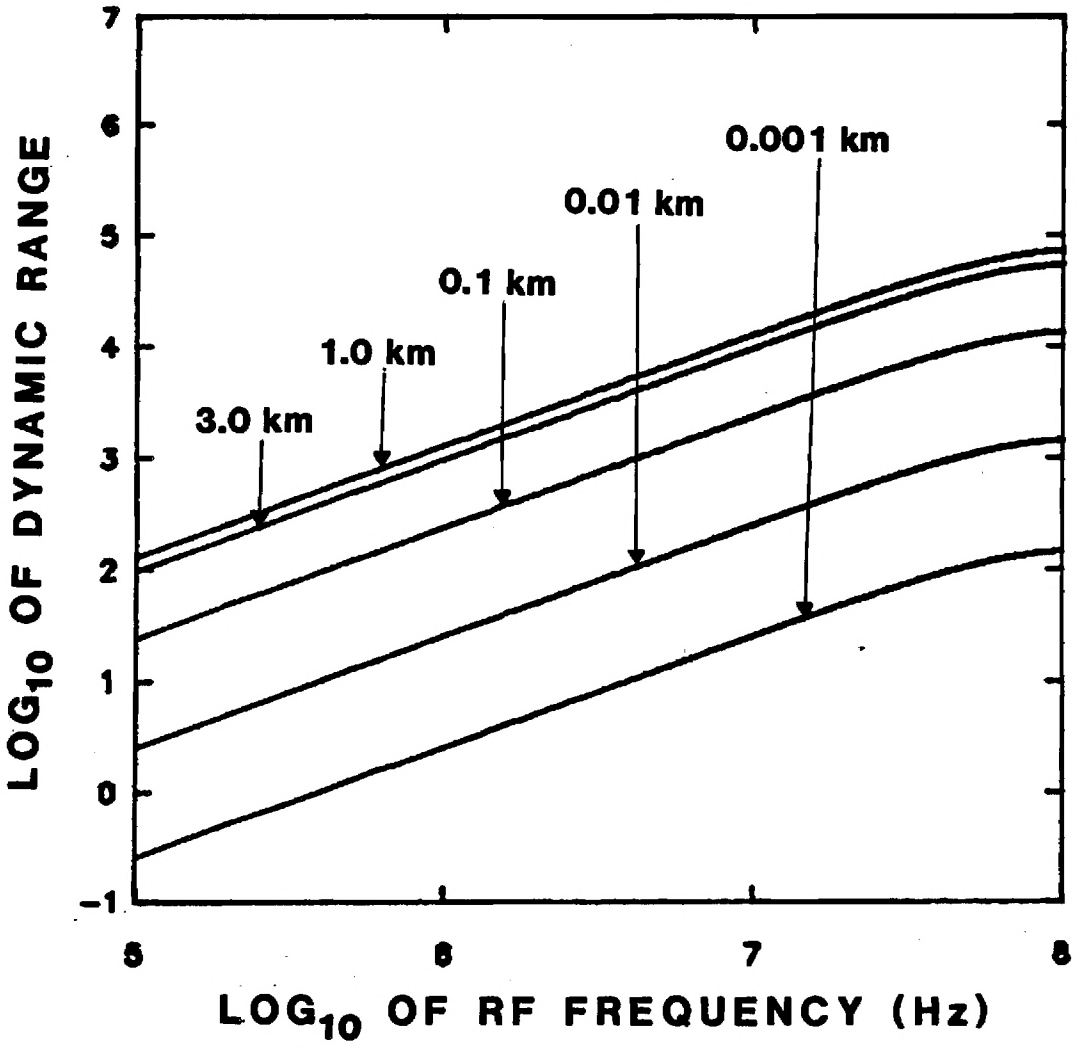

Figure 2-3-4. Expected dynamic range as a function of RF frequency for various fiber lengths. Bandwidth was set to 1 kHz. The optical source is an LED. Maximum strain value is 1.23×10^{-2}. Minimum strain value is strain sensitivity.

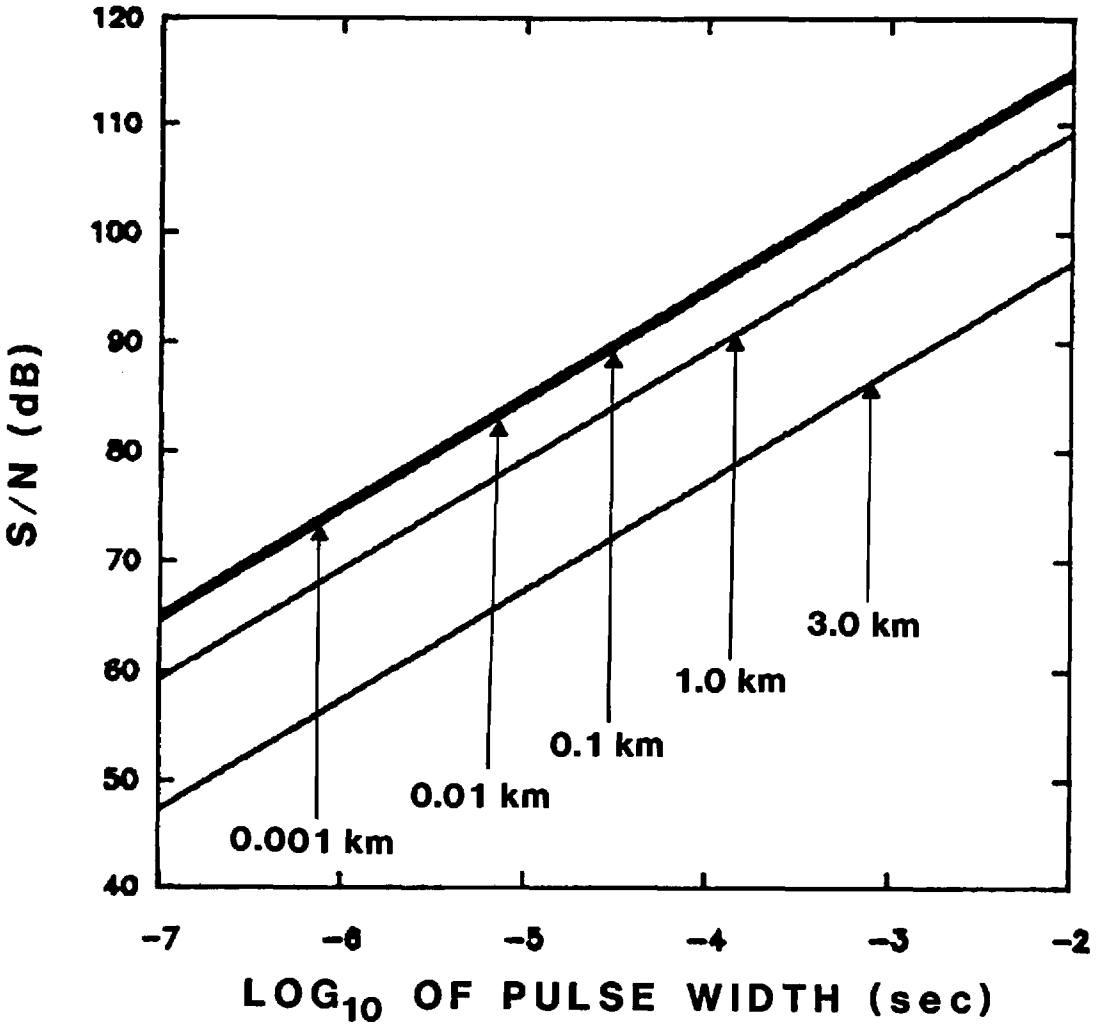

Figure 2-4-1. Signal-to-noise ratio as a function of pulse width for various fiber lengths. RF frequency was set to 100 MHz. The optical source is an LED.

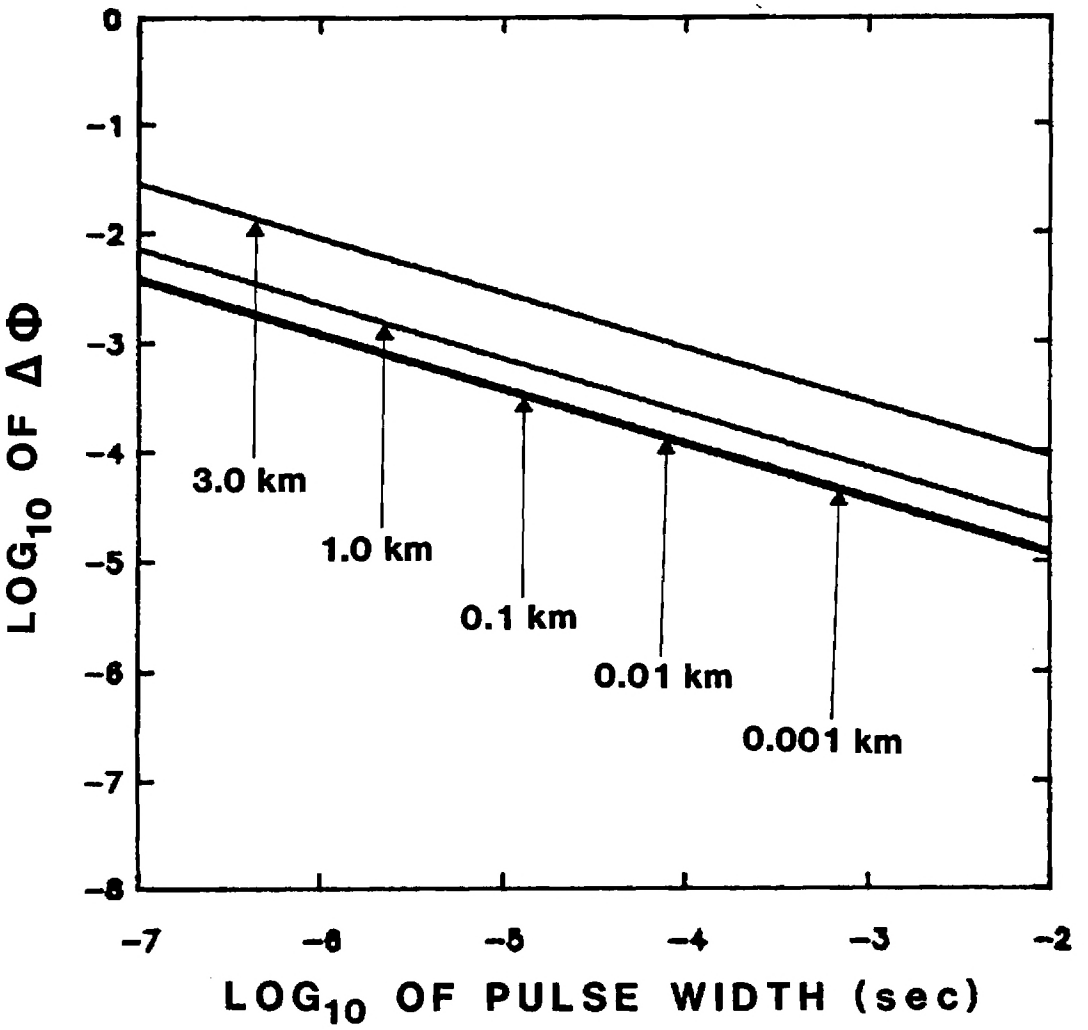

Figure 2-4-2. Minimum observable phase shift, $\Delta\Phi$, as a function of pulse width for various fiber lengths. RF frequency was set to 100 MHz. The optical source is an LED.

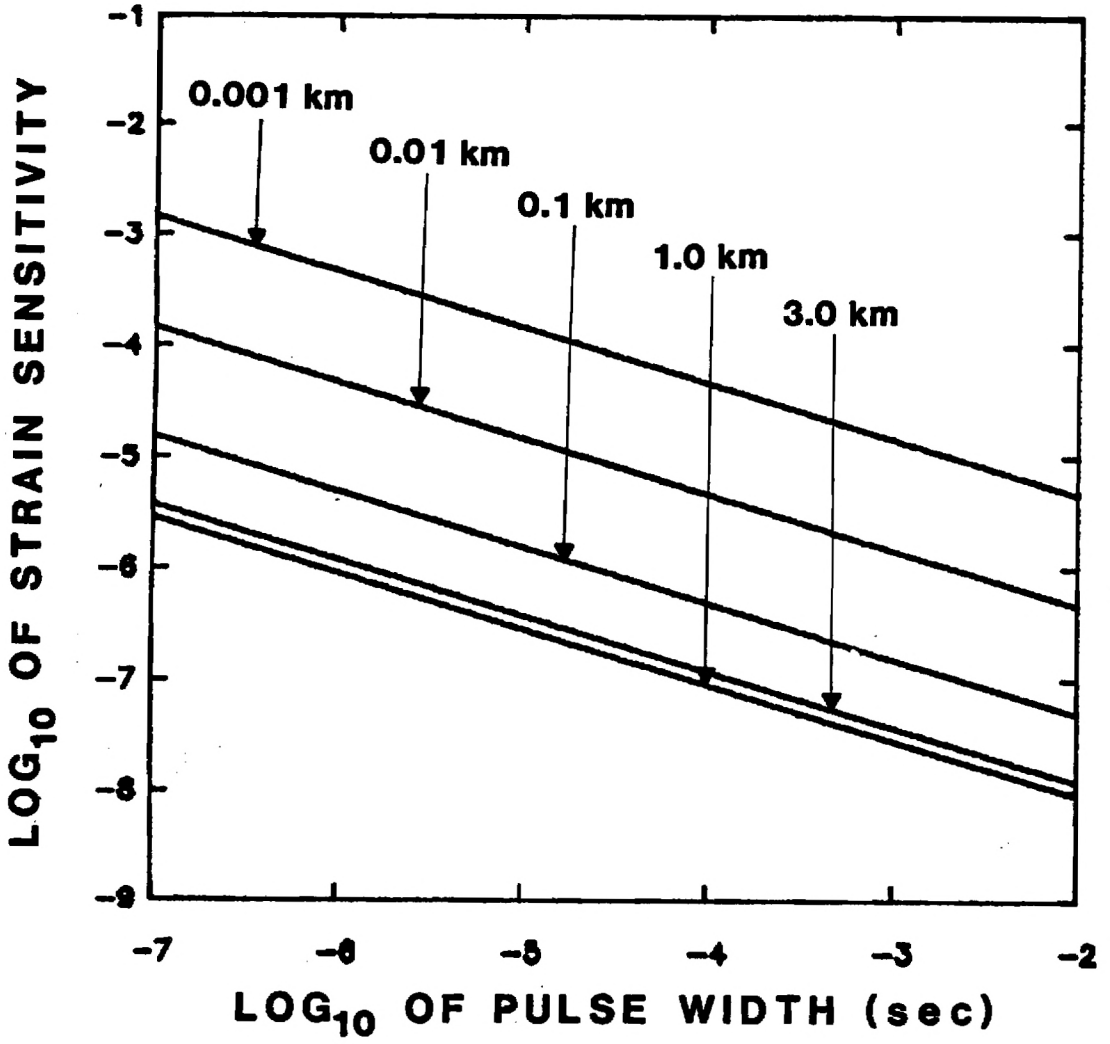

Figure 2-4-3. Minimum observable strain (strain sensitivity) as a function of pulse width for various fiber lengths. RF frequency was set to 100 MHz. The optical source is an LED.

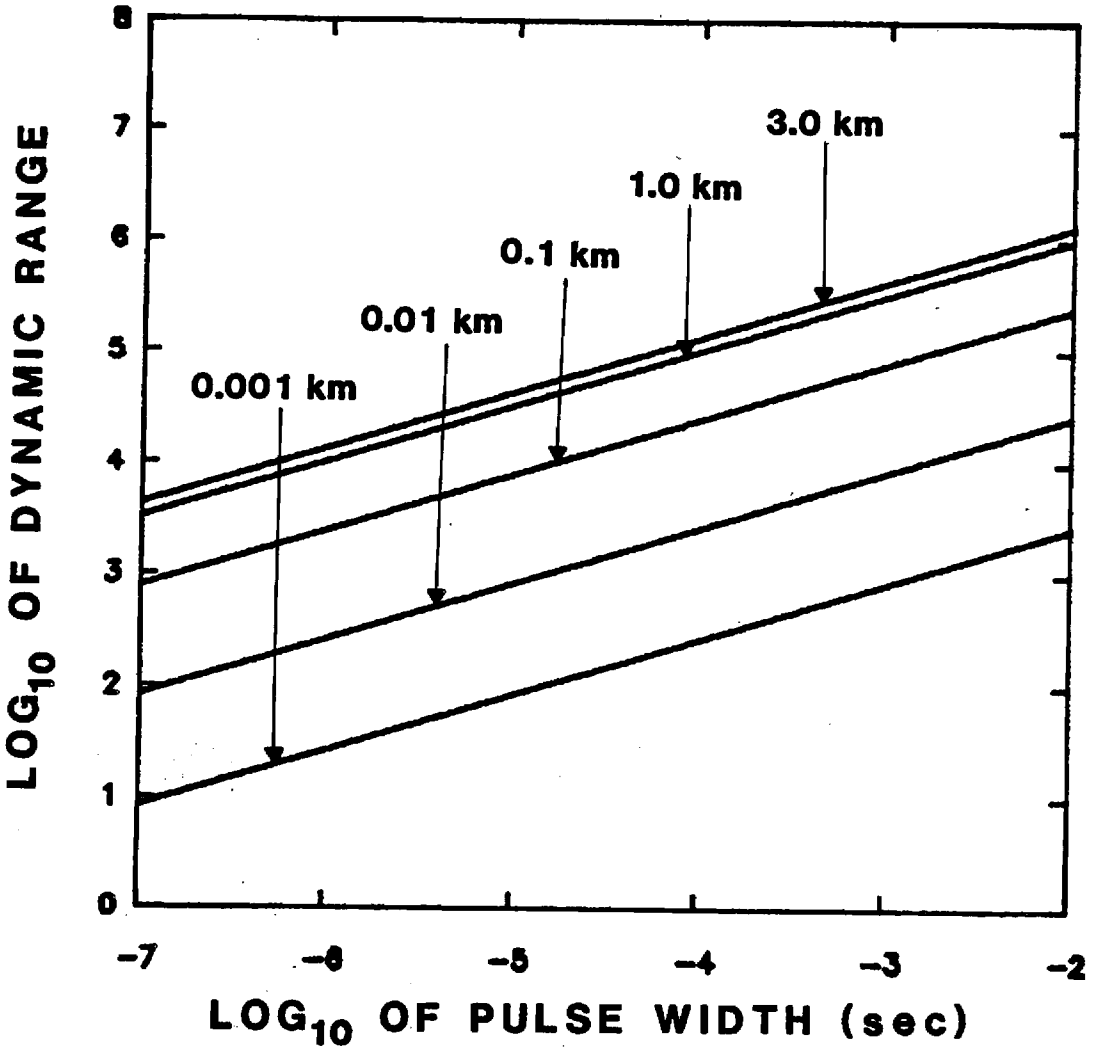

Figure 2-4-4. Expected dynamic range as a function of pulse width for various fiber lengths. RF frequency was set to 100 MHz. The optical source is an LED. Maximum strain value is 1.23×10^{-2}. Minimum strain value is strain sensitivity.

APPENDIX A

THE SUM OF TWO SINUSOIDS

Given two sinusoidal waves y_1 and y_2 with identical frequencies but displaced in phase, i.e.,

$$y_1 = A \sin \omega t$$

$$y_2 = A \sin (\omega t - \phi),$$

the resultant sum is

$$y = y_1 + y_2 = A (\sin \omega t + \sin (\omega t - \phi)) \tag{A.1}$$

Using the trigonometric identity

$$\sin a + \sin b = 2 \cos \left(\frac{a - b}{2}\right) \sin \left(\frac{a + b}{2}\right) \tag{A.2}$$

Equation (A.1) can be rewritten as

$$y = 2A \cos (\phi/2) \sin(\omega t - \phi/2) \tag{A.3}$$

or

$$y = A_R \sin (\omega t - \phi_R) \tag{A.4}$$

where the resultant amplitude A_R and phase ϕ_R are given by

$$A_R = 2A \cos(\phi/2) \text{ and } \phi_R = \phi/2$$

If ϕ is the phase difference between two transverse modes propagating through a fiber, then ϕ is in general non-zero at the output of the fiber. Hence, the resultant amplitude A_R is less than 2A (i.e., the sum of the amplitudes of the two sinusoids).

APPENDIX B

DERIVATION OF THE OUTPUT POWER OF A CW SIGNAL PROPAGATING THROUGH A MULTIMODE FIBER

Given the input power of the signal

$$P_{in}(t) = P\ (1 + m \cos \Omega\ t) \tag{B.1}$$

and the response function of the fiber

$$g(t) = \left[1/(\gamma\ L\sqrt{\pi})\right]\ \exp\left[-t^2/(\gamma^2 L^2)\right], \tag{B.2}$$

$P_{out}(t)$ is then given by the convolution of $g(t)$ with $P_{in}(t)$.

$$P_{out}(\tau) = \int_{-\infty}^{\infty} P_{in}\ (t - \tau)\ g(t)\ dt$$

or

$$P_{out}(\tau) = \int_{-\infty}^{\infty} P(1 + m \cos \Omega(t - \tau)$$

$$1/(\gamma\ L\ \sqrt{\pi})\ \exp\left[-t^2/(\gamma^2 L^2)\right]\ dt \tag{B.3}$$

$$P_{out}(\tau) = P/(\gamma L \sqrt{\pi}) \int_{-\infty}^{\infty} (1 + m \cos \Omega (t - \tau))$$

$$\exp[-t^2/(\gamma^2 L^2)] \, dt$$

$$P_{out}(\tau) = (P/(\gamma L \sqrt{\pi})) \int_{-\infty}^{\infty} \exp[-t^2/(\gamma^2 L^2)] \, dt$$

$$+ ((Pm)/(\gamma L \sqrt{\pi})) \int_{-\infty}^{\infty} \cos \Omega (t - \tau) \exp[-t^2/(\gamma^2 L^2)] \, dt.$$

The solution of the first integral is

$$[P/(\gamma L \sqrt{\pi})] \; (\gamma L \sqrt{\pi}) = P \qquad \text{(B.4)}$$

The solution to the second integral is

$$[(Pm)/(\gamma L \sqrt{\gamma})] \int_{-\infty}^{\infty} \cos \Omega (t - \tau) \exp[-t^2/(\gamma^2 L^2)] \; dt.$$

$$= [(Pm)/(\gamma L \sqrt{\pi})] \int_{-\infty}^{\infty} (\cos\Omega t \cos \Omega\tau + \sin\Omega t \sin \Omega\tau) \exp[-t^2/(\gamma^2 L^2)] \, dt$$

but

$$\int_{-\infty}^{\infty} \sin \Omega t \sin \Omega\tau \exp[-t^2/(\gamma^2 L^2)] \, dt = 0$$

since $\int_{-\infty}^{\infty}$ even function $\cdot$ odd function $= 0$.

Hence, we need to solve only

$$\left[(Pm \cos \Omega\tau)/(\gamma L \sqrt{\pi})\right] \int_{-\infty}^{\infty} \cos \Omega t \exp\left[-t^2/(\gamma^2 L^2)\right] dt$$

which yields

$$\left[(Pm \cos \Omega\tau)/(\gamma L \sqrt{\pi})\right] (\gamma L \sqrt{\pi}) \exp(-\Omega^2 \gamma^2 L^2/4) \qquad (B.5)$$

By combining solutions to the two integrals in Equations (B.4) and (B.5), we can write the output power as

$$P_{out}(\tau) = P\ (1 + m\ \exp(-\Omega^2 \gamma^2 L^2/4) \cos \Omega t)$$

THIS PAGE IS LEFT INTENTIONALLY BLANK

APPENDIX C

THE CONVOLUTION OF A GAUSSIAN PULSE WITH A GAUSSIAN RESPONSE FUNCTION

The objective in Appendix C is to convolve the input pulse $P_{in}(t)$

$$P_{in}(t) = P \quad (1 + m \exp(-\alpha t^2) \cos \Omega t) \tag{C.1}$$

with the response function of the fiber g(t)

$$g(t) = [1/(\gamma L\sqrt{\pi})] \exp \quad [-t^2/(\gamma^2 L^2)] \tag{C.2}$$

The convolution of the two functions is

$$P_{out}(\tau) = \int_{-\infty}^{\infty} P_{in}(t - \tau)\, g(t)\, dt \tag{C.3}$$

or

$$P_{out}(\tau) = [P/(\gamma L\sqrt{\pi})] \int_{-\infty}^{\infty} [1 + m \exp(-\alpha(t - \tau)^2) \cos \Omega(t - \tau)]$$

$$\exp[-t^2/(\gamma^2 L^2)]\, dt \tag{C.4}$$

The integral can be separated

$$P_{out}(\tau) = [P/(\gamma L\sqrt{\pi})] \int_{-\infty}^{\infty} \exp[-t^2/(\gamma^2 L^2)]\, dt \qquad (C.5)$$

$$+ [P/(\gamma L\sqrt{\pi})] \int_{-\infty}^{\infty} m \exp(-\alpha(t-\tau)^2) \exp[-t^2/(\gamma^2 L^2)] \cos \Omega(t-\tau)\, dt$$

The solution of the first integral is

$$[(P/(\gamma L\sqrt{\pi})] \int_{-\infty}^{\infty} \exp[-t^2/(\gamma^2 L^2)]\, dt = (P/(\gamma L\sqrt{\pi}))\,(2\gamma L\sqrt{\pi}/2) \qquad (C.6)$$

$$= P$$

Thus

$$P_{out} = P[1 + 1/(\gamma L\sqrt{\pi})] \int_{-\infty}^{\infty} m \exp(-\alpha(t-\tau)^2) \exp[-t^2/(\gamma^2 L^2)]$$

$$\cos \Omega(t - \tau)dt \qquad (C.7)$$

The integral in Equation (C.7) can be solved by first combining the exponential terms given by

$$E = -\alpha(t - \tau)^2 - t^2/(\gamma^2 L^2) = -\alpha(t^2 - 2t\tau + \tau^2) - t^2/(\gamma^2 L^2)$$

$$E = -[\alpha t^2 - 2\alpha t\tau + \alpha\tau^2 + t^2/(\gamma^2 L^2)]$$

$$E = -t^2[\alpha + 1/(\gamma^2 L^2)] - 2\alpha t\tau + \alpha\tau^2$$

Setting $A = \alpha + 1/(\gamma^2 L^2)$ and completing the square, we obtain

$$E = -A(t^2 - 2\alpha t\tau/A + \alpha^2\tau^2/A^2 + \alpha\tau^2/A - \alpha^2\tau^2/A^2)$$

$$E = -A\left[(t - \alpha\tau/A)^2 + \alpha\tau^2/A - \alpha^2\tau^2/A^2\right]$$

or

$$E = -A(t - \alpha\tau/A)^2 - \alpha\tau^2 + \alpha^2\tau^2/A.$$

Let $C = -\alpha\tau^2 + \alpha^2\tau^2/A$, then

$$E = -A(t - \alpha\tau/A)^2 + C.$$

$P_{out}(\tau)$ can now be rewritten as

$$P_{out}(\tau) = P + P\left[m \exp(C)/(\gamma L\sqrt{\pi})\right] \int_{-\infty}^{\infty} \exp(-A(t - \alpha\tau/A)^2)$$

$$\cos \Omega(t - \tau)\, dt. \qquad (C.8)$$

Set $X = t - \alpha\tau/A$, then $dX = dt$ and $t - \tau = X + \alpha\tau/A - \tau$. The integral becomes

$$\int_{-\infty}^{\infty} \exp(-A(t - \alpha\tau/A)^2) \cos \Omega(t - \tau)\, dt$$

$$= \int_{-\infty}^{\infty} \exp(-AX^2) \cos \Omega (X + \alpha\tau/A - \tau)\, dX$$

$$= \int_{-\infty}^{\infty} \exp(-AX^2) \left[\cos \Omega X \cos \left[\Omega (\tau/(A)(\alpha - A)\right] - \sin\Omega X \sin \left[\Omega(\tau/A)(\alpha - A)\right]\right] dX$$

$$= \int_{-\infty}^{\infty} \left[\exp(-AX^2) \cos \Omega X \cos \left[\Omega (\tau/A)(\alpha - A)\right] dx - \int_{-\infty}^{\infty} \left[\exp(-AX^2) \sin \Omega X\right.\right.$$

$$\left.\left.\sin \Omega\left[(\tau/[A)\ (\alpha - A)]\right]\right] dx.\right.$$

The integral with the sine functions is zero because $\int_{-\infty}^{\infty}$ even function $\cdot$ odd function $dx = 0$. Thus, we need only to evaluate the integral with the cosine functions.

$$\int_{-\infty}^{\infty} \exp(-AX^2) \cos \Omega X \cos \left[\Omega(\tau/A)\ (\alpha - A)\right] dX$$

$$= \cos \left[\Omega\ (\alpha - A)\ \tau/A\right] \int_{-\infty}^{\infty} \exp\ (-AX^2)\ \cos \Omega X\, dX$$

$$= (\sqrt{\pi}/\ \sqrt{A})\ \cos\left[\Omega\ (\tau/A)\ (\alpha - A)\right] \exp(-\Omega^2/4A) \qquad (C.9)$$

The convolution function of Equation (C.8) can now be written as

$$P_{out}(t) = P + \lfloor (P\,m)/(\gamma L)\ \exp(C) \rfloor\ (1/\sqrt{A})\ \cos$$

$$\lfloor \Omega(t/a)\ (\alpha - A) \rfloor\ \exp\ (-\Omega^2/4A) \qquad \text{(C.10)}$$

Evaluating C, $\Omega^2/4A$ and $(t/A)(\alpha - A))$ we obtain

$$C = -\alpha t^2/(\alpha\gamma^2L^2 + 1)$$

$$\Omega^2/4A = (\Omega^2\gamma^2L^2)/(4\alpha\gamma^2L^2 + 4)$$

and

$$(t/A)\ (\alpha - A) = -t/(\alpha\gamma^2L^2 + 1)$$

where

$$A = \alpha + 1/(\gamma^2L^2)$$

and the variable τ was replaced by t.

Substituting these expressions into Equation (C.10), we obtain the final expression of P_{out} (t).

$$P_{out}(t) = P \{1 + (m/\sqrt{\alpha\gamma^2L^2 + 1}) \exp\lfloor(-\Omega^2\gamma^2L^2) /(4\alpha\gamma^2L^2 + 4)\rfloor$$

$$\exp\lfloor(-\alpha t^2)/(\alpha\gamma^2L^2 + 1)\rfloor \cos \Omega \lfloor 1/(\alpha\gamma^2L^2 + 1)\rfloor t\} \qquad (C.11)$$

where α and γ are constants. Equation (C.11) can be simplified by writing

$$m' = (m/\sqrt{\alpha\gamma^2L^2 + 1}) \exp(-\Omega^2\gamma^2L^2)/(4\alpha\gamma^2L^2 + 4)$$

$$\Omega' = \Omega/(\alpha\gamma^2L^2 + 1)$$

$$\alpha' = \alpha/(\alpha\gamma^2L^2 + 1)$$

Hence, $P_{out}(t)$ becomes

$$P_{out}(t) = P\,(1 + m' \exp(-\alpha' t^2) \cos \Omega' t). \qquad (C.12)$$

APPENDIX D
GAUSSIAN STATISTICS

Given two Gaussian probability distributions where $\mu_1 \neq \mu_2$ and $\sigma_1 = \sigma_2 = \sigma$, find the required separation between μ_1 and μ_2 such that integration of the first Gaussian to the right of a threshold b (i.e., from b to ∞) gives 10^{-6} and integration of the second Gaussian from b to ∞ yields nearly 1.0 (see Figure 16).

The integral of the first Gaussian is

$$P(X>b) = \int_b^{\infty} \frac{1}{\sqrt{2\pi}\,\sigma} \exp-((x-\mu)^2/2\sigma^2)\, dx$$

where b denotes the threshold and P (X>b) is the probability of the variable X greater than b.

P (X>b) can be rewritten in terms of a generalized variable z such that

$$P(z>K\alpha) = \int_{K_\alpha}^{\infty} \frac{1}{\sqrt{2\pi}} \exp(-z^2/2)\, dz = \alpha$$

where $K\alpha$ is defined as

$$K_\alpha = \frac{b-\mu}{\sigma} = b/\sigma \quad \text{if} \quad \mu = 0.$$

If α is set to 10^{-6}, then K_α can be found in statistics tables[11] to be 4.7.

Since $K_\alpha = b/\sigma$, we can solve for b

$$b = 4.7\ \sigma\ .$$

If the Gaussians intersect at b, then integration from b to ∞ of the second Gaussian is $1.0 - 10^{-6}$, or nearly 1.0 as required. Thus, the difference $\mu_2 - \mu_1$ must be 2b or $9.4\ \sigma$.

THIS PAGE IS LEFT INTENTIONALLY BLANK

REFERENCES

1. H. F. Wolf, Handbook of Fiber Optics: Theory and Applications, Garland STPM Press, 83 (1979).

2. H. F. Wolf, Handbook of Fiber Optics: Theory and Applications, Garland STPM Press, 94 (1979).

3. C. D. Butter and G. B. Hocker, App. Opt., 17, 2867 (1978).

4. D. E. McCumber, Physical Review, 141, 306 (1966).

5. D. J. Morgan and M. J. Adams, Phys. Stat. Sol. (a), 11, 243 (1972).

6. A. Yariv, Introduction to Optical Electronics, Holt, Rinehart and Winston, (1971).

7. S. D. Personik, Bell System Technical Journal, 50, 843 (1971).

8. A. H. Bowker and G. J. Lieberman, Engineering Statistics, Prentice-Hall Press, 75 (1959).

9. I. H. Malitson, J. Opt. Soc. Amer., 55, 1205 (1965).

10. G. B. Hocker, Optics Letters, 4, 320 (1979).

11. A. H. Bowker and G. J. Lieberman, Engineering Statistics, Prentice-Hall Press, 555, (1959).